Addis Ababa University

Addis Ababa Institute of Technology

School of Mechanical and Industrial Engineering

Dynamic Analysis and Improving Crashworthiness of Side-Impact Beam for Saloon type Vehicles

Presented in Fulfillment of the Requirements for the Degree of Master of Science

(Mechanical and Industrial Engineering)

By: **Bililign Amare**

Advisor: Dr.Ing. Tamirat Tesfaye

Co-advisor: Mr. Araya Abera

June, 2017

ACKNOWLEDGMENT

First of all I want to express my enormous thank to the Almighty God for his creating good environment, continuous and priceless help to accomplish this study.

Next to God, I would like to express my sincere gratitude to my advisor Dr. Tamirat Tesfaye for the continuous support of my research, for his patience, motivation, and immense knowledge. I would also like to express my special gratitude to my co-advisor Mr. Araya Abera for his guidance, support, critical comments, patience and engagement throughout the progress of the study. Without them, this study could have not been completed.

I would also like to thank the school of Electrical and Computer Engineering for giving access to use their advance computer for FEM analysis. This access was accomplished by the help of two dutiful men, Mr. Behailu Mammo and Mr. Fistum; that is why I would like to thank them a lot.

Last but not list, I would like to thank my family and my friends those who are always beside me and played a great role in the completion of this study.

Abstract

Side impact collision of vehicle is one of the awfully hazardous crashes causing injuries and death annually around the word. In this paper, the most important parameters including material, geometry and rib arrangement were studied to improve the crashworthiness during vehicle-to-vehicle side collision. In the side impact, the side door impact structure is responsible to absorb the most possible kinetic energy. Different side impact structures are designed as alternative structure and are modeled with CAD software (CATIA V5) and then analyzed with FEM software (LS-DYNA with ANSYS R15). This research had taken the present geometry and material for side impact beam structure of Lifan-520 model as saloon car type. The side impact collision structure analysis accomplished for different materials to compare the weight and impact behavior. In this study, a side impact beam made of different materials and geometries were studied by impact modeling to determine the deflection, acceleration and energy-absorption behavior. The mentioned characteristics were compared to each other to find appropriate material and geometry. Finally, side impact beam with crossed rib arrangement (⊕-type) and implication of Carbon/PEEK composite material having better specific internal energy absorption, more stable and acceptable deflection within a limited crumple zone are founded for improvement of crashworthiness.

Key Words: Crashworthiness, Energy Absorption, Maximum Deflection, Acceleration, Composite Materials

Table of Contents

List of Figures

List of Tables

Chapter one

1 Introduction

1.1 Background

Side impacts are one of the awfully hazardous crashes causing death and injuries annually around the word. Many of these injuries occur when one car runs into the side of another or into a fixed narrow object such as a trees lamp posts, or poles. Approximately 75% of side impact is Vehicle-to-Vehicle collision and the rest 25% Vehicle-to-fixed object impact [1].

Over the last few decades, critical steps have been taken that increase vehicle occupant safety for frontal impacts: mandatory driver and front-passenger airbags; improved front and rear crumple zones; improved headrest designs; gas tank redesigns; mandatory seat-belt laws; mandatory under ride beams on commercial trucks, and so on. Unfortunately, they do not provide similar protection for side-impact collisions. Although frontal crashes occur more often, the type of crash that is now more likely to result in a fatality or a serious injury is a side-impact collision [2]. Approximately 25% of all crashes are side impacts. Over 13,000 deaths, due to side impact occurred during 1998 in United States alone [3]. Approximately 46% of total fatalities are due to side impacts [4].

The main difficulty in designing for side impact collision is the limited crumple zone between the impacting vehicle and impacted occupant [5]. Strengthening vehicle body-door in side impacts demands more attention due to having less impact zone area and lower rigidity compared with the bumper. A good structure behavior is necessary to absorb most of the kinetic energy.

Crashworthiness may be assessed either prospectively, using computer models or experiments, or retrospectively by analyzing crash outcome. Data obtained from a crash simulation indicate the capability of the vehicle body to protect the vehicle occupants during a collision against injury. Computer aided parametric design software will be used for modeling of the problem to define all the coordinate values and geometrical details, then this CAD data would be transferred to an FEM software (LS-DYNA, MADYMO, ANSYS etc.) for pre-processing, solution and post-processing followed by generation and interpretation of results related to energies, acceleration and displacements/deflections with different loads & boundary conditions possible in various accidental situations during side collision [6].

1.2 Crashworthiness

Crashworthiness is the ability of the vehicle to absorb energy and to prevent occupant injuries in the event of accident. Crashworthiness features includes air bags, seat belts, crumple zones, side impact protection, interior padding and head rests.

Structural crashworthiness involves absorption of kinetic energy by considering designs and materials suitable for controlled and predictive energy absorption. In this process, the kinetic energy of the colliding bodies is partly converted into internal work of the bodies involved in the crash. Crash events are non-linear and may involve material failure, global and local structural instabilities and failure of joints. Strain-rate and inertia effects may play an important role in the response of the structures involved.

Crashworthiness of a material is expressed in terms of its specific energy absorption. In order to protect passengers during an impact, a structure based on strength and stiffness is far from being optimal. Rather, the structure should collapse in a well-defined zone and keep the forces will below dangerous accelerations. The rate of absorbing energy has also its own influence on the brain skull. This leads the decelerated of vehicle should not greater than 20 g, [13].

1.3 Crash Statistics

Side-impact crash is the second most severe crash scenario after frontal-impact. The recent crash statistics shows that 51%, 25%, 15% and 9% are frontal, side, rollover and rear-impact, respectively, [1, 8, 12]. As figure 1 indicates the frontal-impact is higher than the side-impact [1]. However, the space requires for any structure in the event of a side-impact to absorb energy is very less than the frontal-impact.

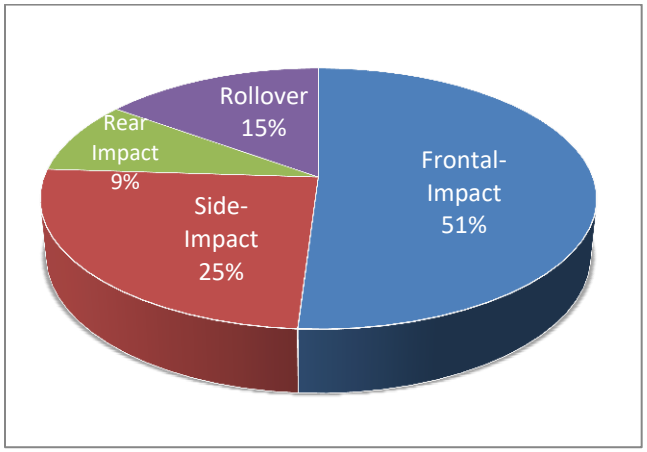

Figure 1 Crash Type

The occupant injuries in the side-impact crash are severe when compared with the frontal crash. Other crashes involved are the rear impact and rollover. These amounts are lesser crash scenario than the side or the frontal crash. In the recent time approximately 46% of total fatalities are due to side impacts; and the other 54% are (fontal = 38%, rear = 6% and rollover = 10%), [4].

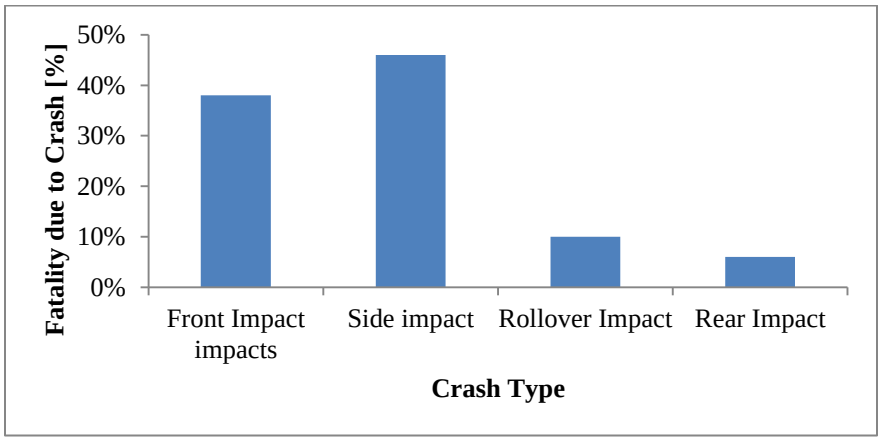

Figure 2 Fatality due to crash

1.4 Basic Research Questions

- Which types of structure and geometry will be appropriate for absorbing high kinetic energy with acceptable deflection in limited crumble zone during side collision?
- Which available materials (inexpensive and lightweight) are suitable for side impact beams?
- Which types of geometry and material combination will absorb energy in more stable condition with acceptable acceleration limits?

1.5 Statement of Problems

Over the last few decades, critical steps have been taken that increase vehicle occupant safety for frontal impacts: mandatory driver and front-passenger airbags; improved front and rear crumple zones; improved headrest designs; gas tank redesigns; mandatory seat-belt laws; mandatory under ride beams on commercial trucks, and so on. Unfortunately, they do not provide similar protection for side-impact collisions, [2]. The main difficulty in designing for side impact collision is the limited crumple zone between the impacting vehicle and impacted occupant. To avoid the occupant injuries it is necessary to absorb the whole kinetic energy both of the vehicle and the occupant. Kinetic energy of the occupant can absorbed by using three or four point seat belts, side air bags, padding materials and crumble zone during side collision [10]. Most researches of side impact protection focused on low-speed (<20 km/h) impacts [3], [10], [9], [5], [7] and also in fixed object collision [10], [5], [4], [7]. Whereas approximately 75% of side impact is Vehicle-to-Vehicle collision and also 60% of vehicle-to-vehicle side collisions are occurred at a speed more than 32 km/h [1]. Therefore absorbing high kinetic energy of vehicles during high speed side collision between vehicles needs a special structure which can sustain the effect of severe condition of side collisions. Some researchers were introduced the optimum structure for side-impact beam [7, 8, 9] and the other researchers were investigated on appropriate materials for side-impact structure, [11, 15]. But crashworthiness structure needs optimum combination of structures and intended materials.

1.6 Objective of the Study

There are several areas in the field of crash-impact dynamics that need to be studied to improve the crashworthy design of the side-door.

1.6.1 General Objective:

The general objective of this study is to find a compatible side door impact-beam having better energy absorption during severe side collision in limited crumple zone to enhance crashworthiness.

1.6.2 Specific Objective:

- ☞ Designing appropriate structure for vehicle side collision.
- ☞ Identifying appropriate material for side impact structure.
- ☞ Analyzing the energy absorption of different alternative of side impact structures.

1.7 Significance of the Study

This study will have a contribution to increase vehicle occupant safety for constrained fatality or a serious injury due to side-impact collision. The study can also indicate a clue how crashworthiness design could implement in limited crumple zone. The side impact structure is designed from the lightweight materials, so automotive industries may use this concept for lightweight design of vehicles parallel with occupant safety.

1.8 Scope and limitation of the Study

The study included designing of side impact structure with preparing its model and analyzing with respect to speed of collision. The design of the structure focused on five-seater saloon (Lifan 520) type vehicle. It analyzed the specific energy absorption of the structure with selecting appropriate material. The failure of the bonding between the beam tube and rib is taken as negligible and it is supposed that any set of parts is constrained to each other in all degree of freedom without modeling the mechanical strength of the coupled part. The crashworthiness experimental analysis is expensive and not available in Ethiopia; this limits the study to apply only computational finite element analysis using Computer Aided Drafting (CAD) and Computer Aided (CAE) software such as CATIA, AutoCAD, and ANSYS_LS-DYNA. For the accuracy of the result, experimental test should be conducted in the future work.

Chapter Two

2 Literature Review

2.1 Related Work in side impact protection mechanism

Side impact protection mechanism will install in the door of vehicle. They will have different geometries and will construct from different materials. This research focuses on the side impact protection mechanisms by studying Lifan-520 model car. This existed model has four side impact beams with a circular cross-section and constructed from steel 1006. Thought time to time, crashworthiness has been a growing realization of importance in virtually every transportation sector. Newer designs are proposed every day to improve the crashworthiness of the structure. There is no limit in the field of crashworthiness in reducing the injuries sustained by the occupant. It is preferable to design a vehicle to collapse in a controlled manner, thereby ensuring the safe dissipation of kinetic energy.

Panagiotis Bazios [7], discussed energy absorption and deflection of five conventional vehicle door components (side panel, inner skin of door, outer skin of door, impact beam and hinges) of two-seater electrical vehicle in side impact conditions. He applied dynamic structural analysis type and found optimum thickness of the door components in order to minimize impact energy and the intrusion of the door to the cabin. After recognizing as the impact beam is the main impact energy absorber, he redesigned to having variable thickness.

Javier Luzon-Narro [8], presented six innovative occupant near side lateral impact protection concepts including a dynamic door, high-volume side airbag, a large external airbag that covers doors, sill and B-pillar of the struck vehicle and other concepts for increasing the distance between the occupant and the door panel (active armrest, inflatable door beam and moving seat). All systems are based on pre-crash detection of the impact and are activated as soon as 0.8 second before the impact. This paper also details the task of integrating these systems into a vehicle using FE models, sled tests, and full scale crash tests.

John Townsend [9], discussed The design and development of the side impact modular door system for different size vehicles with and without Door and Chassis-Frame Integration Technology (DACIT). This paper presents a side impact protective door system within the space between the outer skin of a car door and the occupant, which will be as efficient as that already standard in frontal impact by integrating the structural modular door with the vehicle body.

Sandeep Dalavi, [10], discussed the effectiveness of car interior door trim parts (top roll, insert, armrest, main carrier and Ma-pocket) in reducing loads transferred to the occupant during side impact and suggested strengthening those parts can protect injuries of side collisions. He indicated that addition of energy absorbing padding material in the door area can greatly improve the energy dissipation in the car interior.

Gustavo Zini [11], indicated some feasible innovations that may lead to a better side impact protection, pointing out some aspects that can be developed thoroughly within the corresponding settings and using the appropriate resources. The mentioned innovations analyzed from a general point of view, using basic engineering and physics principles. Simulations performed using a simplified model consisting on mass spring system. The protection offered by current safety devices analyzed, segmented into three groups (pre-impact, impact and post-impact).

Ashwin Sheshadri [12], demonstrated that the new designed composite beam with carbon/epoxy is more effective than the present steel beam. A composite side impact beam has designed to replace the present beam and the injuries sustained by the occupant are recorded. The research had used Carbon/Epoxy and Glass fiber/epoxy composite materials in the designed side-impact beam. In addition, a parametric study was carried out on the beam to determine the maximum possible energy absorbing parameters. It demonstrated that the new designed beam with the use of carbon/epoxy present more energy absorption than the present steel beam. Energy absorption, displacement and the acceleration of the present and the new design were also compared and discussed in detail. The research demonstrated that the new designed composite beam with carbon/epoxy is more effective than the present steel beam.

2.2 Injury Criteria's

Injury criteria can be defined as a biomedical index of exposure severity, which indicates the potential for impact induced injury by its magnitude. There are several kinds of injury criteria's that related to the human body. These are basically the impact loads acting on the human body.

2.2.1 Head Injury Criterion (HIC)

The head injury criterion is defined as:

$$\text{HIC} = \max\left[\frac{1}{t1-t2}\int_{t1}^{t2} R(t)dt\right]^{2.5}(t_2\text{-}t_1) \quad (1)$$

For, T0 ≤t1≤ t2≤ TE

Where, T_0 = start time of simulation

TE= end time of simulation

R(t) = is the resultant head acceleration in g's measured at head's center of gravity over the time interval T0 ≤ t ≤ TE.

t_1 and t_2 are the initial and final times (in seconds) of the interval during which the HIC attains a maximum value.

In the event of an impact, crashworthy materials would have work done on them to absorb this kinetic energy over a time frame that ensures the deceleration of the car to be less than 20g, above which the passengers will experience irreversible brain damage because of the relative movements of various parts of the brain within the skull cavity, [13].

2.2.2 Thoracic Trauma Index (TTI)

The thoracic trauma index (TTI) provides an indication of the severity of injuries received by motor vehicle occupants in side-impact collision environments.

The Thoracic Trauma Index (TTI) can be defined as:

$$\text{TTI} = 1.4 * \text{AGE} + 0.5 * (\text{RIBg} + \text{T12}) * \text{MASS}/\text{MSTD} \quad (2)$$

Where AGE = age of the test subject in years,

RIBg = maximum absolute value of acceleration in g's of the 4^{th} and 8^{th} rib on the struck side,

T_{12g} = maximum absolute acceleration values in g's of the 12^{th} thoracic vertebra, in lateral direction,

MASS = test subject mass in kg

MSTD = standard reference mass of 75 kg.

The TTI is the acceleration criterion based on accelerations of the lower thoracic spine and the ribs. The TTI can be used as an indicator for the side impact performance of passenger cars. The specific benefit of the TTI is that it can be used to address the entire population of vehicle occupants because the age and the weight of the cadaver are included.

There is also a definition for the TTI that could be used for dummies without a specific age, called the TTI (d). It is defined for 50th percentile dummies with a mass of 75 kg:

$$TTI(d) = 0.5 * (RIBg + T12g) \quad (3)$$

The dynamic performance requirement, as stated in FMVSS 214 regulations of 1990, is that the acceleration on the structure shall not exceed 85 g for passenger cars with four side doors and 90 g for two side doors [17].

2.3 NHTSA/ Standard

The National Highway Traffic Safety Administration (NHTSA) is an agency of the Executive Branch of the U.S. government, part of the Department of Transportation. There are some of the important standards/regulations related to crash situations which are referred for the modeling and testing purpose. The Most common standard in US is FMVSS (Federal Motor Vehicle Safety Standards) regulations [17], and the other standards are ECE (Economic Commission of Europe) regulations in Europe, ARAI (Automotive Research Association of India), [12].

2.3.1 Federal Motor Vehicle Safety Standard (FMVSS 214)

The US dynamic side impact requirement, FMVSS-214, is used to evaluate the performance of passenger vehicles in car-to-car side crashes. FMVSS 214 was amended in 1990 to assure occupant in a dynamic test that simulates a severe right-angle collision. It is one of the most important and promising safety regulation issued by the NHTSA. It was phased into new passenger cars during model years 1994-97. In 1993, side impacts accounted for 33% of the fatalities to passenger car occupants. The current FMVSS 214 is a culmination of many years of research to make the passenger car less vulnerable in side impacts and especially to reduce fatalities risk to the nearside occupant, when a car is struck in the door area by another vehicle. This modeling protocol is more familiar than Insurance Institute for Highway Safety (IIHS), Side Impact Test Protocol, which is described in the next article, [17].

This study applied the FMVSS for modeling the impacter. The test configuration as specified by the National Highway Traffic Safety Administration (NHTSA) is shown in the next figure. Schematically, a moving deformable barrier (MDB) is shown impacting the side of a stationary vehicle at 54 km/h (33.5 mph). The MDB is towed at a crabbed angle of 27^{o} to its longitudinal axis. This configuration is intended to simulate a striking generic vehicle moving at 48.4 km/h, perpendicular to the side of the struck vehicle traveling at 24.2 km/h. The crabbed angle configuration allows the simulation of a two-vehicle side impact, both in motion condition, using a simplified test method where only one vehicle is in motion.

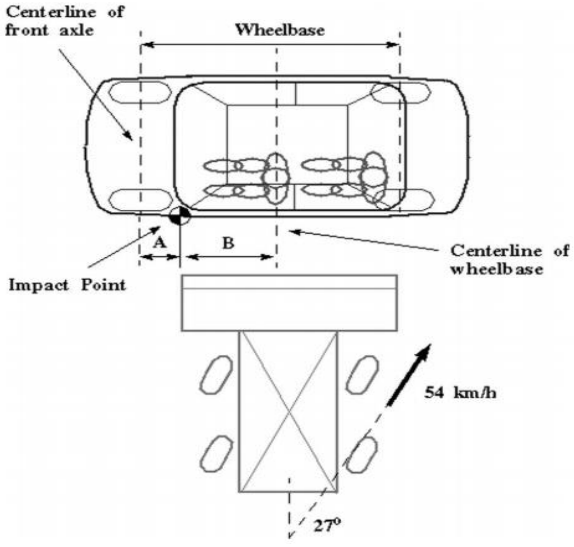

Figure 3 FMVSS - 214 test procedure [17]

The NHTSA MDB represents an average passenger vehicle in the US. The following figure shows the MDB's specifications. The MDB consists of the following components [17]:

- ✓ Main frame assembly
- ✓ barrier face
- ✓ Hub assembly
- ✓ Rear guide assembly
- ✓ Axle assembly

The geometrical specifications of the MDB are shown in the next figure.

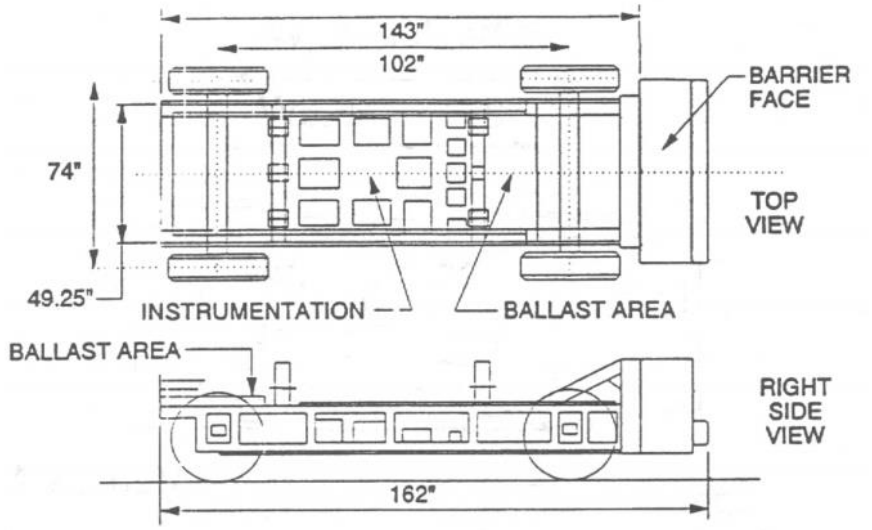

Figure 4 Moveable Deformable Barrier (MDB) specifications [17]

The barrier face specifications of the MDB are shown in the next figure.

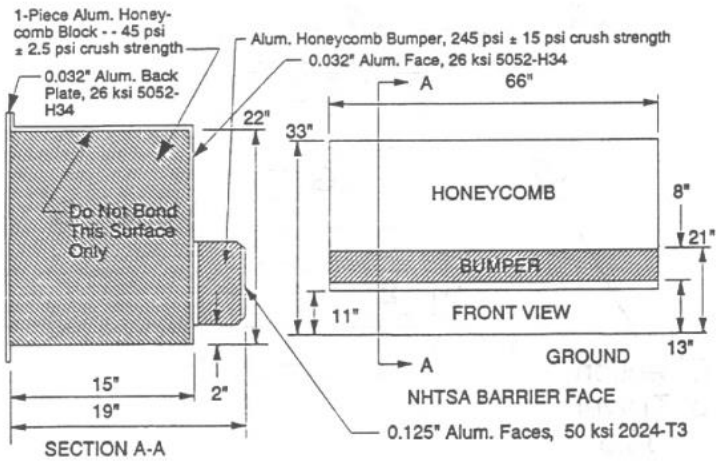

Figure 5 barrier face specifications [17]

2.3.2 Insurance Institute for Highway Safety (IIHS), Side Impact Test Protocol

The Institute's side impact test is relatively very severe. Given the design of today's vehicles, it is unlikely that people in real world crashes, as severe as this test would emerge uninjured. However, with good side impact protection, people should be able to survive crashes of this severity without serious injuries.

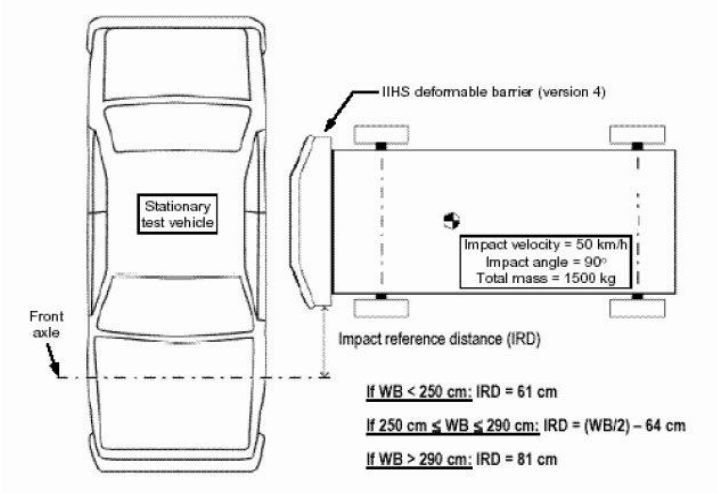

Figure 6 IIHS Test Configuration [14]

In this test procedure the crash is similar to the one used in Federal Motor Vehicle Safety Standard (FMVSS 214) but the wheels on the moving deformable barrier(MDB) are aligned with the longitudinal axis of the cart (zero degrees) to allow for 90 degree impact with velocity of 50 Kph(31 mph).

2.4 Requirements of side-Impact Beam

Federal Motor Vehicle Safety Standards (FMVSS) No. 214 establishes the minimum strength required for side doors of passenger cars. The side doors must be able to withstand an initial crush resistance of at least 2,250 pounds after 6 inches of deformation, and intermediate crush resistance of at least 3,500 pounds (without seats installed) or 4,375 pounds (with seats installed) after 12 inches of deformation. A peak crush resistance of two times the weight of the vehicle or 7,000 pounds whichever is less(without seat installed) or 3-1/2 times the weight of the vehicle or 12,000 ponds whichever is less(with seats installed) after 18 inches of deformation [13].

The major factors in considering the materials for the side door are load path and maximum resisting load of the door. The load carrying capacity and intrusion of the side door structure

mainly depends on mechanical properties, shape, size and thickness of its components. The proper combination of these features can dramatically change the behavior of the structure, providing an efficient design [12].

2.5 Collision Dynamic Modeling and Analysis Techniques

2.5.1 Finite Element Analysis

Simulation using finite element method comprises of three major phases:

- Pre-processing, in which the analyst develops a finite element mesh to divide the subject geometry into sub domains for mathematical analysis, and applies material properties and boundary conditions,
- Solution, during which the program derives the governing matrix equations from the model and solves for the primary quantities, and
- Post-processing, in which the analyst checks the validity of the solution, examines the values of primary quantities (such as displacements and stresses), and derives and examines additional quantities (such as specialized stresses and error indicators).

2.5.2 Various Crash Test

A crash test is a form of destructive testing usually performed in order to ensure safe design standards in crashworthiness and crash compatibility for various types of vehicle like small, medium and heavy duty and its related systems and components for the sake of getting the performance of the vehicle under the different conditions of crash at different angles with taking certain object like rigid wall, cables specially three-strand cable, concrete barriers, guardrail systems etc. It will be performed either by numerical simulations or experimentally. The following figure depicts different types of crash test generally used.

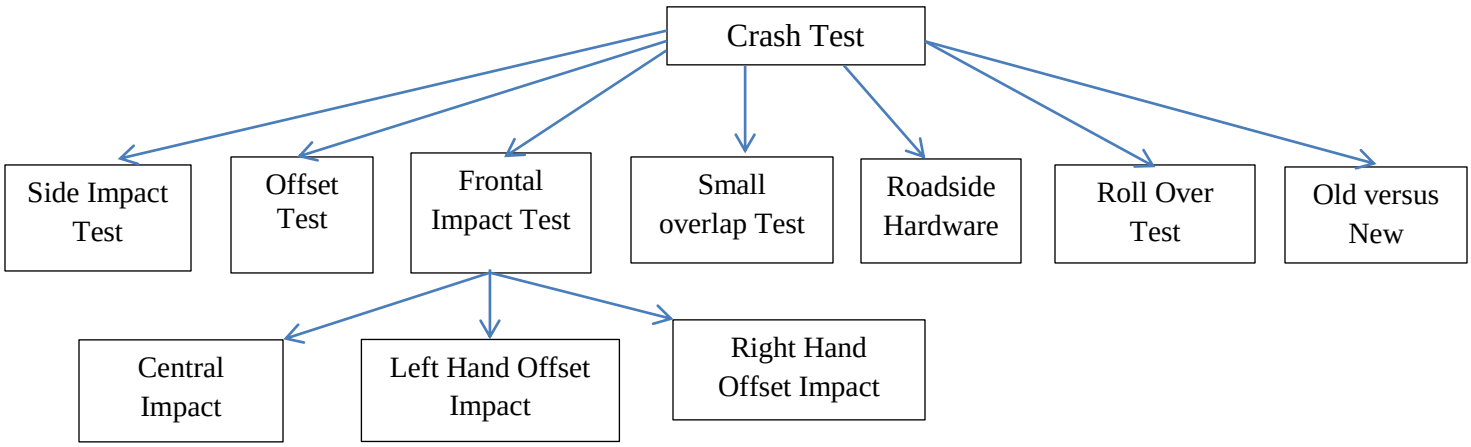

Figure 7 Classification of various crash test used in testing

- Side Impact Test- In this test sometimes the vehicle is in static condition or in dynamic and another vehicle or an object collide at the side surface having some speed.
- Offset Test- In this test only a part of front portion of the vehicle strikes on some barrier usually a vehicle at a given speed.
- Frontal Impact test- In this test a fully front structure of the vehicle collides with another object like another vehicle, rigid wall etc. at a given speed.
- Small Overlap Test- In this only a small portions of the vehicle strikes an object like tree, pole or if a car were to clip another. This situation loads a maximum value of force into the vehicle structure at a particular given speed. This test usually comprises of 15% to 20% of the front structure.
- Roll-Over Test- In this test a vehicle is in rollover condition having certain angle by which they tests ability (specifically the pillars holding the roof) to support itself in a dynamic impact. It is also done for the static crash testing condition.
- Roadside Hardware- These are performed to ensure that the crash barriers and crash cushions will protect vehicle occupants from roadside hazards.
- Old Versus New- In this an impact is done between old car against a new car and the big car against a small car; it is performed to show the advancements in crashworthiness.

2.5.3 Test Methodologies

Crush tests can be carried out in two conditions namely quasi-static and impact conditions.

1) Quasi-static Testing

In quasi-static testing, the test specimen is crushed at a constant speed. Quasi-static tests may not be a true simulation of the actual crash condition because in an actual crash condition, the structure is subjected to decreasing in crush speed, from an initial impact speed, finally to rest. Many materials used in designing crashworthy structures are rate sensitive. That means their energy absorption capability is dependent on the speeds at which they are crushed. So the determination of materials as good energy absorbers after quasi-statically testing them does not ensure their satisfactory performance as crashworthy structures in the event of an actual crash. The following are some advantages of quasi-static testing.

- ✓ Quasi-static tests are simple and easy to control.
- ✓ Impact tests require very expensive equipment to follow the crushing process because the whole crushing takes place in a split second. Hence quasi-static tests are used to study the failure mechanisms in composites, by selection of appropriate crush speeds.

The major disadvantage of quasi-static testing is that it may not be a true simulation of the actual crash conditions since certain materials are strain rate sensitive.

2) Impact Testing

The crushing speed decreases from the initial impact speed to rest as the specimen absorbs the energy. The major advantage of impact testing that it is a true simulation of the crash condition since it takes into account the stress rate sensitivity of materials. But the crushing process takes place in a fraction of a second. Therefore it is difficult to study the crushing unless provided with expensive equipment like a high-speed camera. This is one disadvantage of impact testing. This study applied this impact test with finite element analysis.

2.6 Energy Absorption in different materials

Steel has higher young's modulus, yet fails to absorb higher energy absorption. In composites, there are different kinds of fibers having different stiffness. For instance, carbon fibers are stronger than glass, yet glass fiber withstand load for a longer time than carbon fibers. The energy absorption capability of the composite materials offers a unique combination of reduced weight and improves crashworthiness of the vehicle structures [12, 15].

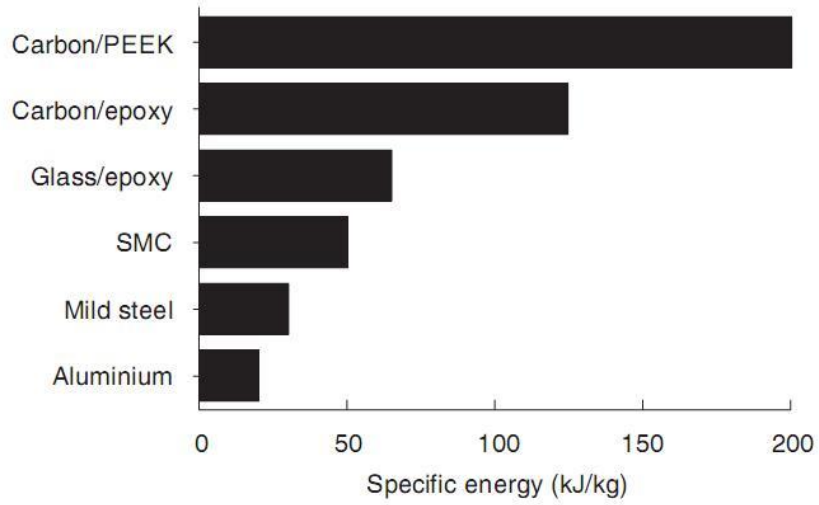

Figure 8 Specific Energy of some materials [12]

Factors on Energy Absorption of Composite Materials

The effect of a particular parameter (such as fiber type, matrix type, fiber orientation, specimen geometry, processing conditions, fiber content, test speed and test temperature) on the energy absorption of a composite material is summarized below [15].

Fiber Type: The density of the reinforced fibers has a lot to do with the energy absorption characteristics of a composite material. As the density of the fiber decreased from a higher to a lower value, the specific energy of the fiber reinforced tubes increased from a lower to a higher value respectively. Tubes reinforced with fibers having higher strain to failure result in greater energy absorption properties. Changes in fiber stiffness affect energy absorption capability less than changes in fiber failure strain provided the different materials crush in the same mode.

Matrix Type: If one is restricted to discussing the energy absorption capability of a reinforced fiber thermoplastic matrix material it could be concluded that a higher interlaminar fracture toughness, GIC, of the thermoplastic matrix material would increase the energy absorption capability of the composite material. Also an increase in matrix failure strain causes greater energy absorption capabilities in brittle fiber reinforcements. Conversely, the energy absorption in ductile fiber reinforcements decreases with increasing matrix failure strain. The role of thermosetting resin matrices in energy absorption is not clear and further studies are essential.

Fiber Orientation: Regarding the effects of fiber orientation on the energy absorption capability of a composite material, the fiber orientations that enhance the energy absorption capability of the composite material requires them to:

- Increase the number of fractured fibers.
- Increase the material deformation.
- Increase the axial stiffness of the composite material.
- Increase the lateral support to the axial fibers.

Specimen Geometry: Studying the effect of tube dimensions it can be said that the crush zone fracture mechanisms are influenced by the tube dimensions and these fracture mechanisms determine the overall energy absorption capability of the composite tubes. For a given fiber layup and tube geometry, the specific energy follows the order, circular> square> rectangle.

Processing Conditions: The cooling rate dependence of fracture toughness of semi-crystalline thermoplastic composite materials is the cause for variation in energy absorption capability with cooling rate. Fracture toughness increases with increase in cooling rate and hence causes an increase in the energy absorption capability. There has been no systematic study reported in literature on the effect of processing conditions on the energy absorption characteristics of thermoset composite tubes.

Fiber Content: There has been no systematic study reported in literature on the effect of fiber content on the energy absorption of composites. It should be noted that an increase in the fiber content might not always necessarily improve the specific energy absorption capability. As the fiber volume fraction increases, the volume of the matrix between the fibers decreases. This causes the interlaminar strength of the composite to decrease. As interlaminar strength decreases, interlaminar cracks form at lower loads, resulting in a reduction in the energy absorption capability. Also, as fiber volume fraction increases, the density of the composite increases which results in a lower energy absorption capability.

Test Speed: Upon reviewing the literature there seems to be a lack of consensus about the influence of test speed on the energy absorption. However it is known that energy absorption capability is a function of testing speed when the mechanical response of the crushing mechanism is a function of strain rate. The rate at which the structure is loaded has an effect on both the material's behavior and also the structural response of the target. The strain energy absorbing capabilities of the fibers and the geometrical configuration of the target are very important to the impact resistance of composites at low rates of strain. However the strain energy absorbing capabilities of the fibers and the geometrical configuration of the structure is less important at very high rates of strain since the structure responds in a local mode. What is important is the magnitude of energy dissipated in delamination, debonding and fiber pull out.

2.7 Common Material used for Side Crash Structures

These are some material found in the literature survey [3,5,8,12, 18] which is generally used in crash analysis of automobile components and the MDB. Specifically, for this study the materials related to component used are list and summarized as shown in the next table.

Table 1 Materials used in crash analysis

Material and their Specification		**Components**
Aluminum	AA 5182	Door trim
	Aluminum 5052-H34	NHTSA MDB_ Aluminum Face
	Aluminum 5052-H34	NHTSA MDB_ Aluminum Back
	Aluminum 2024-T3	NHTSA MDB_ Aluminum Face
Steel	A514	Beam support, door trim
	Steel 1006	Impact Beam
Composites	Carbon/PEEK	Impact beam
	Glass/PEEK	
	Carbon/PEI	
	Carbon/Epoxy	
	Carbon/PAS	
Honeycomb material	Honeycomb_245 Psi	NHTSA MDB_ Face
	Honeycomb_45 Psi	NHTSA MDB_ Main Block

Where, PEEK: polyetheretherkeetone, PEI: polyetherimide, PAS: polyarylsulfone,

2.8 Computer Aided Engineering (CAE) Tools used for Crash Analysis

Due to increasing cost on conducting real-time crash simulations, CAE tools are very widely used in auto industry. As a result, automakers have reduced product development cost and time while improving safety, comfort, and durability of the vehicles they produce. The predictive capability of CAE tools has progressed to the point where much of the design verification is now done using computer simulations rather than physical prototype testing. Tools used in this study are briefly explained below.

2.8.1 Ls-Dyna

LS-DYNA is a general-purpose, explicit finite element program used to analyze the nonlinear dynamic response of three-dimensional inelastic structures. Its fully automated contact analysis

capability and error-checking features have enabled users worldwide to solve successfully many complex crash and forming problems.

An explicit time integration scheme offers advantages over the implicit methods found in many FEA codes. A solution is advanced without forming a stiffness matrix (thus saving storage requirements). Complex geometries may be simulated with many elements that undergo large deformations. For a given time step, an explicit code requires fewer computations per time step than an implicit one. This advantage is especially dramatic in solid and shell structures. In extensive car crash, airbag and metal forming benchmark analyses, the explicit method has been shown to be faster, more accurate, and more versatile than implicit methods. LS-DYNA has over one hundred metallic and nonmetallic material models like Elastic, Elastoplastic, Elasto-viscoplastic, Foam models, Linear Viscoelastic, Glass Models, Composites, etc.

Some of the prime application areas of LS-DYNA are as follows:

- Crashworthiness simulations: automobiles, airplanes, trains, ships, etc
- Occupant safety analyses: airbag/dummy interaction, seat belts, foam padding, etc
- Biomedical applications.
- Bird strike
- Metal forming: rolling, extrusion, forging, casting, spinning, ironing, superplastic forming, sheet metal stamping, profile rolling, deep drawing, hydroforming (including very large deformations), and multi-stage processes.

2.8.2 Msc Patran

It is a finite element modeler used to perform a variety of CAD/CAE tasks including modeling, meshing, and post processing for FEM solvers LSDYNA, NASTRAN, ABAQUS Etc. Patran provides direct access to geometry from the world's leading CAD systems and standards. Using sophisticated geometry access tools Patran addresses, many of the traditional barriers to shared geometry, including topological incompatibilities, solid body healing, mixed tolerances, and others. MSC. Patran provides an open, integrated, CAE environment for multi-disciplinary design analysis. This feature can be used to simulate product performance and manufacturing process early in the design-to-manufacture process.

2.8.3 Madymo

MADYMO (MAthematical DYnamical MOdels) is a general-purpose software package, which can be used to simulate the dynamic behavior of mechanical systems. Although originally developed for studying passive safety, MADYMO is now increasingly used for active safety and general biomechanics studies. It is used extensively in industrial engineering, design offices, research laboratories and technical universities. It has a unique combination of fully integrated multi body and finite element techniques. MADYMO offers in addition to standard output quantities, the possibility to calculate injury parameters like femur and tibia loads, Head Injury Criterion (HIC), Gadd Severity Index (GSI), Thoracic Trauma Index (TTI) and Viscous Injury Response (VC). Special output can be obtained through user-defined output routines. Results of the simulation are stored in a number of o/p files, to be accessible by post-processing programs.

2.8.4 Easi Crash Dyna (ECD)

EASI CRASH DYNA is the first fully integrated simulation environment specially designed for crash engineering requiring large manipulation capability. It can directly read files in IGES, NASTRAN, PAM-CRASH, MADYMO and LSDYNA data. ECD has unique features, which enable the crash simulation more realistic and more accurate.

2.8.5 Easi-Crash Mad

EASi-CRASH is based on EASi's 20+ years of practical experience in crash simulations. It greatly enhances the simulation process by allowing concurrent access to the model and simulation results. Animation, visualization and synchronized curve plotting make EASi-CRASH MAD a high performance CAE environment.

This study applied the Ls-Dyna explicit finite element since it has a capability for crashworthiness simulation and also available in ANSYS workbench.

2.9 Implicit and Explicit Philosophy

Most software's would normally solve the dynamic equilibrium equation in an implicit approach however the foremost widespread approach that ought to be used for highly non-linear issues is to use explicit(specific) time integration scheme like a central difference scheme.

- **Implicit:** A global stiffness matrix is computed, inverted, and applied to the nodal out-of-balance force to obtain a displacement increment. The advantage of this approach is that time step size may be selected by the user. The disadvantage is the large numerical effort required to form, store, and factorize the stiffness matrix. Implicit simulations therefore typically involve a relatively small number of expensive time steps.
- **Explicit:** Internal and external forces are summed at each node point, and a nodal acceleration is computed by dividing by nodal mass. The solution is advanced by integrating this acceleration in time. The maximum time step size is limited by the Courant condition, producing an algorithm which typically requires many relatively inexpensive time steps. There are several benefits of such a procedure and therefore the most significant is that it results in an algorithmic programmed which may be simplified programmed, does not need any matrix operation procedure and more is very appropriate for a quick parallel computing methodology.
- **Comparision of explicit and implicit**

  The explicit method requires short time step for an accurate solution, whereas the implicit method can give reliable results with large time steps. The implicit methods are unconditionally stable, whereas the explicit methods are mostly conditionally stable. In implicit method contact cannot be easily controlled.

2.10 Common Element used in Crash FE Analysis

- Shell element- Quadrilateral, Triangular, Belytschko-Lin-Tsay shell element
- Beam element- Hughes-Liu beam element
- Hexahedron element
- Solid element

Chapter Three

3 Research Methods, Materials and Procedures

3.1 Modeling of side-impact Components

Information related to geometry and material for side crash components are collected in Yangfan (Lifan Motor) offices, garage and spare parts. Two basic components for energy absorption of side impact are impact beam and impact beam support. They are constructed from steel 1006. Their basic geometries are shown in the next drawings. All dimensions are in mm.

3.1.1 Modeling of Side Impact Beam

The present impact beam for Lifan-520 is a circular tube which constructed from steel 1006 as shown below.

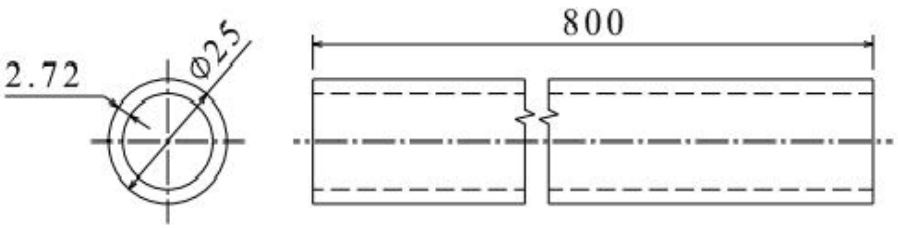

Figure 10 Side Impact Beam

3.1.2 Side-impact Beam Supporter

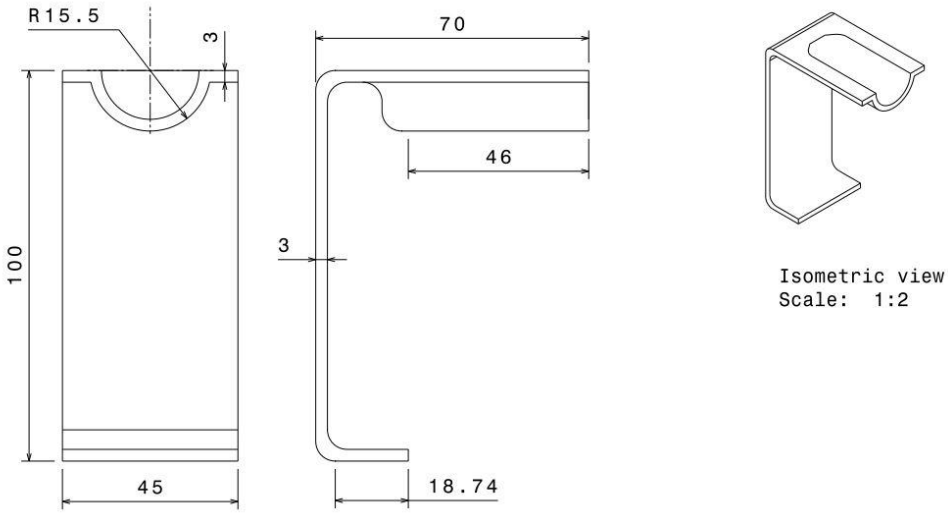

Figure 11 Side-impact Beam Supporter

3.1.3 Front -door Trim

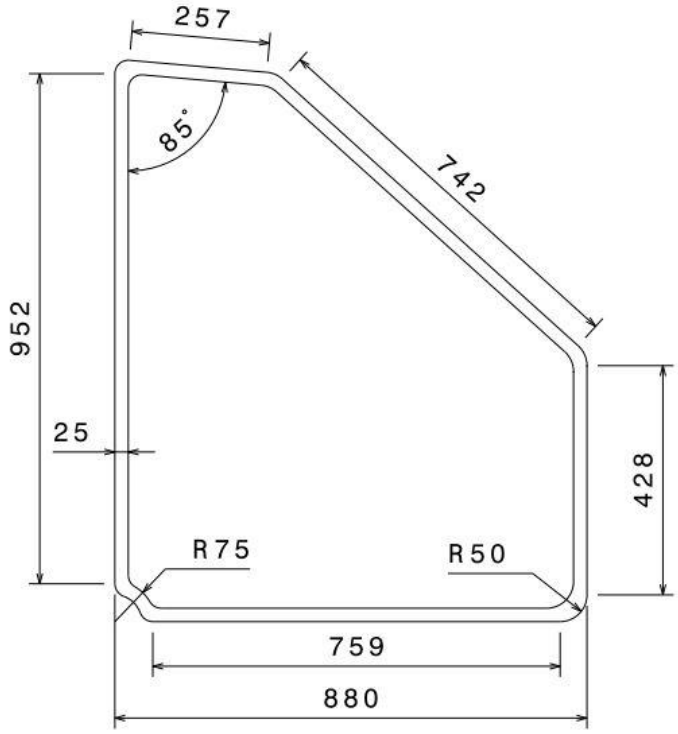

Figure 12 Front -door trim

3.1.4 Rear-door Trim

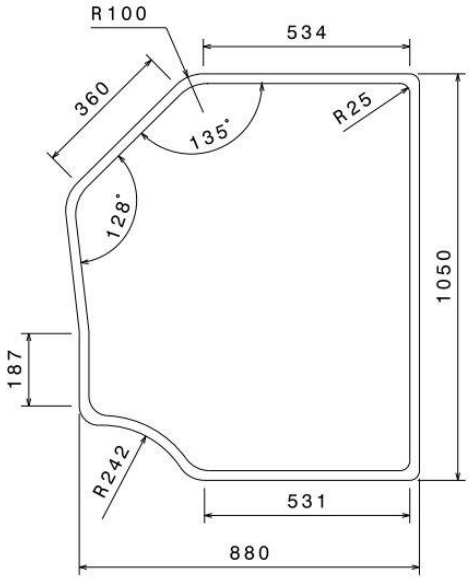

Figure 13 Rear-door Trim

3.1.5 Assembly of side impact structure

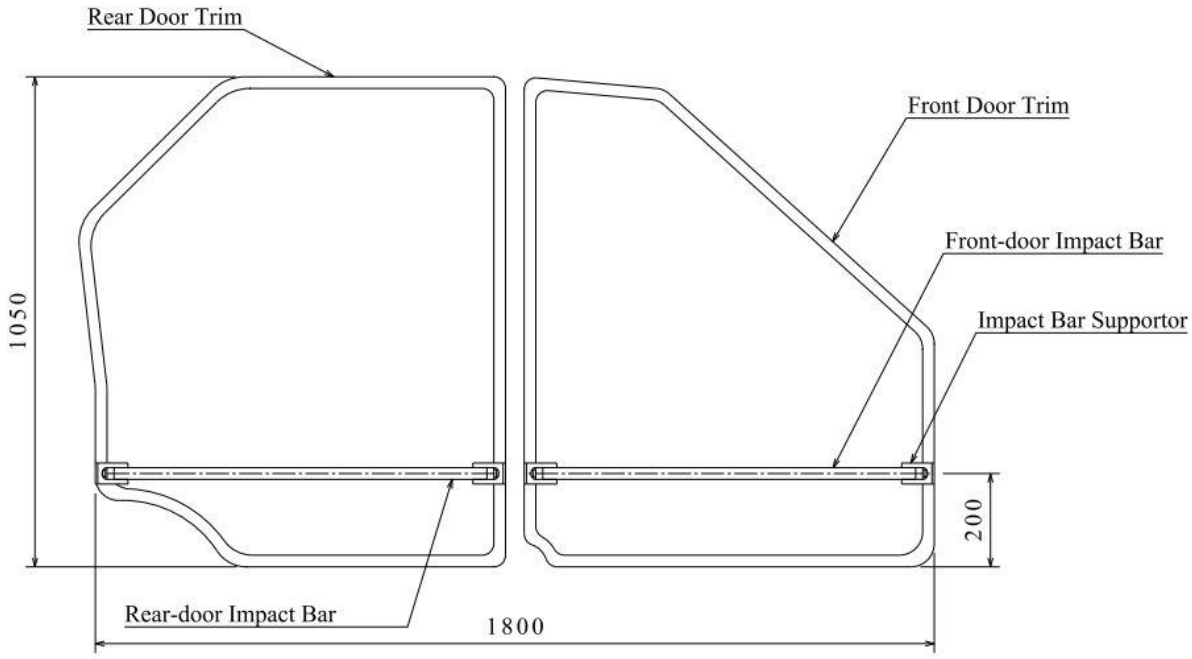

Figure 14 Assembly of side impact structures

3.2 Side Impacting Protocol Modeling

Some institute generated a crash modeling for side impact. This research applies the test configuration as specified by the NHTSA (National Highway Traffic Safety Administration). The model is prepared with the help of CATIA V5. The assembly drawing with section-view, the overall assembly drawing and bill of materials for the model is shown in the next figures.

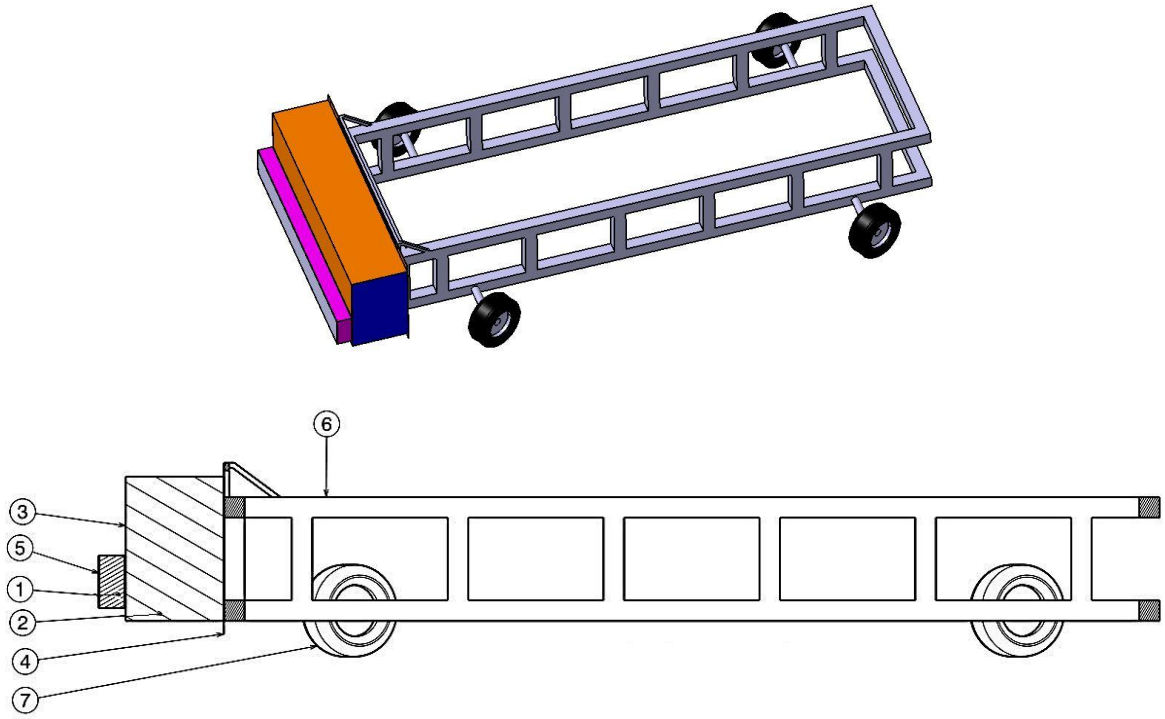

Figure 15 Side impact protocol NHTSA MDB

Table 2 Bill of Materials

No.	Part Name	Quantity	Material	Remark
1	NHTSA MDB_ Face Bumper	1	Honeycomb_1.67 MPa	
2	NHTSA MDB_ Honeycomb Main Block	1	Honeycomb_0.31 MPa	
3	NHTSA MDB_ 0.032 Aluminum Face	1	Aluminum 5052-H34	0.8128 mm thickness
4	NHTSA MDB_ 0.032 Aluminum Back	1	Aluminum 5052-H34	0.8128 mm thickness
5	NHTSA MDB_ 0.125 Aluminum Face	2	Aluminum 2024-T3	3.175 mm thickness
6	NHTSA MDB_ Base Frame	1	Steel 1006	
7	Tyre Rim	4	Aluminum 5454	

All the components of MDB are model in CATIA V5 with their geometrical specification. Their intended volume is measured/calculated form the model. The mass of each component is calculated by multiplying their volume with their density. Then the overall mass is gained with the summation of each specified component's mass. All calculation results are summarized in the next table. The total mass became approximately 1368 Kg.

Table 3 Calculation of total mass of the modeled MDB

No.	Part Name	Quantity	Material	Density [Kg/m^3]	Volume [m^3]	Mass [Kg]
1	NHTSA MDB_ Face Bumper	1	Honeycomb_1.67 MPa	85	0.034	2.89
2	NHTSA MDB_ Honeycomb Main Block	1	Honeycomb_0.31 MPa	26.2	0.356	9.32
3	NHTSA MDB_ 0.032 Aluminum Face	1	Aluminum 5052-H34	2680	0.0016	4.36
4	NHTSA MDB_ 0.032 Aluminum Back	1	Aluminum 5052-H34	2680	0.0018	4.83
5	NHTSA MDB_ 0.125 Aluminum Face	2	Aluminum 2024-T3	2780	0.00088	4.90
6	NHTSA MDB_ Base Frame	1	Steel 1006	7896	0.153	1208
7	Tyre Rim	4	Aluminum 5454	2785	0.012	133.68
Total Mass [Kg]						**1367.8**

All material properties for the component are listed in the material property APPENDIX A.

The MDB had modeled to have a track width of, 1880mm, wheelbase of 2,591 mm and the following center of gravity and moment of inertia with the same as mentioned in [13].

Table 4 Center of gravity and moment of inertia of MDB

Center of gravity			**Moments of inertia**		
X	Y	Z	Pitch	Roll	Yaw
1121 mm rear of front axle	5 mm left of longitudinal center	500 mm from the ground	2263 Kg-m^2	508 Kg-m^2	2572 Kg-m^2

3.3 Designing of Impact Beams

The alternative geometries for impact beam are generated with inserting different rib structures inside the circular tube. The circular tube has the same external diameter with the present Lifan-520 model which is 25 mm. The thicknesses of circular tubes are depending on the rib geometries and structures. This study applies the following concepts for searching which type of rib structure and arrangement are better for crashworthiness having equivalent volume with the existed impact beam.

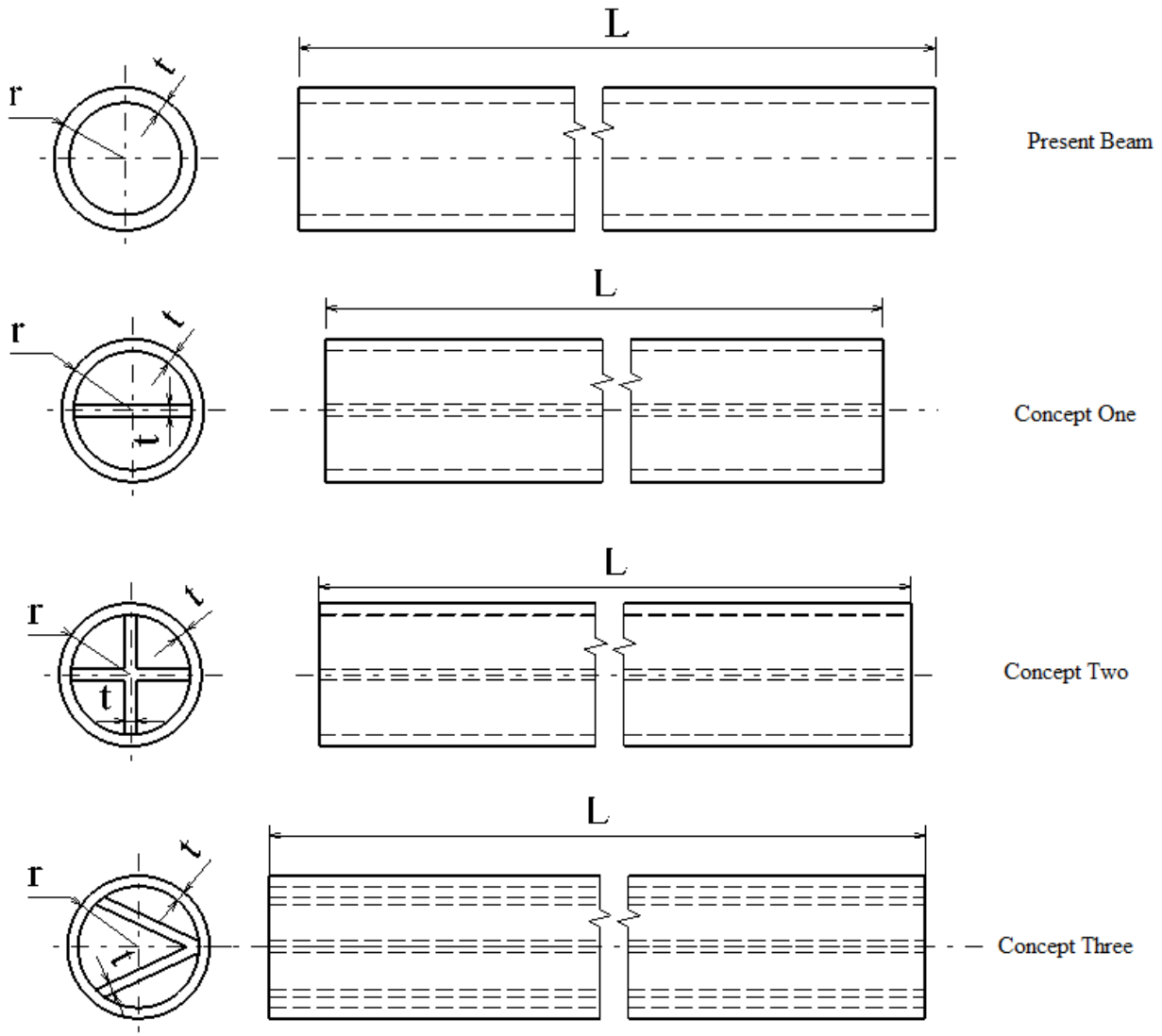

Figure 16 Alternative Geometry of impact beam

The equivalent thickness of each concept was analyzing by considering having the same cross-sectional area and volume with the present beam. The following table summarized the parameters intended for the new concept models and present beam structure.

Table 5 Calculation of thickness for each concept

	Reference (Present Model)	**Concept One (Model One)**	**Concept Two (Model Two)**	**Concept Three (Model Three)**
Profile	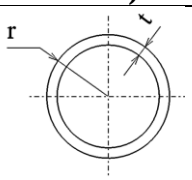	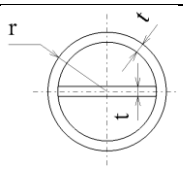	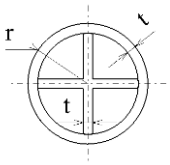	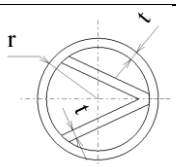
Radius (r), [mm]	25	25	25	25
Length (L) [mm]	800	800	800	800
Cross-sectional Area (A) [mm^2]	190.38	190.38	190.38	190.38
Volume (V) [mm^3]	152308.4	152308.4	152308.4	152308.4
Equivalent Thickness (t) [mm]	$A = \pi(r^2 - (r-t)^2)$	$A = \pi(r^2 - (r-t)^2) + 2t(r-t)$	$A = \pi(r^2 - (r-t)^2) + t(4r - 5t)$	$A = \pi(r^2 - (r-t)^2) + (r-t)(r - 1.41t)$
	$190.38 = \pi(12.5^2 - (12.5 - t)^2)$	$190.38 = \pi(12.5^2 - (12.5 - t)^2) + 2t(12.5 - t)$	$190.38 = \pi(12.5^2 - (12.5 - t)^2) + t(50 - 5t)$	$190.38 = \pi(12.5^2 - (12.5 - t)^2) + (12.5 - t)(12.5 - 1.41t)$
	$\gg \ t = 2.72$	$\gg \ \boldsymbol{t = 2.06}$	$\gg \ \boldsymbol{t = 1.66}$	$\gg \ \boldsymbol{t = 1.72}$

The orientation of rib arrangement will have some variation. This study only applied the ribbed position as shown in the previous table.

3.4 Material for impact beam

Once the geometries are decided, the next step is to find a material that has higher energy absorption for the impact beams. Materials have a great role in the crashworthiness improvement of structures. Steel sheet has been used in vehicle side impact beam more than a century. Its low production cost, consistent properties and being familiar for production make it chosen for as impact structure. Steel 1006 material is the present material used for present impact beam of Lifan-520, and its property is shown in the material property APPENDIX A.

In recent time, the lightweight materials are chosen for minimizing fuel consumption. This study searches for good material to absorb the energy form the impact vehicle. The high energy absorption property of carbon/Epoxy and Carbon/PEEK material took the attention of this study. As previously mentioned in detail from the literature topic, the energy absorption of composite material are depend on fiber type, matrix type, fiber orientation, processing condition, and fiber contents. This research applied Carbon-IM10 for composite fiber and Epoxy-8552 and Teca-PEEK for matrix of composite which are commercially available and having good energy absorption properties rather than steel. For both composites, the fibers are aligned parallel to tube axis and the process condition is rapidly cooled. The proper amount of fiber contents for better energy absorption is not clearly shown in literatures. But some researchers [15] conducted some experiment on the volume fraction of 0.35, 0.4, 0.45, and 0.5 and among them, 0.4 volume fraction was recommended as better energy absorber. This study applied the volume fraction of 0.4 for the composites.

This study took the intended material properties from the literatures. But there were some difficulties to find all material properties within a literature. This study filled those gaps by searching those properties from different literature and also by applying matrix compositions rule as shown in composite property APPENDIX B. The material specifications which used in this study are shown in the material property APPENDIX A. The total mass of impact beams can be summarized as shown in the next table. Since, the volume of all beams are the same (V=152308 mm^3), the only variation is due to their density (ρ=7896, 1580 and 1419 Kg/ m^3 for steel 1006, carbon/Epoxy and Carbon/PEEK, respectively). Their intended mass is then m = 1.2026 Kg, 0.2406 Kg and 0.2161 Kg for steel 1006, Carbon/Epoxy, and carbon/PEEK, respectively.

3.5 Impact Mechanics

In the impact theory, it is important to distinguish between elastic and plastic impacts. In elastic impact a negligible amount of energy is lost between impacting bodies. A plastic impact involves a significant amount of energy dissipated during collision. An impact between two vehicles is one example of an elasto-plastic impact.

A principle of energy conservation in the elastic impact is used; the kinetic energy before impact is conserved and converted to elastic energy and the kinetic energy of the Moving Deformable Barrier (MDB) and the automobile at its maximum deflection, i.e.,

$$0.5m_Av^2_A = 0.5K_{eq}\delta^2_{max} + 0.5m_Bv^2_0 \quad (4)$$

Where, m_A is the mass of the impactor (MDB), m_B the mass of vehicle, v_A the velocity of the impactor before impact and v_0 the final velocity of the impactor, δ_{max}, vehicle in maximum deflection point, K_{eq} is an inherent characteristics of a material which depends on the reaction force and deflection of impact beam.

An important consideration of momentum is that it can be neither created nor destroyed. Thus, the momentum before an impact is equal to the momentum after the impact. At the moment of its maximum deflection, a principle of momentum conservation before and after impact can be expressed as follows:

$$m_Av_A = (m_A + m_B)v_0 \quad (5)$$

By combining the above two equations δ_{max} is obtained as follows

$$\delta_{max} = \sqrt{\frac{1}{K_{eq}}\frac{m_A m_B}{m_A + m_B}v_A^2} \quad (6)$$

After separation point, the conservation of energy and momentum equation can be expressed as follows:

$$0.5m_Av^2_A = 0.5m_Av^2_{A2} + 0.5m_Bv^2_{B2} \quad (7)$$

$$m_Av_A = m_Av_{A2} + m_Bv_{B2} \quad (8)$$

where v_{A2} and v_{B2} are the final velocities of the impactor and the vehicle, respectively in separation point. In the elasto-plastic impact, the principle of linear momentum conservation satisfies, since impact forces are equal and opposite.

$$m_A v_{A+} m_B v_B = m_A v_{A2} + m_B v_{B2} \quad (9)$$

In this case, the velocities after impact may be determined with the coefficient of restitution (COR). The coefficient of restitution is the ratio of speed of separation to speed of approach in a collision.

$$\mathrm{COR} = \frac{v_{B2} - v_{A2}}{v_A - v_B} \quad (10)$$

An object with a COR equals to 1 collides elastically, while an object with a COR of 0 will collide inelastically, effectively sticking to the object it collides with, not bouncing at all. The coefficient of restitution is a number which indicates how much kinetic energy (energy of motion), remains after a collision of two objects. If the coefficient is high, it means that very little kinetic energy was lost during the collision. If the coefficient is low, it indicates that a large fraction of the kinetic energy was converted into the heat or was otherwise absorbed through deformation.

The energy dissipating can be found by subtracting the kinetic energy of the two masses after impact, and the kinetic energy of the impactor before impact.

$$E_{plastic} = 0.5(m_A v^2_A + m_B v^2_B - m_A v^2_{A2} - m_B v^2_{B2}) \quad (11)$$

3.6 Specific Energy Absorption E_s

Specific energy absorption, ES, is defined as the energy absorbed per unit mass of material.

$$W = \int_0^{S_b} P dS \tag{12}$$

Where, W is the total energy absorbed in crushing of specimen. A more characteristic property of progressive crushing mode is

$$W = \int_{S_i}^{S_b} P dS = \bar{P}\,(S_b - S_i) \tag{13}$$

Where, S_b and S_i are the crush distances intervals and $\bar{P}$ is the mean crush load. The specific energy absorption capability, E_S, of a material defined as the energy absorbed per unit mass of material is given by

$$E_s = \frac{W}{m} \tag{14}$$

Combining the above two equations we get

$$E_s = \frac{W}{m} = \frac{\bar{P}\,(S_b - S_i)}{V\rho} \tag{15}$$

Where, V is the volume of the crushed portion of the specimen and ρ is the density of the material. We can also write

$$E_s = \frac{W}{m} = \frac{\bar{P}\,(S_b - S_i)}{V\rho} = \frac{\bar{P}\,(S_b - S_i)}{AL\rho} \tag{16}$$

Where, A and L are the cross sectional area and length of the crushed portion of the specimen respectively.

$$E_s = \frac{\bar{P}\,(S_b - S_i)}{AL\rho} = \frac{\bar{P}\,S_b}{AL\rho} \tag{17}$$

If S_i is much less than S_b, the ratio $(S_b / L) = K$ is a measure of the collapsibility of the specimen. Substituting $(S_b / L) = K$ in the above equation we have

$$E_s = \frac{\bar{P}\,K}{A\rho} = \frac{\bar{\sigma}\,K}{\rho} \tag{18}$$

Where, $\bar{\sigma}$, is the mean crush stress.

3.7 Finite Element Modeling

The principle of virtual work can be used to derive the governing equations in finite element model which stated that the work done by the external loads is equal to the work done by internal loads. The principle of virtual work can be applied to both linear and no-linear problems. Applying this principle to a finite element with elemental volume (V_e), it can be formulated as follows:

$$\Delta(U_{int})e_v = \Delta(W_{ext})e_v \quad (19)$$

Where $\Delta(U_{int})e_v$ and $\Delta(W_{ext})e_v$ are rate of work done by internal force and external force on elemental volume, respectively. Special approximation using finite element method and time approximation where the ordinary differential equations are further approximated in time are computed by reaching the dynamic equilibrium equation at the end of every time step can be expressed as follows.

$$[M]\left\{\frac{d^2X}{dt^2}\right\} + c\left\{\frac{dX}{dt}\right\} + k\{X\} = \{F_{ext}(t)\} \quad (20)$$

Where M= mass matrix, C= damping matrix, K= stiffness matrix, F_{ext} = external force, t = time. Crash analysis requires a dynamic analysis formulation and also a non-linear transient dynamic explicit type of finite element analysis. The non-linear describes the relation between the applied condition and the result of its effect. In most crash scenarios large amount of plastic deformation occurs which by itself needs a non-linear investigation. In crash conditions, the time frame is short and the analysis is highly dynamic.

Explicit finite element model has been found as outstanding tool to solve complex tasks that include large deformation of structures, great inertial effects and analysis of contact is developed in several algorithms which makes it much easier to perform and control the response than in implicit solver. Explicit Finite Element Method is based on Central Difference Method.

In Explicit time integration schemes above equation can be written as:

$$[M]\left\{\frac{d^2X}{dt^2}\right\}_n + c\left\{\frac{dX}{dt}\right\}_n + k\{X\}_n = \{F_{ext}(t)\}_n \quad (21)$$

Where 'n' represents a time level index. Physically it refers to:

$$\text{Inertial force} + \text{Damping force} + \text{Stiffness force} = \text{External force} \quad (22)$$

Using second order accurate Explicit Central Difference Operator $\left\{\frac{dX}{dt}\right\}_n$ and $\left\{\frac{d^2X}{dt^2}\right\}_n$ can be expressed as

$$\left\{\frac{dX}{dt}\right\}_n = \frac{\{X\}_{n+1} - \{X\}_{n-1}}{2\Delta t} \quad (23)$$

$$\left\{\frac{d^2X}{dt^2}\right\}_n = \frac{\{X\}_{n+1} - 2\{X\}_n + \{X\}_{n-1}}{\Delta t^2} \quad (24)$$

Substituting and rearranging equation (23) and (24) into equation (20), the final governing equation for crash analysis can be obtained as:

$$\frac{1}{\Delta t^2}[M] + \frac{1}{2\Delta t}[C]\{X\}_{n+1} = \{F_{ext}\}_n - \{F_{int}\}_n + \frac{1}{\Delta t^2}[M][2\{X\}_n - \{X\}_{n+1}] + \frac{1}{2\Delta t}[C]\{X\}_{n-1} \quad (25)$$

Time increment in dynamic explicit is as follows

$$t^{n+1/2} = {}^1/_2\,(t^{n+1} + t^n) \quad (26)$$

$$\Delta t^n = t^{n+1/2} - t^{n-1/2} \quad (27)$$

$$t^{n+1} = t^n + \Delta t^{n+1/2} \quad (28)$$

The velocity and displacement vector can be obtained as follows.

$$v^{n+1/2} = \frac{x^{n+1} - x^{n+1}}{\Delta t^{n+1/2}} \quad (29)$$

$$x^{n+1/2} = v^{n+1/2}\Delta t^{n+1/2} + x^n \quad (30)$$

$$a^n = \frac{v^{n+1/2} - v^{n-1/2}}{t^{n+1/2} - t^{n-1/2}} \quad (31)$$

Acceleration at a^{n+1} can be calculated by

$$a^{n+1} = m^{-1}\left(f_{ext}^{n+1} - f_{int}^{n+1} - Cv^{n+1/2}\right) \quad (32)$$

Where, C is damping factor and f_{ext} *and* f_{int} are, external force and internal force, respectively.

The general working principle of explicit dynamics can be summarized in the next chart [19].

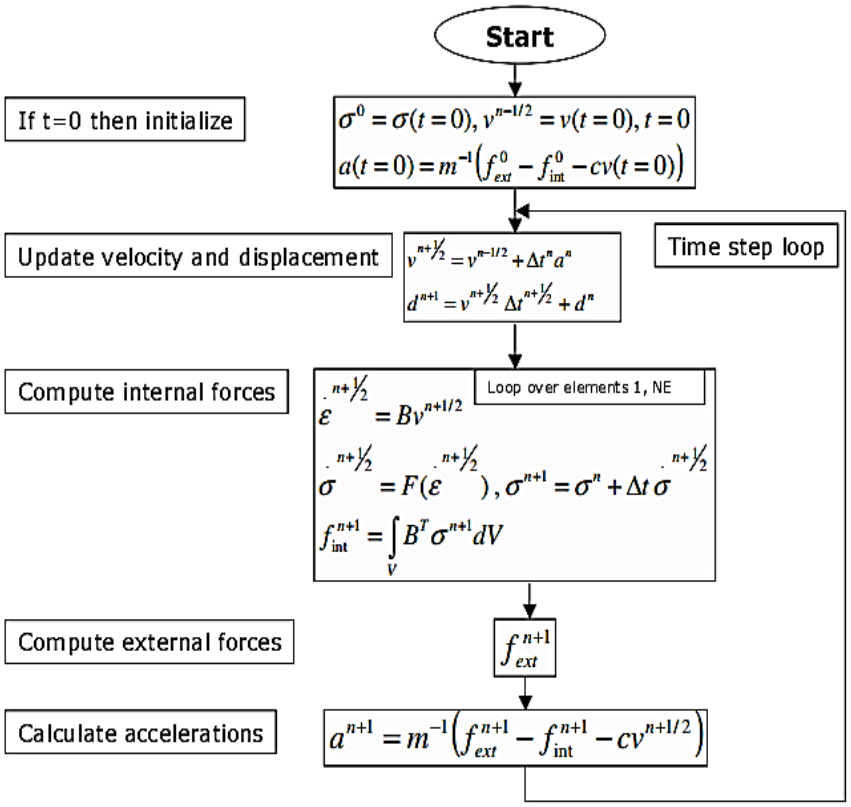

Figure 17 Flow chart of Explicit Dynamics

Finite Element Method Computational Analysis Procedure

ANSYS LS-DYNA is a non-linear transient dynamic finite element program that planned to solve short duration dynamic problems. This study used the explicit dynamic analysis system of ANSYS R15 workbench for solving the impact analysis. The overall procedures of FEM analysis for this study after selecting explicit dynamics from ANSYS workbench are summarized as follows.

a) **Adding materials in Engineering Data**:

All materials used for the assignment of each component of Moving Deformable Barrier and vehicle impact structures are added in material library. All properties of material are filled with their specific units (if having) from engineering data toolbox. Properties of each material used for this study are shown in the material property APPENDIX A.

b) **Importing Geometries:**

The assembled model of impact structures and Moving Deformable Barrier with the format of IGS file is imported into Geometry workbench and aligned to with global coordinate system. And also the impact beam surfaces were generated for the compatibility of shell element type in the analysis.

c) **Assigning intended material for each component:**

The perspective material for each component was assigned from the Model workbench

d) **Defining the connections and contacts**

The contact interaction among the component of Moving Deformable Barrier was defined as bonded/un-bonded based on the NHTSA-MDB criteria. The failure of the connection (spot-welded type) between the beam tube and rib is taken as negligible and it is supposed that any set of parts is constrained to each other in all degree of freedom without modeling the mechanical strength of the coupled part. This also was taken for the connection between the tube and beam support.

e) **Meshing**

The meshing element size for the MDB is set to be 55 mm as recommended with NHTSA. Since the average thickness of impact beams are smaller than the other

dimension of the part, the best meshing for the element was the shell element with the type of four node-quadrilateral element, Belytschko-Lin-Tsay is applied.

The meshed model and statistics for the parts of model are attached in the meshing APPENDIX C. The statistics of mesh is shown in the next table,

Table 6 Meshed statistics for the parts of model

	MDB	Present Model	Model One	Model Two	Model Three	Beam Support
Number of Element	39,537	11,318	14,856	17,292	16,686	12,080
Number of Node	16,801	19,723	28,396	30,006	32,092	3,380

f) Assigned initial velocity of MDB

The initial velocity of moving deformable barrier (MDB) was assigned to be 15 m/s for all analysis with the perspective direction of collision as ruled by NHTSA.

g) Setting the Analysis

Maximum number of cycles and end time for analysis were assigned to be 10^7 and 0.08 s, respectively. Normally, the number of cycle depends on the time increment/step which by itself depends on the number of element size and material properties. Small numbers of elements end up faster than large amount element size. Most side impact analysis taken assigned to be 0.1 s. In this study 0.08 s was enough for the end of collisions.

h) Assigning Boundary Condition

This study applied the boundary condition to the impact beam to be fixed at the contact surface between the beam and its supports. The geometry for present type of supports (as taken from Lifan-520 model) is supposed to be support for all models. The MDB wheels are assigned to constrain in the vertical direction, they are allowed to free in the horizontal movement.

i) Solve/Run the Analysis

Once all necessary input parameters are set, the analysis was run and information related to collision dynamic is recorded with figures, chart and also exporting in excel files. Generally, this study conducted 12 explicit dynamics analysis with the combination of four models and three materials. Those analyses are summarized as shown in next table.

Table 7 Conducted Analysis with material and model combination

Analysis	Material	Model
Analysis One	Steel 1006	Present Model
Analysis Two	Steel 1006	Model One
Analysis Three	Steel 1006	Model Two
Analysis Four	Steel 1006	Model Three
Analysis Five	Carbon/Epoxy	Present Model
Analysis Six	Carbon/Epoxy	Model One
Analysis Seven	Carbon/Epoxy	Model Two
Analysis Eight	Carbon/Epoxy	Model Three
Analysis Nine	Carbon/PEEK	Present Model
Analysis Ten	Carbon/PEEK	Model One
Analysis Eleven	Carbon/PEEK	Model Two
Analysis Twelve	Carbon/PEEK	Model Three

Chapter Four

4 Result and Discussion

The results generated from the LS-DYNA analysis with the help of ANSYS R15 of Explicit Dynamics is summarized in the following subtopics. Three materials (Steel 1006, Carbon/Epoxy and Carbon/PEEK) were assigned for each concept/model of impact beam. The result from the analysis includes total deformation, total acceleration, and internal energy for each of impact beams. The equivalent stress (Von-Mises stress) is attached at the stress APPENDIX D. The results are shown with help of figures which were taken from the ANSYS modeling workbench and with graphs which were exported from ANSYS workbench results in the excel file format. The intended geometry specifications of the four models are as shown in the next table.

Table 8 Geometry Specification of models

	Present Model	**Model One**	**Model Two**	**Model Three**
Profile	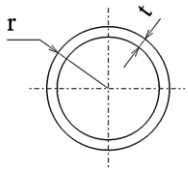	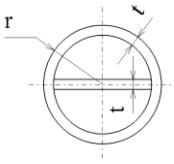	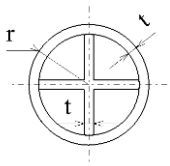	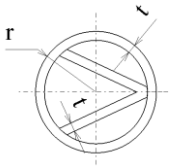
Radius (r), [mm]	25	25	25	25
Length (L) [mm]	800	800	800	800
Thickness (t) [mm]	$\gg \ t = 2.72$	$\gg \ t = 2.06$	$\gg \ t = 1.66$	$\gg \ t = 1.72$

The assigned materials are also shown in the following table.

Table 9 Assigned materials for models

Present Material	**Material One**	**Material Two**
Steel 1006	Carbon/Epoxy	Carbon/PEEK

4.1 Deformation

4.1.1 Total Deformation of Present Material (Steel 1006) Beam

The deformation of each impact beam when the Steel 1006 material assigned is shown in the next figures.

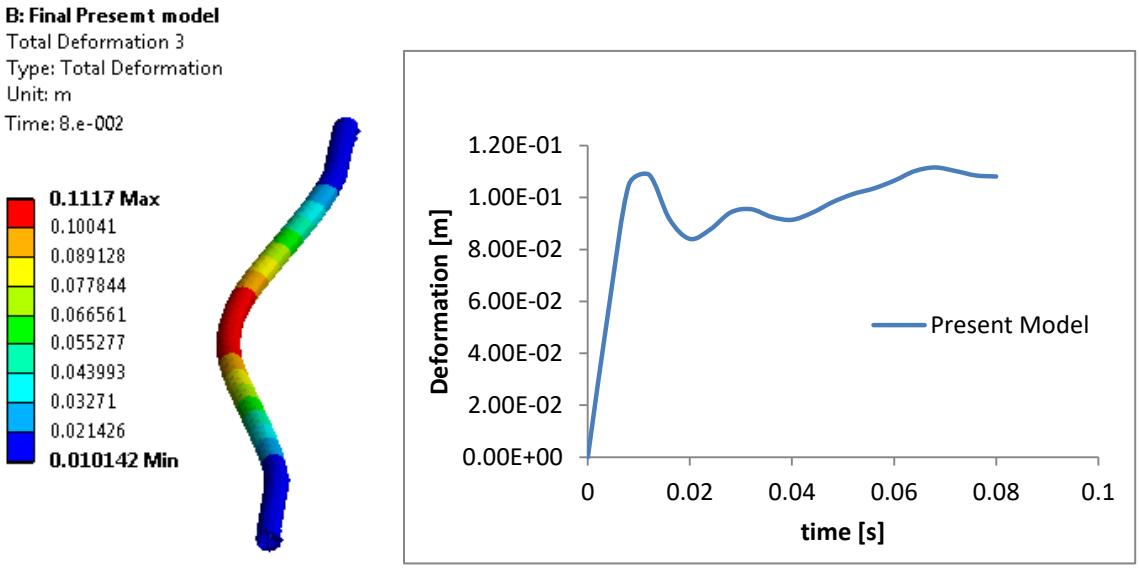

a)

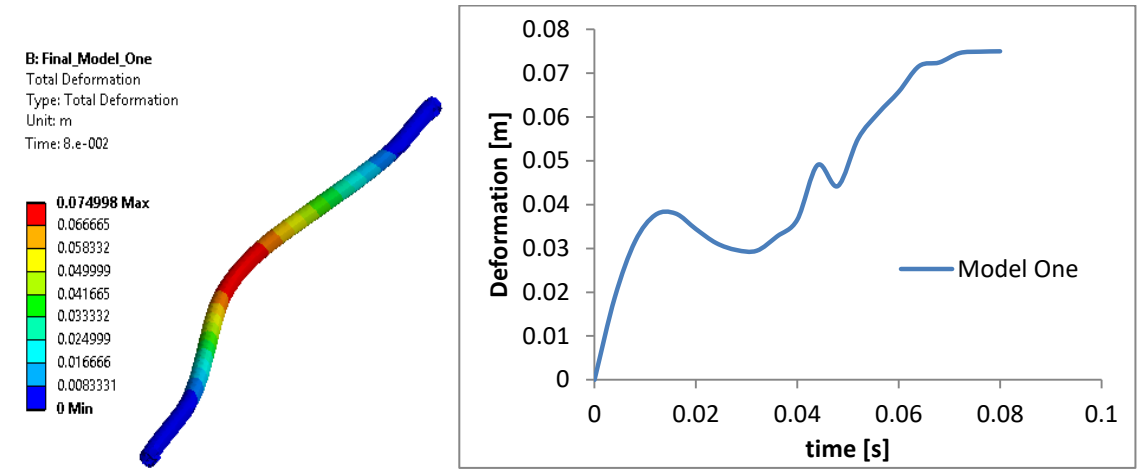

b)

Figure 18 Total deformation in Steel 1006 beam a) Present Model b) Model One

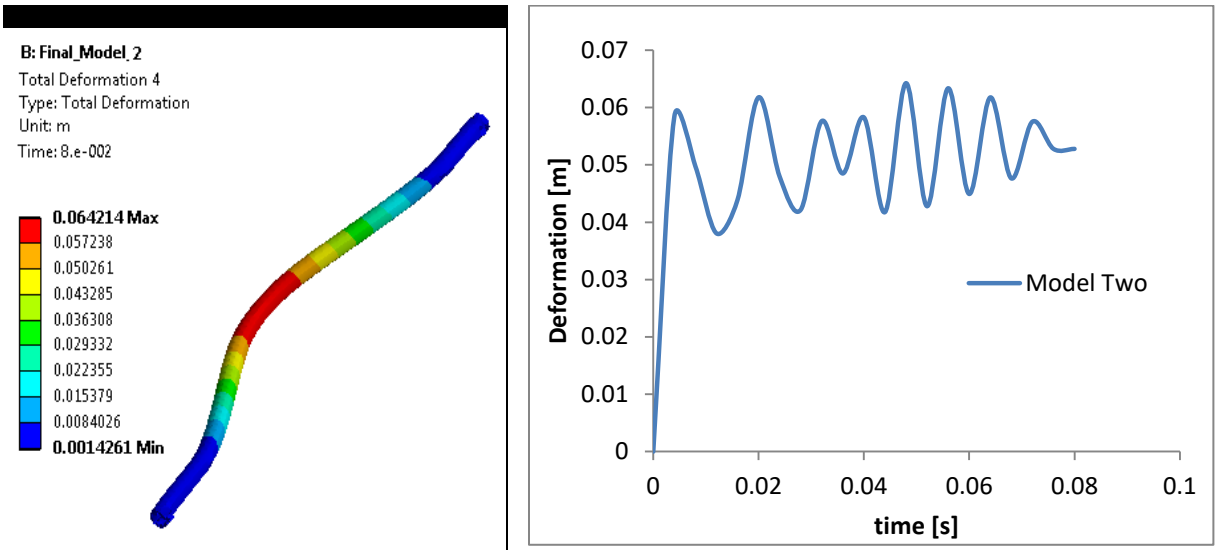

a)

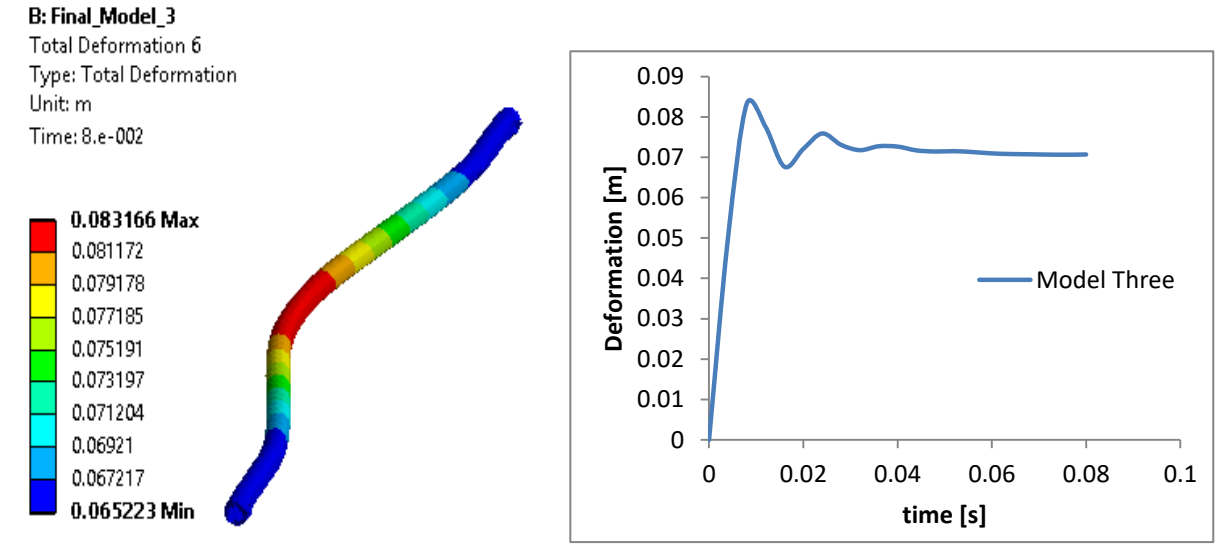

b)

Figure 19 Total deformation in Steel 1006 beam **a)** Model Two **b)** Model Three

The total deformation on each beam with the applied of steel material is shown in the above four figures. As their perspective graph indicates, the deformation history is varies when the time rise. Specially, model two deforms dynamically unstable. Such types of behaviors may be the material and geometry combination properties. It needs further study. The maximum deflection was scored 111.7 mm for present model, 75 mm for model one, 64 mm for model two and 83 mm for model three, respectively.

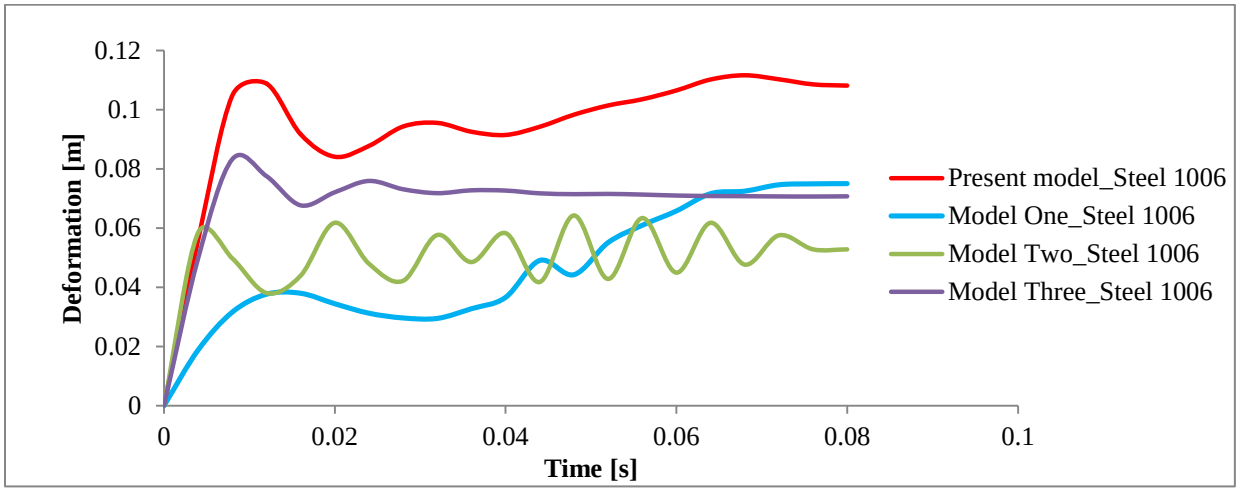

Figure 20 Total Deformation on steel 1006 beams

As the above graph shows, inserting ribs in the tube (model -one, -two and -three) can minimize the deformation of beam. Model one, model two and model three can reduce the maximum deflection with 32.8%, 42.4% and 25.4%, respectively when compared to present model. The improvement on the maximum deflection due to inserting ribs is shown in the next column graph.

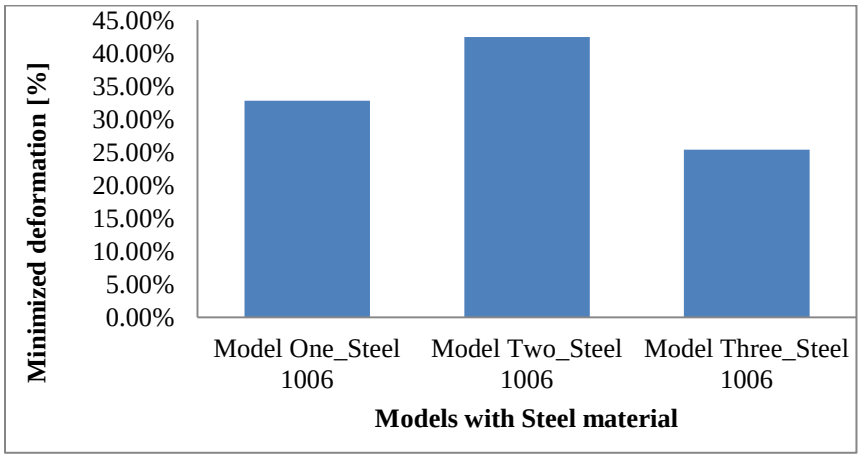

Figure 21 Minimized Deflection due to inserting rib for steel beams

4.1.2 Total Deformation of Material One (Carbon/Epoxy) Beam

The deformation of each impact beam when the Carbon/Epoxy composite material assigned is shown in the next figures.

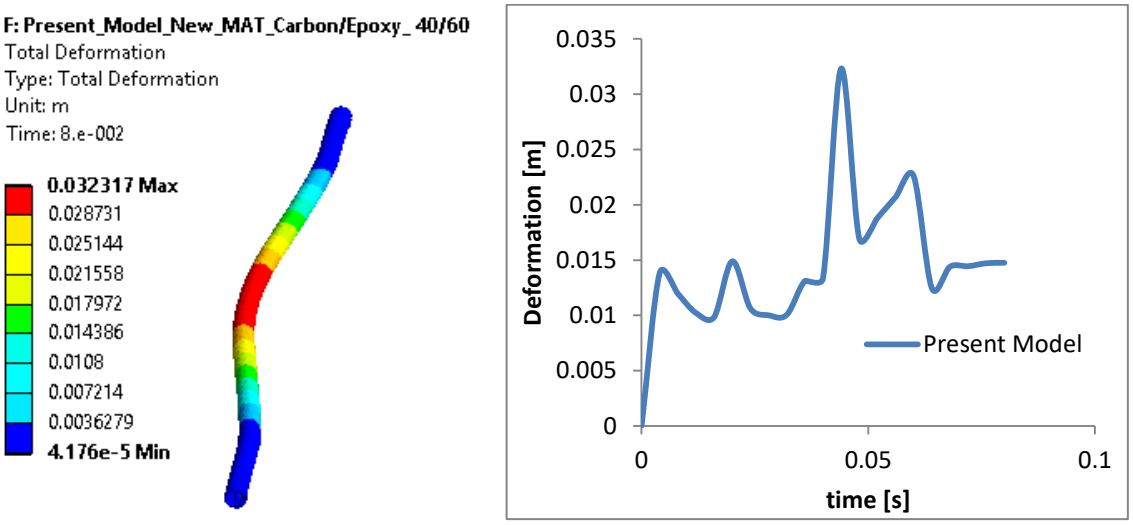

a)

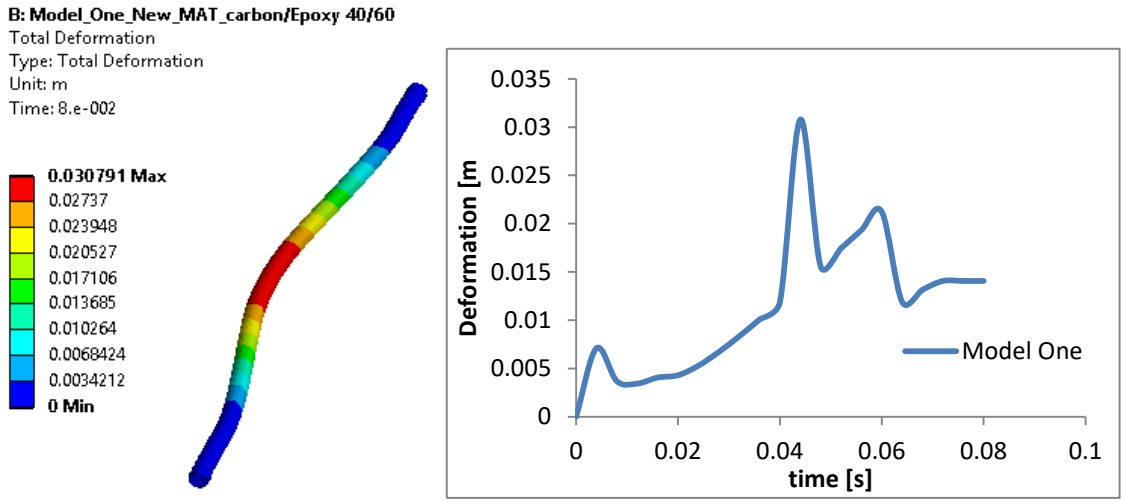

b)

Figure 22 Total deformation in Carbon/Epoxy beam a) Present Model b) Model One

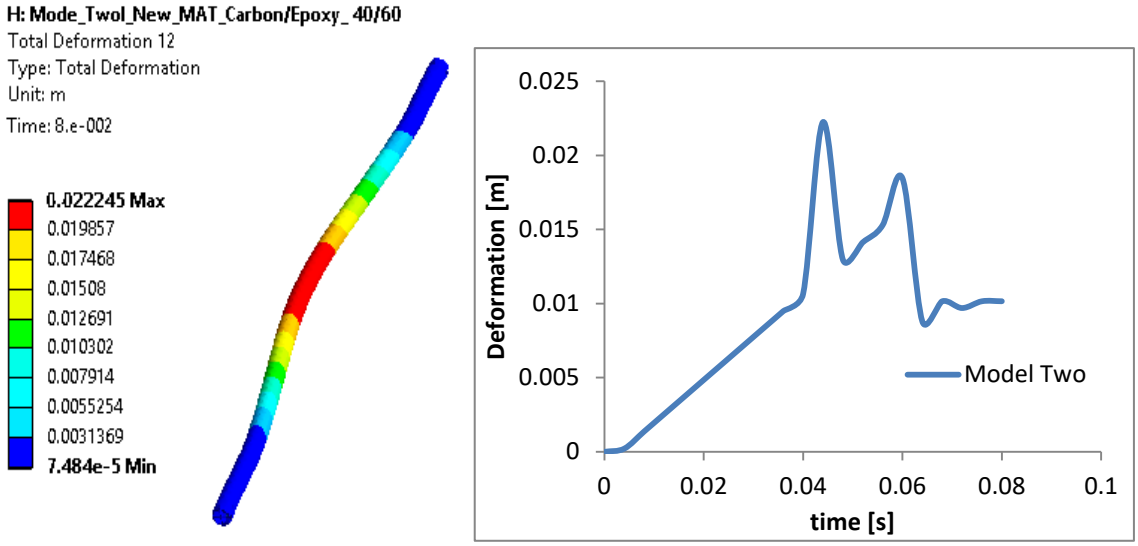

a)

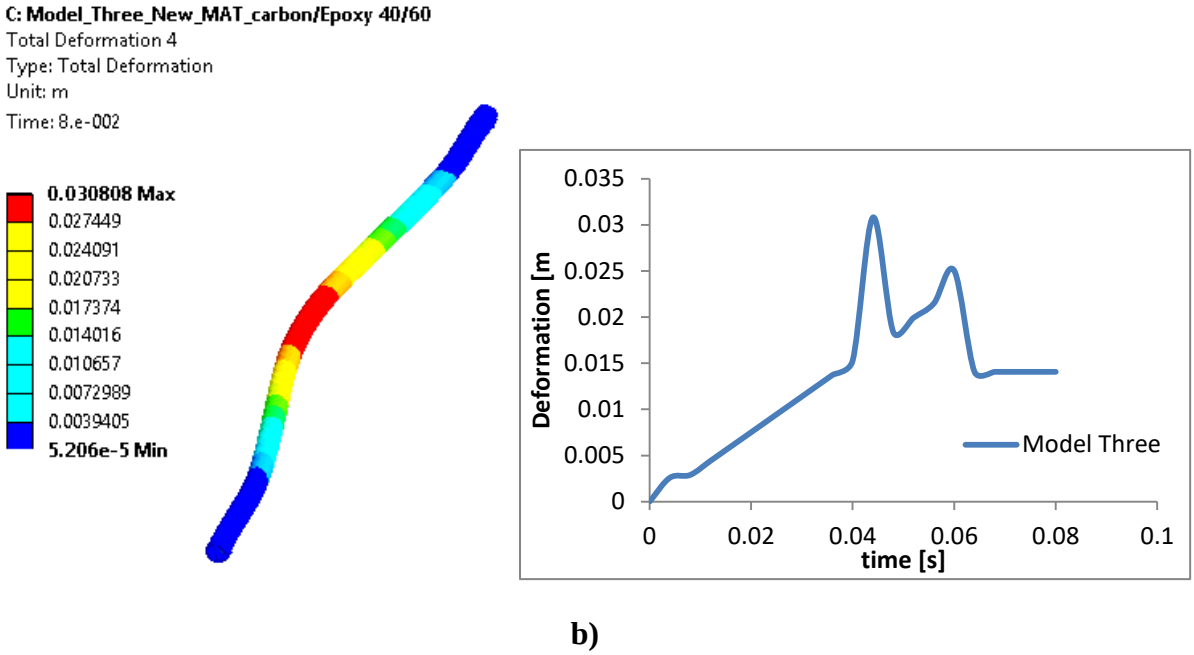

b)

Figure 23 Total deformation in Carbon/Epoxy beam a) Model Two b) Model Three

The total deformation on each beam with the applied of carbon/epoxy composite material is shown in the above four figures. As their intended graph indicates, the deformation history is varies when the time rise. The maximum deflection is scored 32.32 mm, 30.79 mm, 22.2 mm and 30.81 mm for present model, model one, model two and model three, respectively

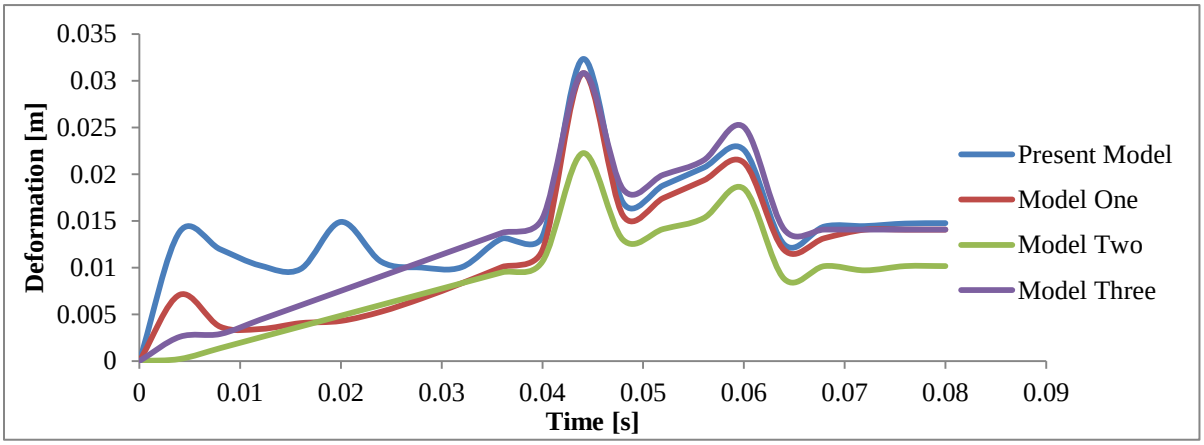

Figure 24 Total Deformation on Carbon/Epoxy beams

For carbon/epoxy composite beams, the maximum deflection of model one and model three are approximately equivalent to the present model. They didn't show significant variation with present model. But model two can reduce the maximum deflection of beam with 31.17% when comparing with the present model with same application of Carbon/Epoxy material.

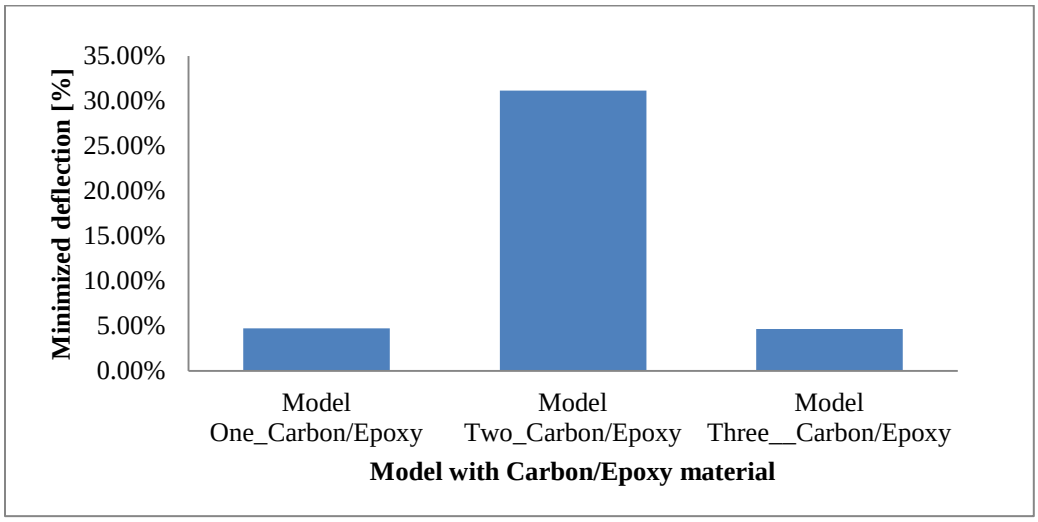

Figure 25 Minimized Deformation due to inserting rib for Carbon/Epoxy beams

4.1.3 Total Deformation of Material Two (Carbon/PEEK) Beam

The deformation of each impact beam when the Carbon/PEEK composite material assigned is shown in the next figures. The figures were taken at the end of simulation and the unit is in m.

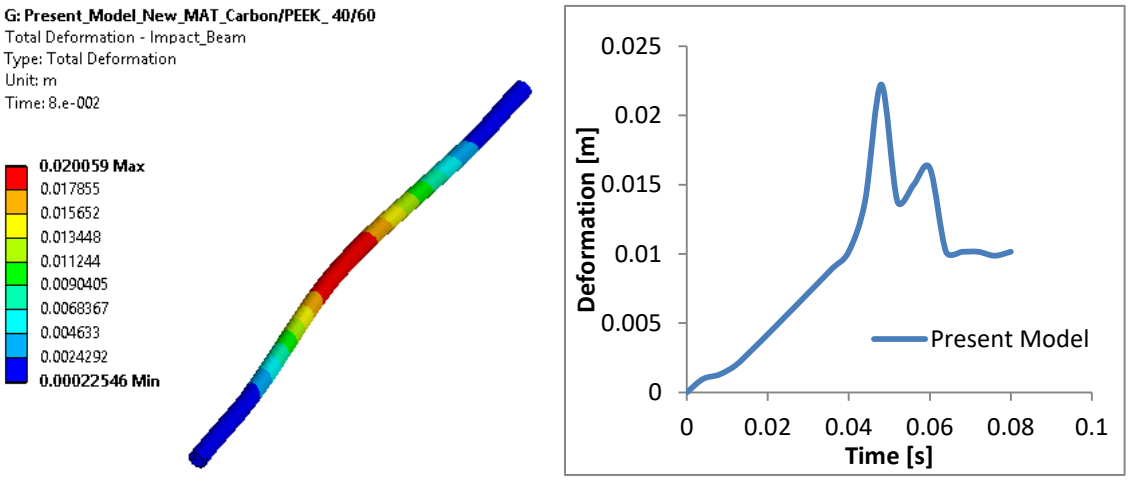

a)

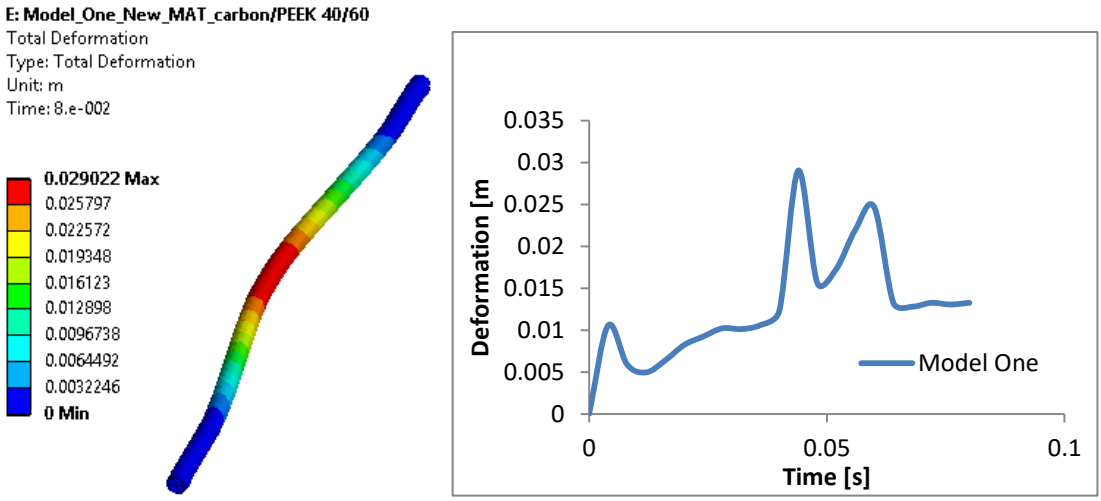

b)

Figure 26 Total deformation in Carbon/PEEK beam a) Present Model b) Model One

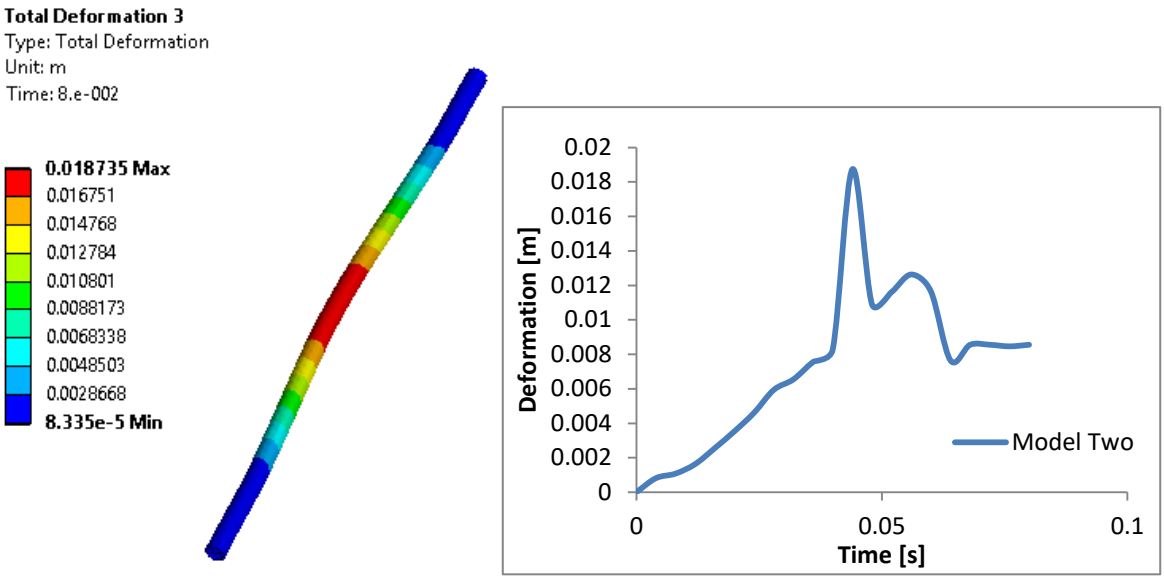

a)

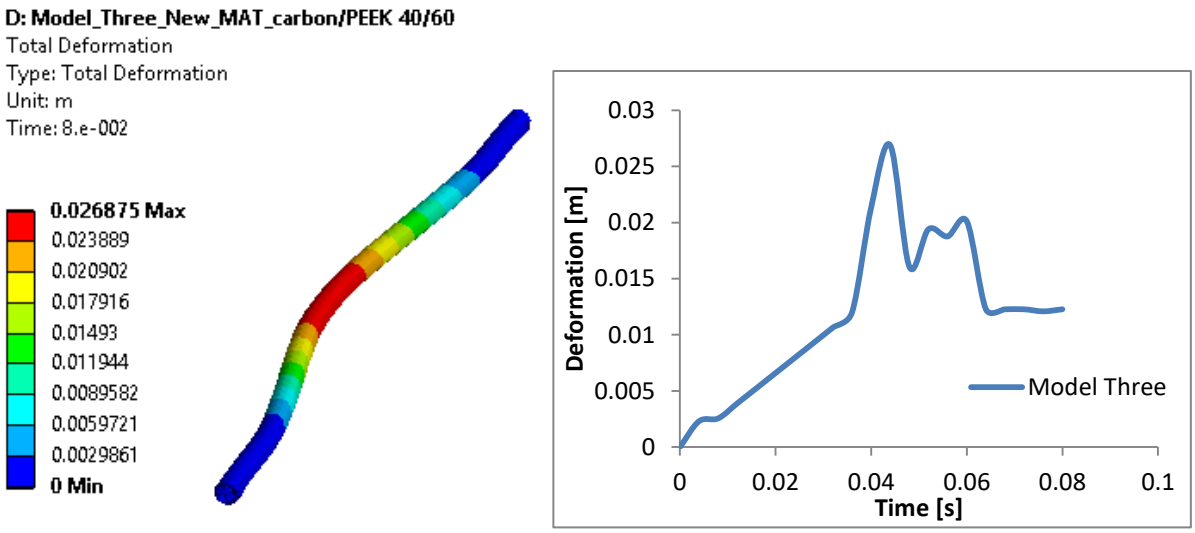

b)

Figure 27 Total deformation in Carbon/PEEK bean a) Model Two b) Model Three

The total deformation on each beam with the applied of Carbon/PEEK composite material is presented in the above four figures. As their graph indicates, the deformation history is varies when the time rise. The maximum deflection is scored 22.25 mm, 29.03 mm, 18.74 mm and 26.88 mm for present model, model one, model two and model three, respectively.

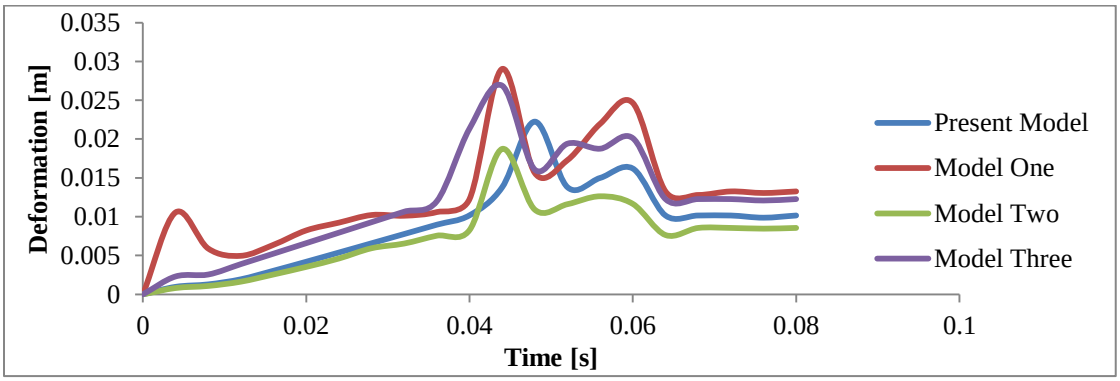

Figure 28 Total Deformation on Carbon/PEEK beams

For Carbon/PEEK composite beams, the maximum deflection of model one and model three are unexpectedly greater than present model. The present model with Carbon/PEEK composite can reduce the deflection 30.5% beyond model one and 20.81% beyond model three. The rib orientation of model one and model three greatly affects the beam performance. This type of variation indicated that the thicknesses of rib and tube of model one and model three with the implication of Carbon/PEEK material could not sustain the impact when compared to the present model. But model two can reduce the maximum deflection of beam with 15.78% when comparing with the present model with same application of carbon/PEEK material.

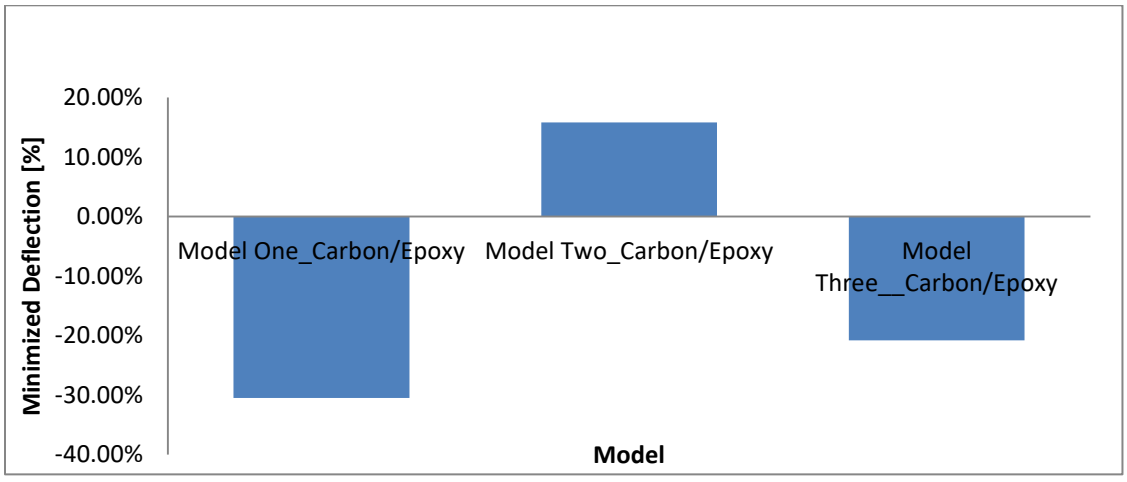

Figure 29 Minimized deflection due to inserting rib for Carbon/PEEK beams

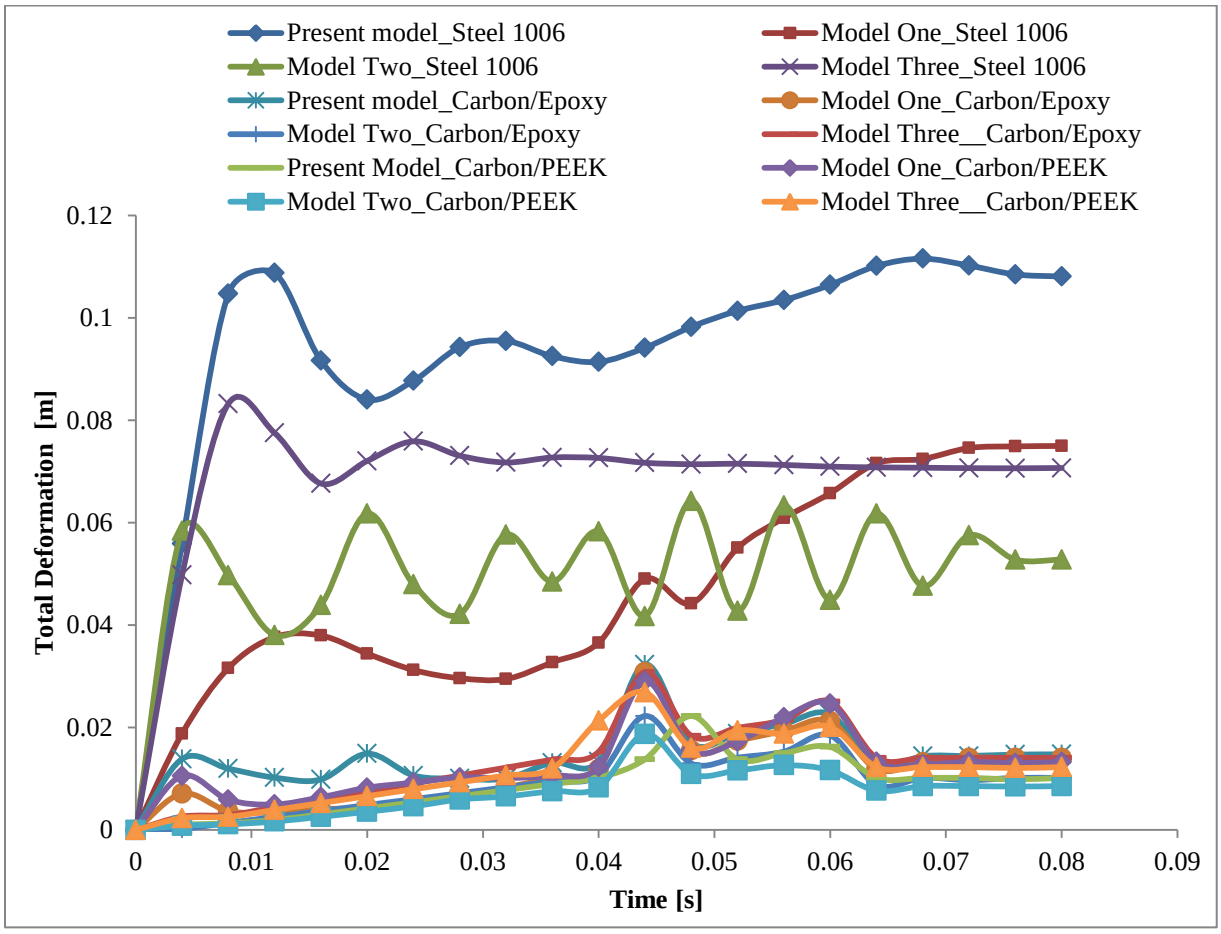

Figure 30 The influence of modification of material and geometry on deformation

The influence of modification of material on the maximum deflection of each beam is shown in the next column graph.

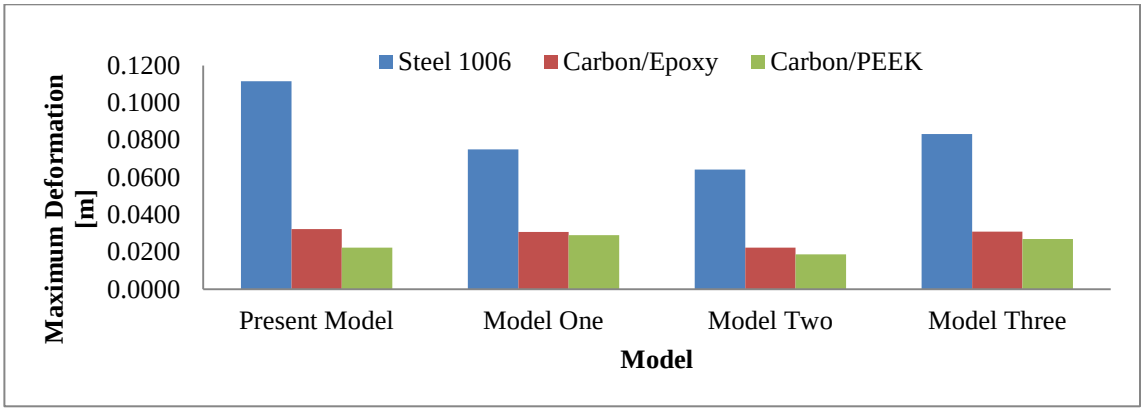

Figure 31 Influence of modification of material on deflection

The influence of modification of material on the maximum deflection is shown in the next column graph

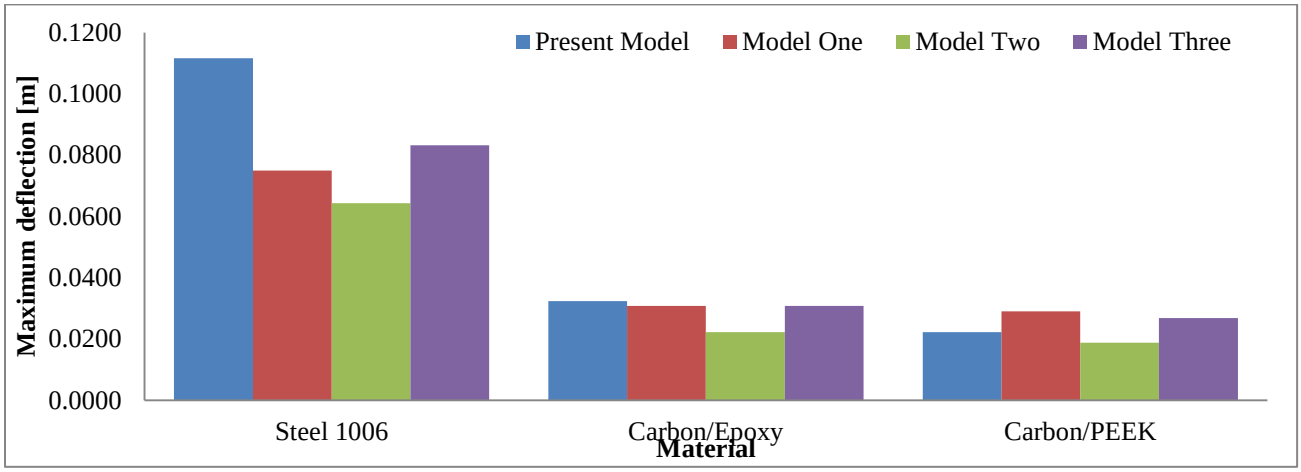

Figure 32 Influence of modification of geometry on deflection

From the previous discussions of deformation, influences of material and geometry modification are compared and discussed. Now the whole result of maximum deflection on each geometry and their perspective material could be summarized as shown in the next column graph.

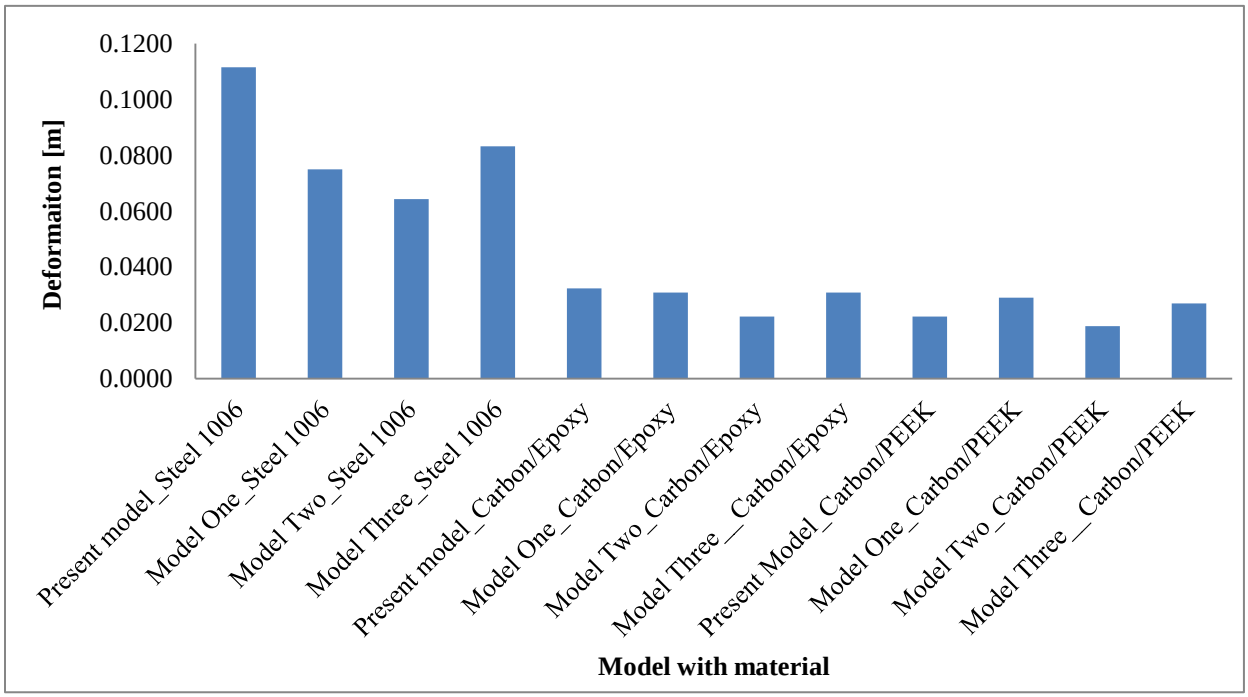

Figure 33 Summary of maximum deflection

4.2 Acceleration

4.2.1 Acceleration of Present Material (Steel 1006) Beams

The total acceleration on four beams with present material (steel 1006) is generated as the next graph shows. Those values are expressed in terms of gravity g (they were divided by 9.81 and in the unit of m/s^2).

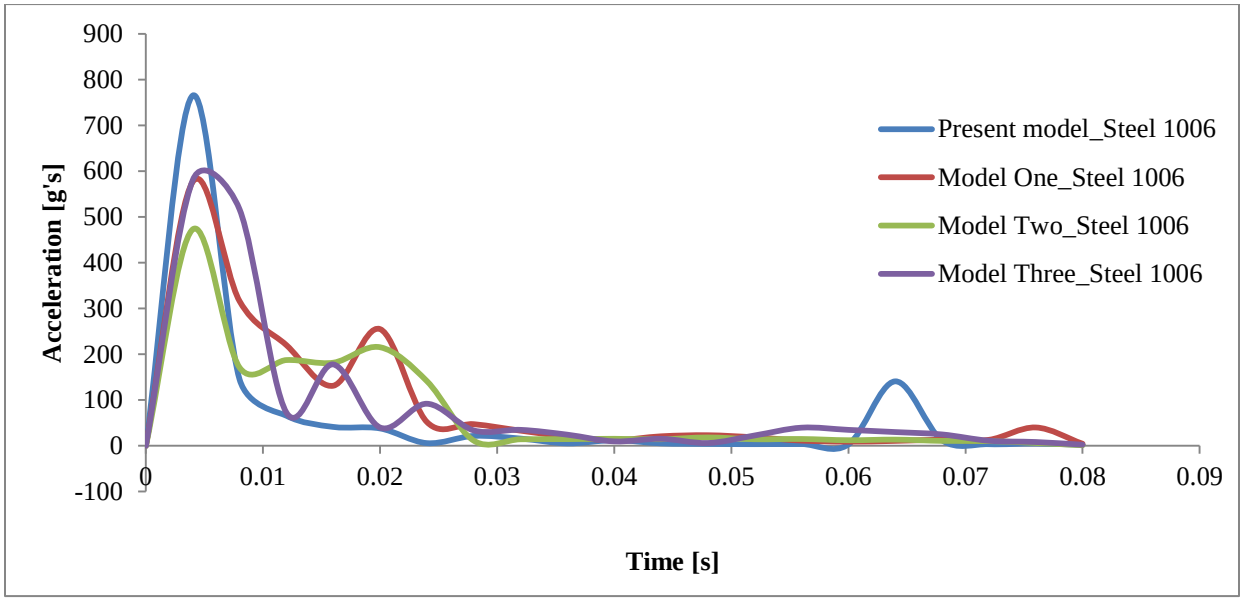

Figure 34 Acceleration on Steel 1006 Beams

The maximum acceleration generated on the steel beams are 765 g, 577 g, 473 g, and 580 g for the present model, model one, model two and model three, respectively.

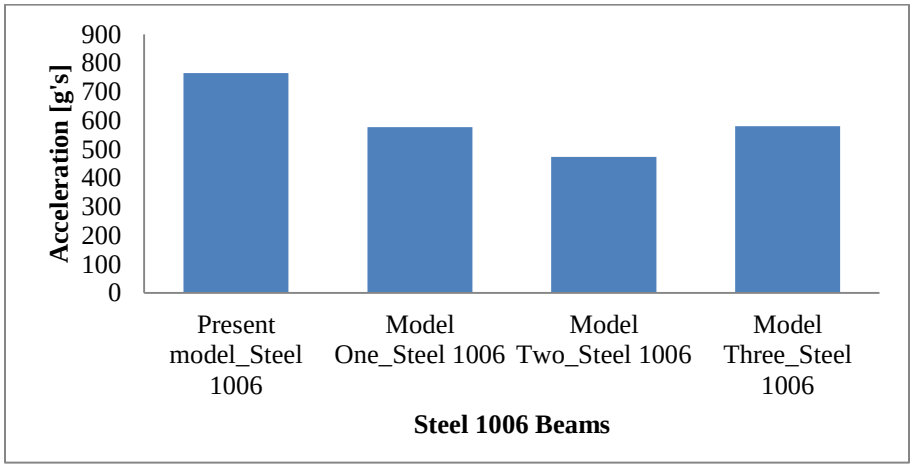

Figure 35 Maximum acceleration on steel 1006 beams

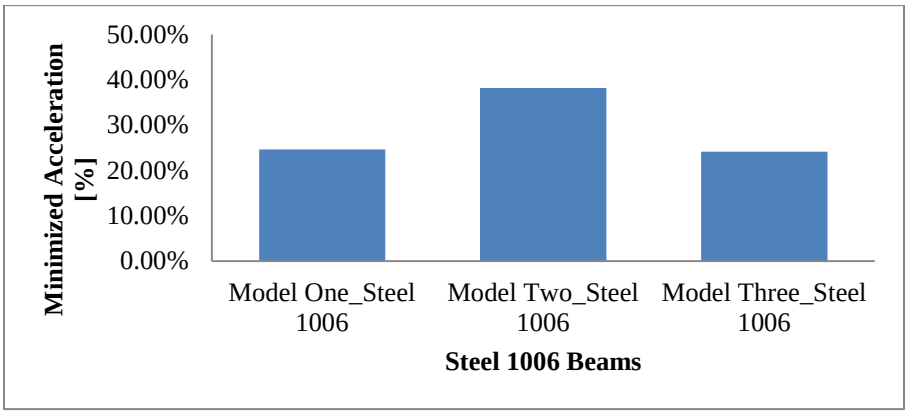

Figure 36 Minimized acceleration due to inserting ribs for steel beams

As the above column graph indicates, using ribbed beams instead of tube alone can enhance the stability of beam structure. When comparing the acceleration of model one, model two and model three with the present beam, they can reduce the acceleration with 24.63%, 38.2% and 24.17%, respectively. Thought the acceleration reduction values are better than the present beam, all beams with implication of steel 1006 materials may not be acceptable when compared with the standard regulation of FMVSS 214 (which states that the maximum acceleration of the structure shall not exceed 85 g) [13].

4.2.2 Acceleration of Material One (Carbon/Epoxy) Beams

The total acceleration on four beams with material one (Carbon/Epoxy) is generated as the next graph presented. Those values are expressed in terms of gravity g (they were divided by 9.81 and have m/s^2 unit).

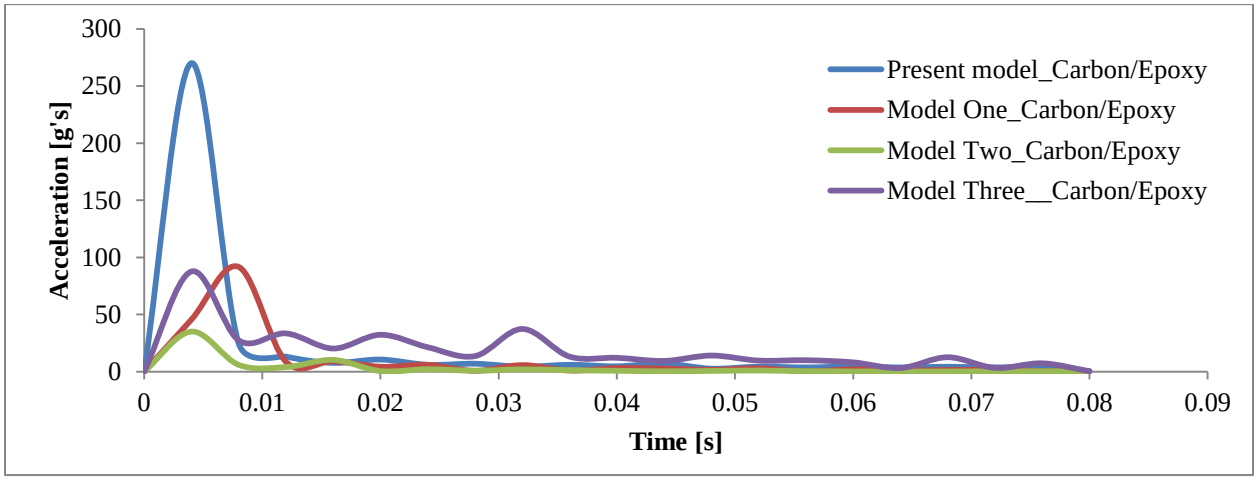

Figure 37 Acceleration on Carbon/Epoxy Beams

The maximum acceleration generated on the Carbon/Epoxy Composite beams are 125 g, 92 g, 45 g, and 98 g for the present model, model one, model two and model three, respectively.

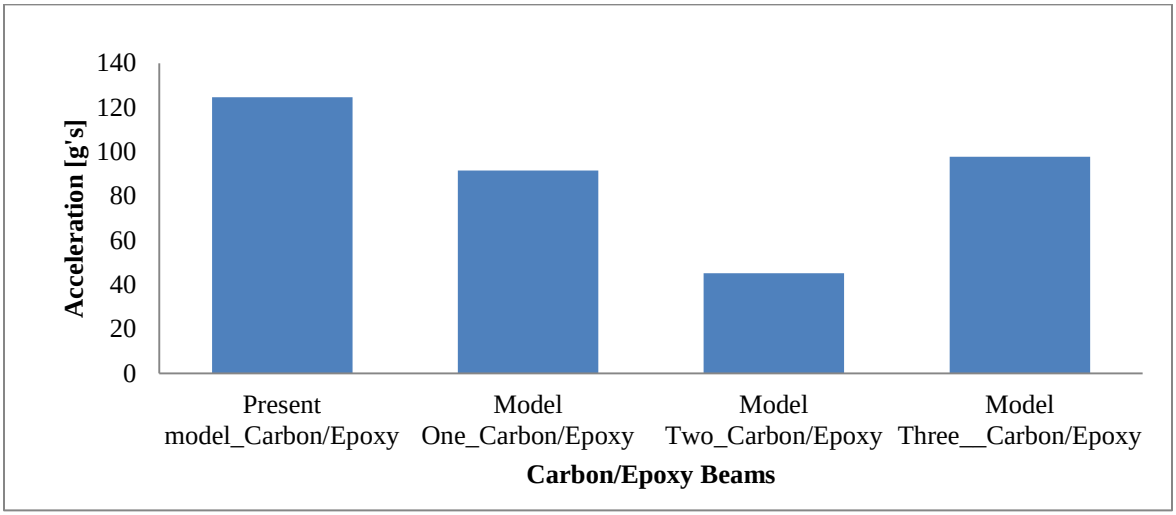

Figure 38 Maximum acceleration on Carbon/Epoxy beams

As the next column graph indicates, using Carbon/Epoxy ribbed beams instead of tube alone can enhance the stability of beam structure. Model one, model two and model three with the material implication of Carbon/Epoxy, can reduce the acceleration by 26.52%, 63.74% and 21.537%, respectively. Thought the acceleration reduction values are better than the present beam, except model two may not be acceptable when compared with the standard regulation of FMVSS 214 (which states that the maximum acceleration of the structure shall not exceed 85 g) [13].

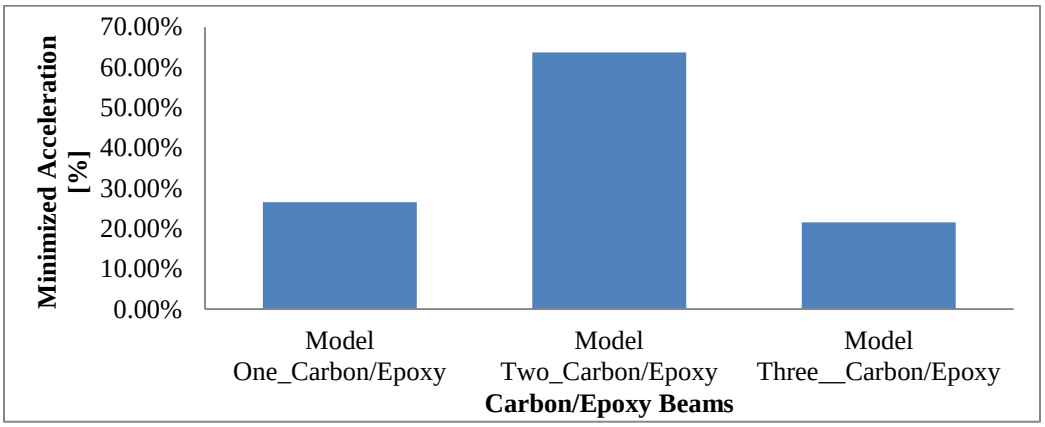

Figure 39 Minimized acceleration due to inserting ribs for Carbon/Epoxy beams

4.2.3 Acceleration of Material Two (Carbon/PEEK) Beams

The total acceleration on four beams with material two (Carbon/PEEK) is generated as the next graph presented. Those values are expressed in terms of gravity g (they were divided by 9.81 and have m/s^2 unit).

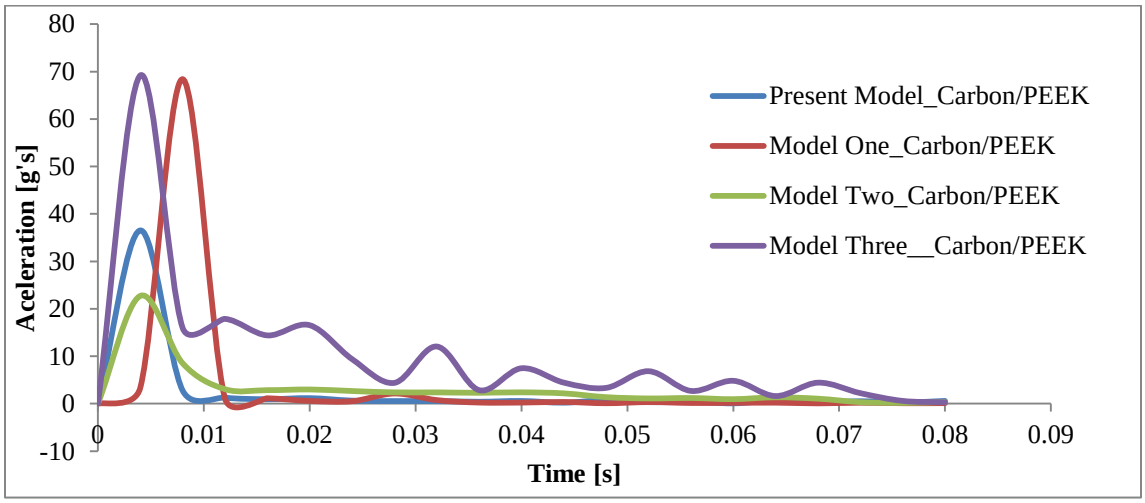

Figure 40 Acceleration on Carbon/peek Beams

The maximum acceleration generated on the Carbon/PEEK Composite beams are 37 g, 68 g, 23 g, and 69 g for the present model, model one, model two and model three, respectively.

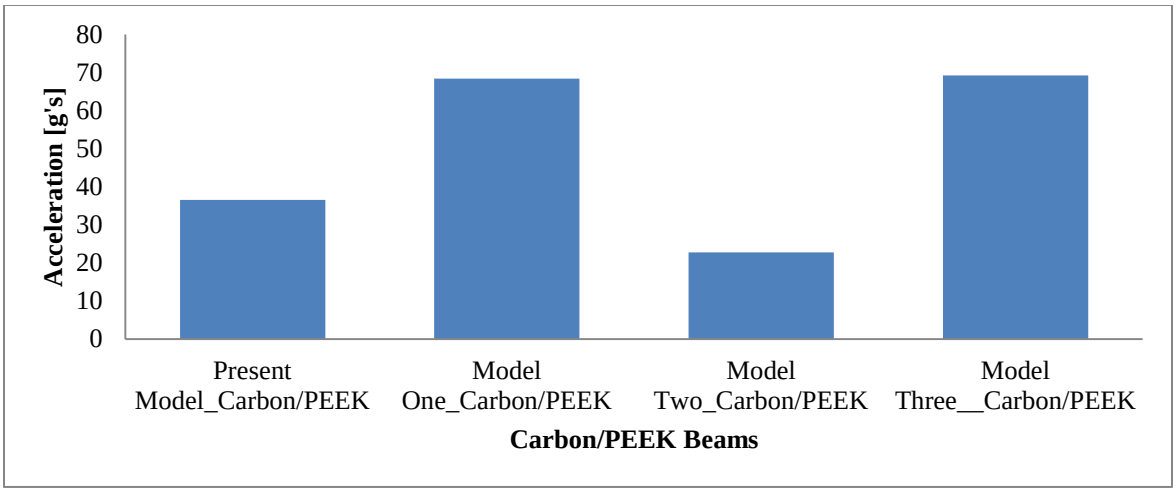

Figure 41 Maximum acceleration on Carbon/PEEK beams

As the next column graph indicates, using Carbon/PEEK ribbed beams instead of tube alone can enhance the stability of model two. When observing the resulted acceleration of all

carbon/PEEK models, they can satisfy the regulation of FMVSS 214 rules. But the two models (model one and model three) are less stable when comparing with the present model with Carbon/PEEK composite material. Model two could reduce the acceleration with 37.8% when compared to the present model. Inserting ribs as model one and model three are less stable when compared to the tube alone beam.

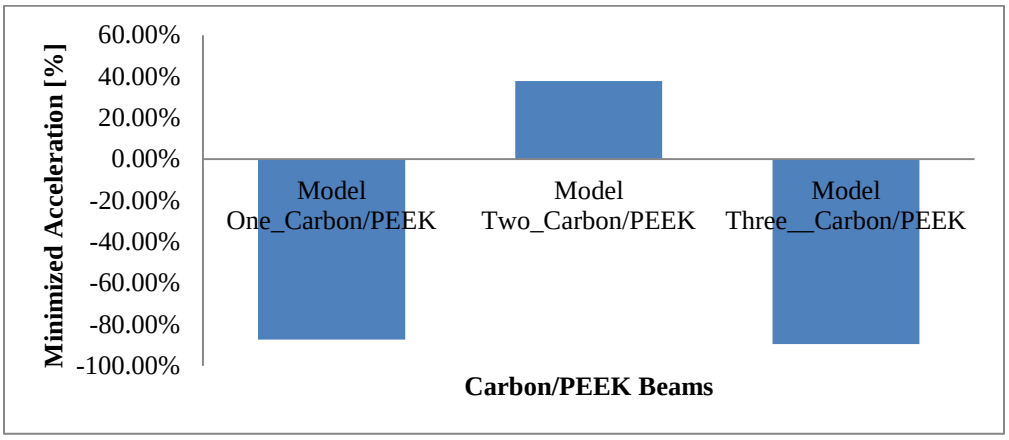

Figure 42 Minimized acceleration due to inserting ribs for Carbon/PEEK beams

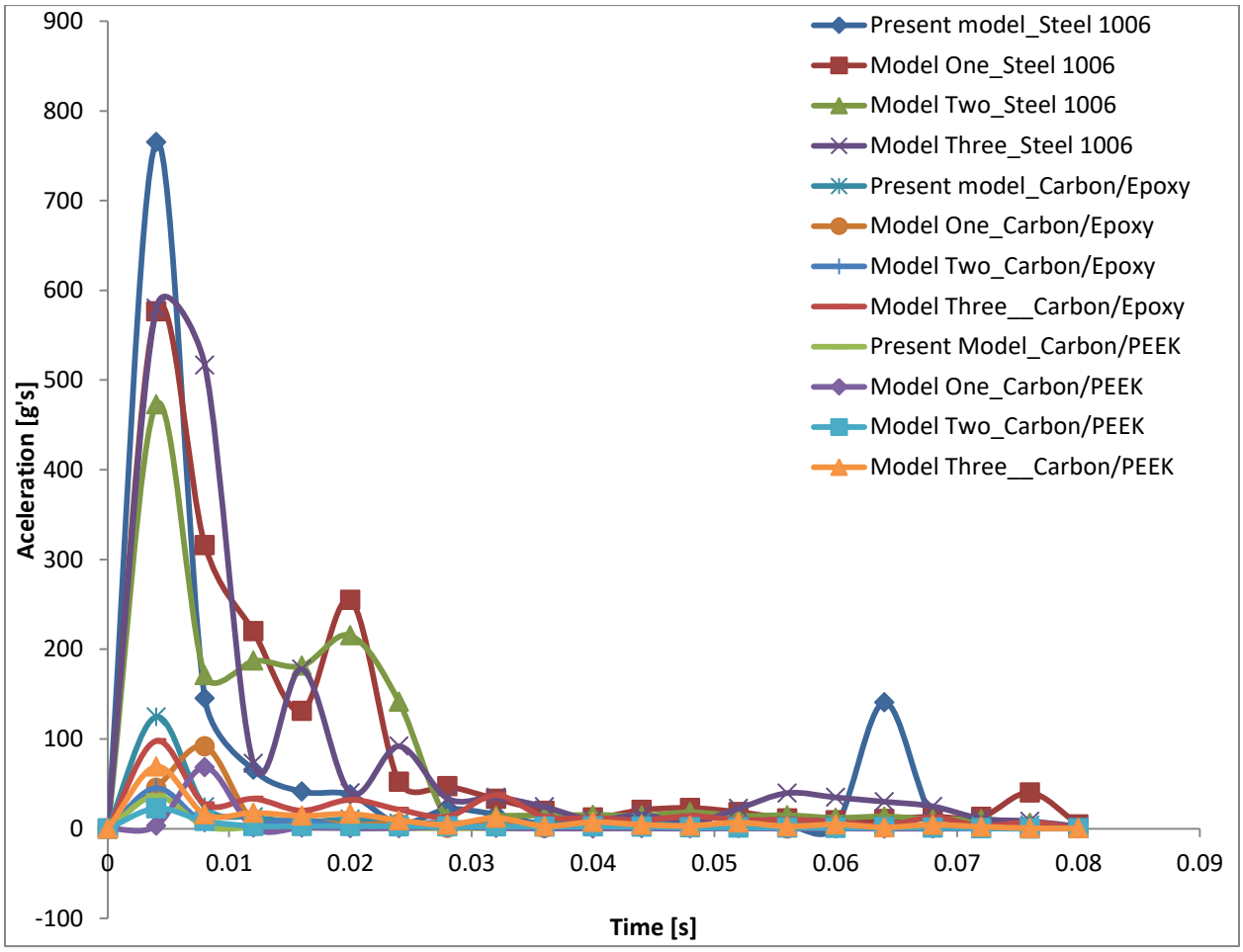

Figure 43 The influence of material and geometry on acceleration

The influence of modification of material on acceleration is shown in the next column graph

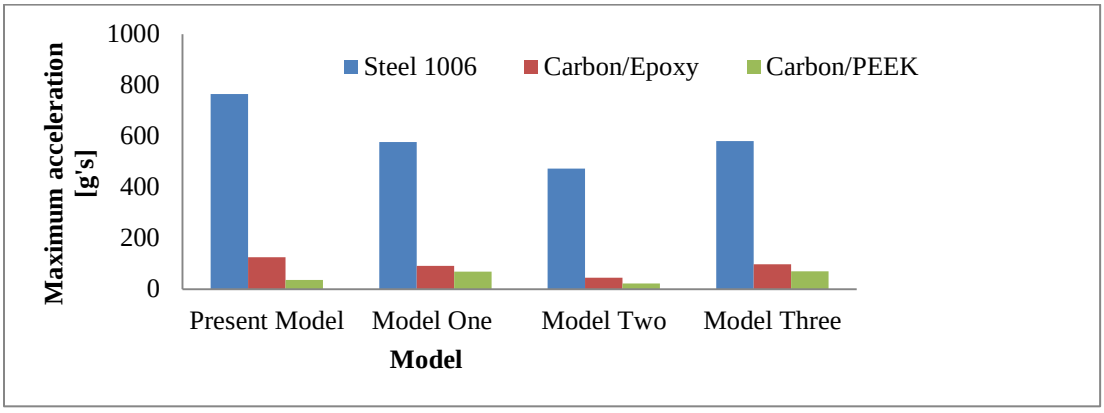

Figure 44 Comparison of modification of material on acceleration

The influence of modification of geometry on acceleration is shown in the next column graph

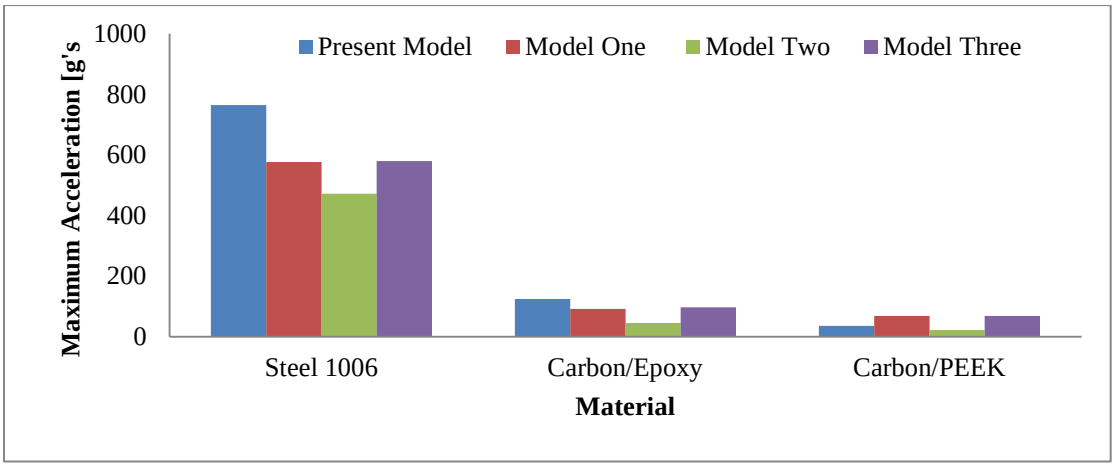

Figure 45 Comparison of modification of geometry on acceleration

From the previous discussions of acceleration, influences of material and geometry modification are compared and discussed. Now the whole result acceleration on each geometry and their perspective material are summarized as shown in the next column graph.

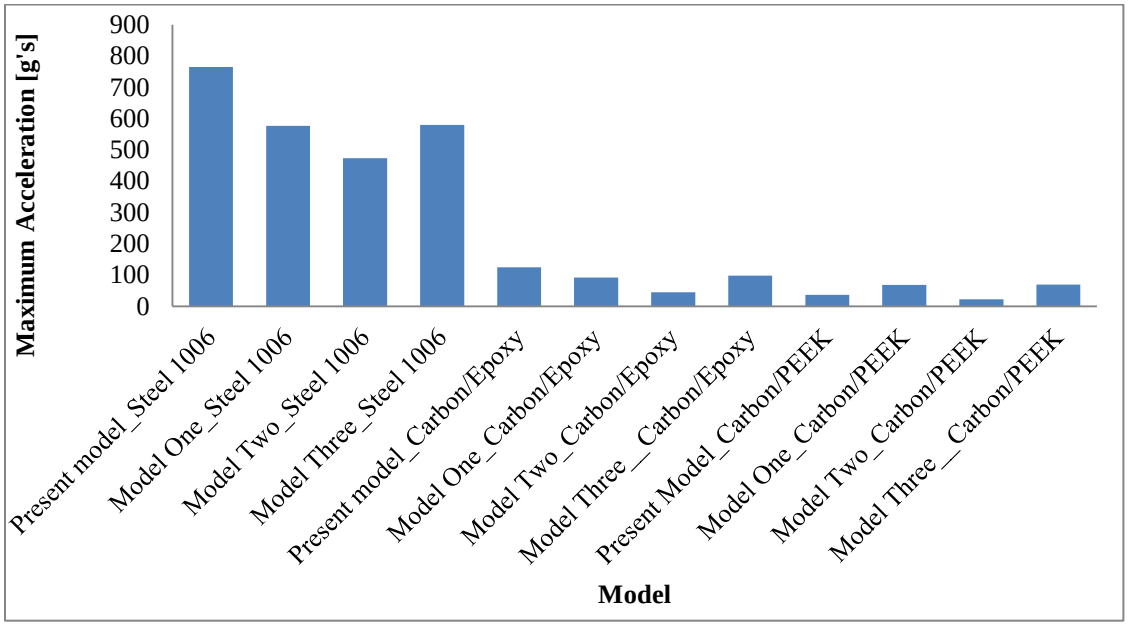

Figure 46 Summary influence of modifying material and geometry on acceleration

4.3 Internal Energy in Beam

The resulted internal energy of the impact beams is show in the next subtopics.

4.3.1 Internal Energy of Present Material (Steel 1006) Beams

The internal energy of each impact beam when the Steel 1006 material assigned is shown in the next graphs. The figures were generated at the end of simulation and the unit is in J.

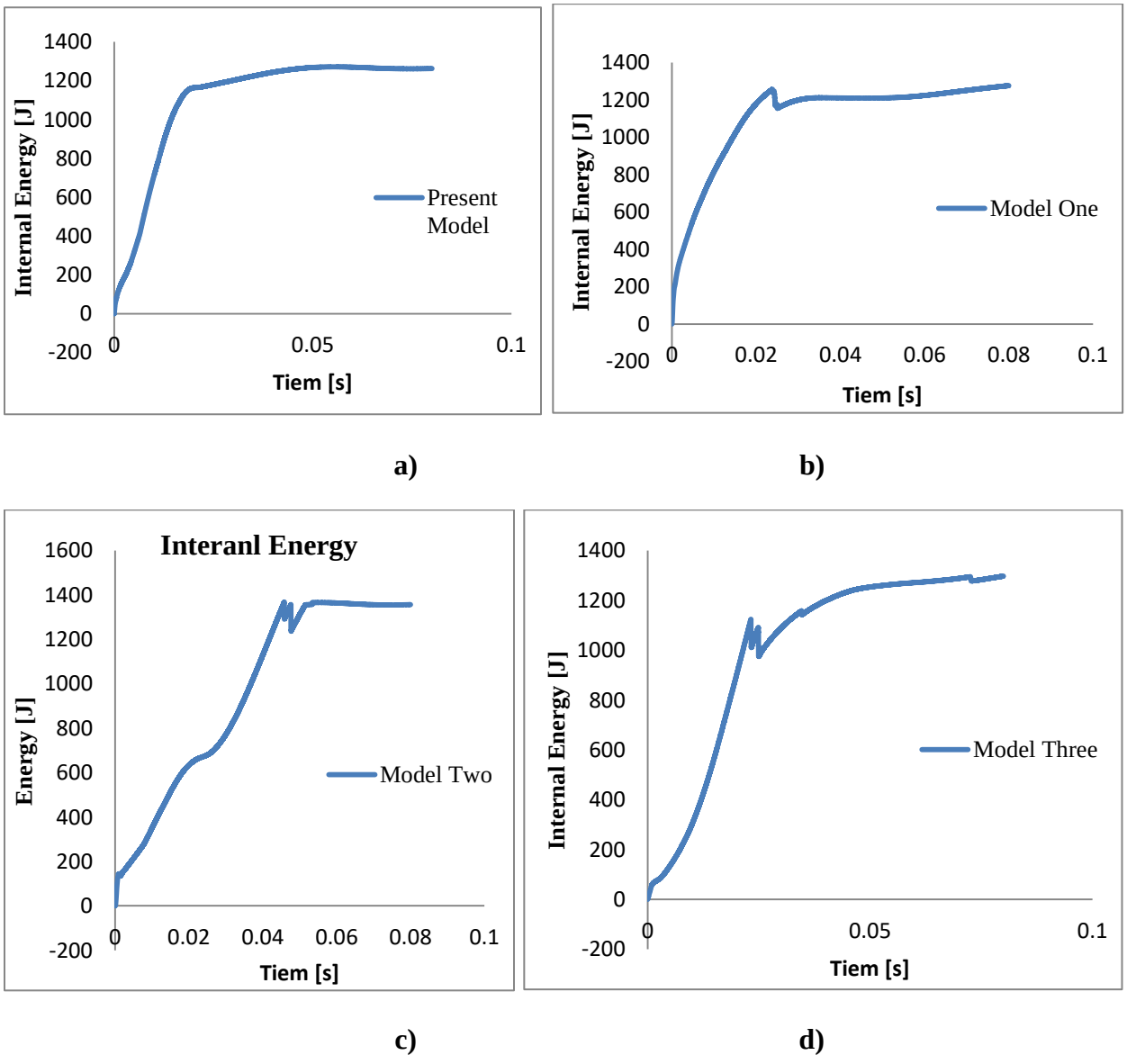

Figure 47 Internal energy in Steel 1006 beam **a)** Present Model **b)**Model One **c)**Model Two **d)** Model Three

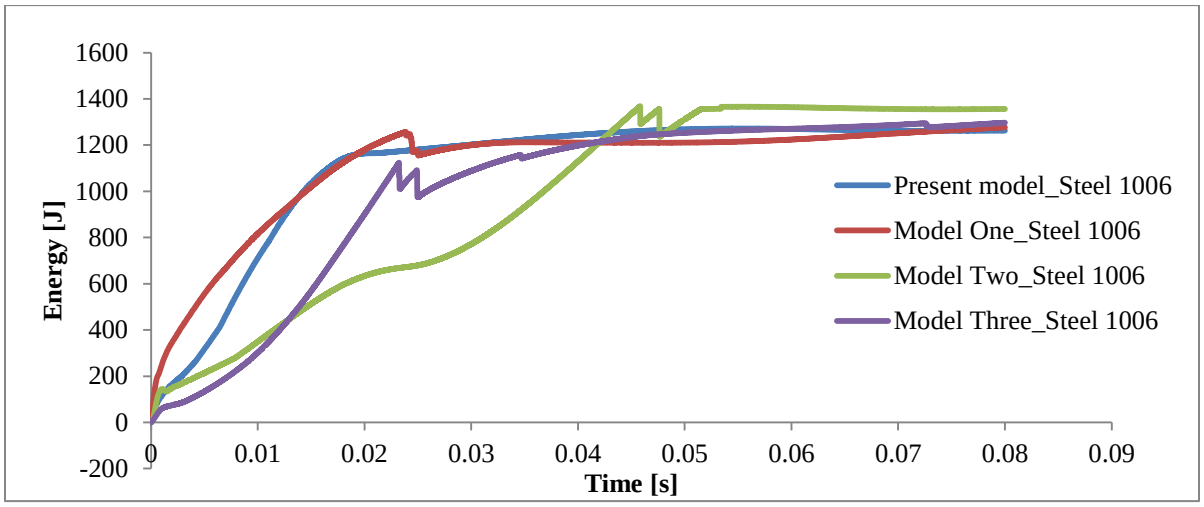

Figure 48 Internal energy absorbed by steel 1006 beams

As it can be seen from the above figure, model one absorbed the highest energy up to the collision time reached about 15 milliseconds. But once the collision time reached about 45 milliseconds, model two became dominant over the other one. The maximum energy absorbed by present model, model one, model two and model three were 1272 J, 1277 J, 1368J and 1297 J, respectively. Which means the maximum specific energy absorption, SEA (dividing the internal energy absorbed by their own mass) for present model, model one, model two and model three are 1057.7 J/Kg, 1061.86 J/Kg, 1137.53 J/Kg and 1075.45 J/Kg, respectively. When model one, model two and model three are compared to present model, they increased the specific absorbed energy by 0.4%, 7.54% and 1.96%, respectively. Inserting ribs in steel 1006 tube couldn't show that much significant improvement as of model one and model three.

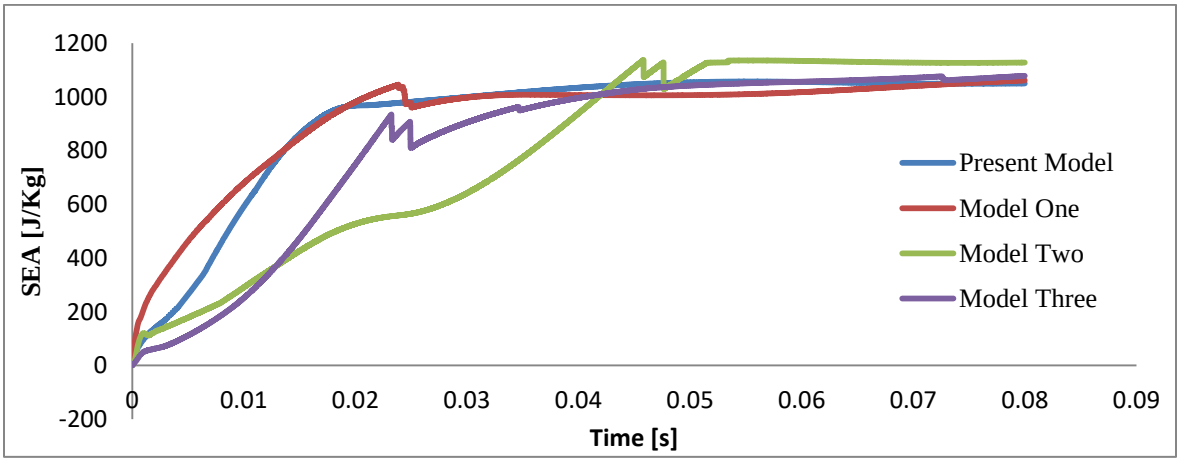

Figure 49 Specific Energy Absorption of steel 1006 beams

4.3.2 Internal Energy in Beam for Assignment of Material One (Carbon/Epoxy)

The internal energy of each impact beam when the Carbon/Epoxy material assigned is shown in the next graphs. The figures were generated at the end of simulation and the unit is in J.

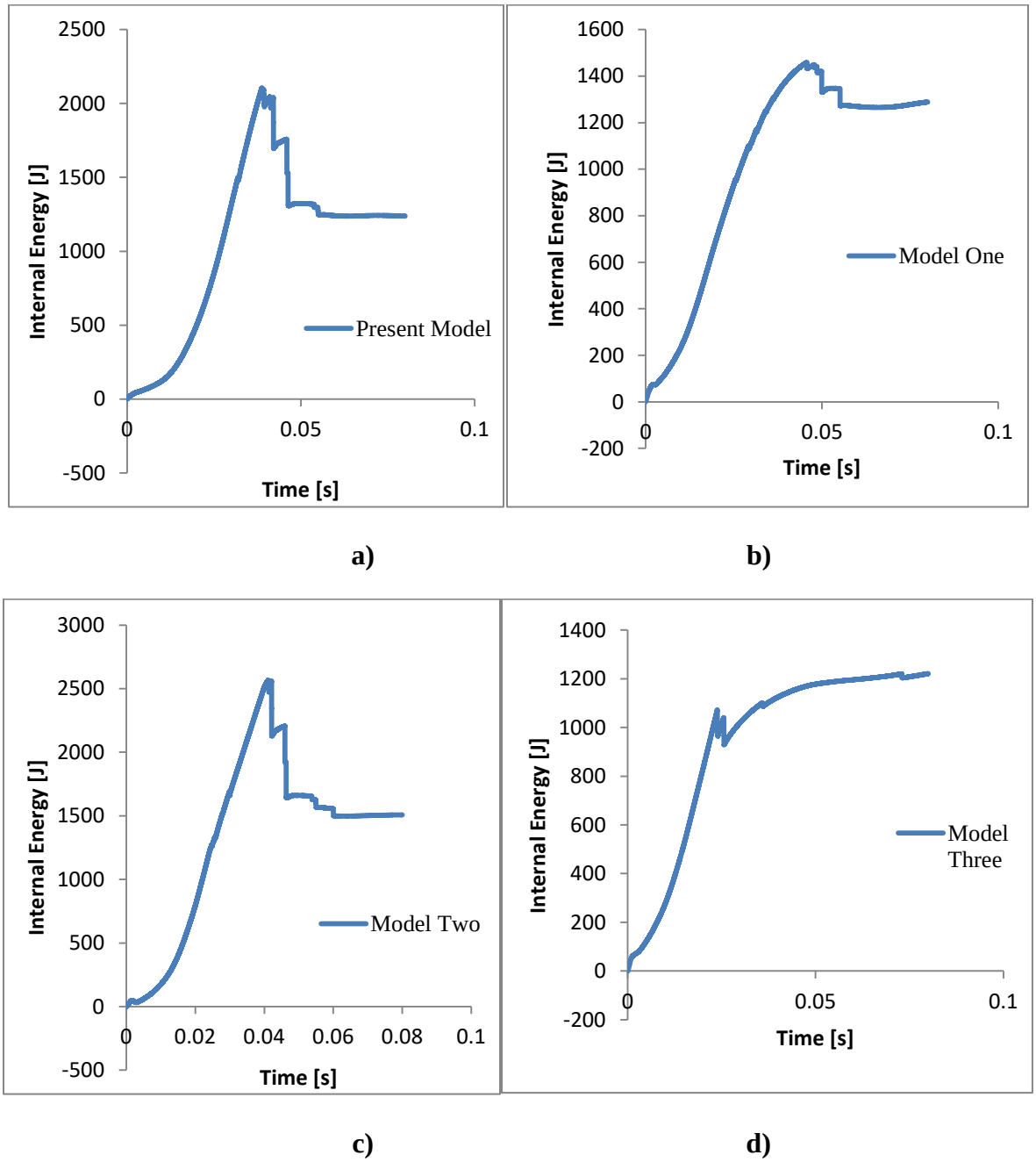

Figure 50 Internal energy in Carbon/Epoxy beam **a**) Present Model **b**)Model One **c**) Model Two **d**) Model Three

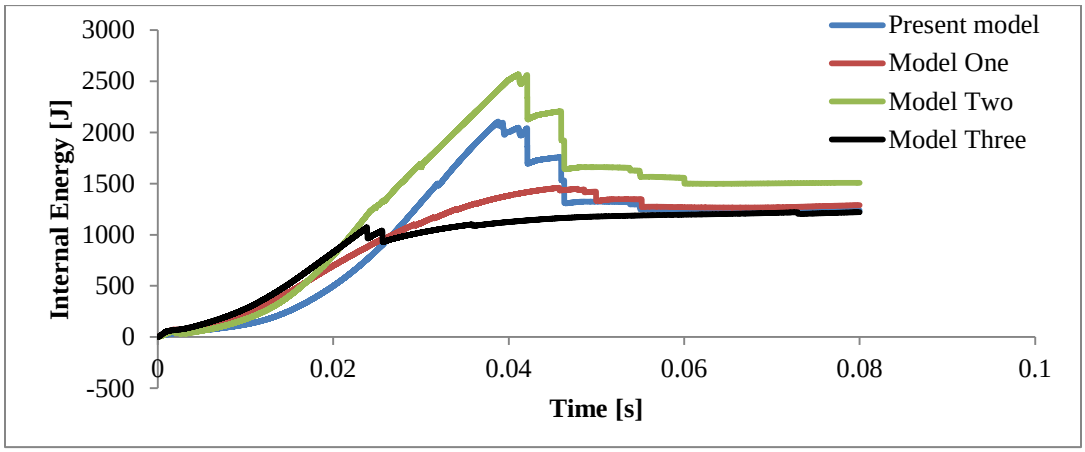

Figure 51 Internal energy absorbed by Carbon/Epoxy beams

As shown in the above graph, the internal energy absorbed by model two became highest once after the collision time reached 20 milliseconds. Even the maximum internal energy absorption of model two is less compared to model two and present model, it absorbs energy consistently next to model three. The maximum energy absorbed by present model, model one, model two and model three were 2106 J, 1459 J, 2568 J and 1221 J, respectively. Which means the maximum specific energy absorption, SEA for present model, model one, model two and model three are 8754 J/Kg, 6065 J/Kg, 10673 J/Kg and 5075 J/Kg, respectively When comparing the internal energy absorbed by present model and model two, inserting rib could enhance by 21.9%. But inserting ribs as of model one and model three could absorb less energy compared with the tube alone beam (present model).

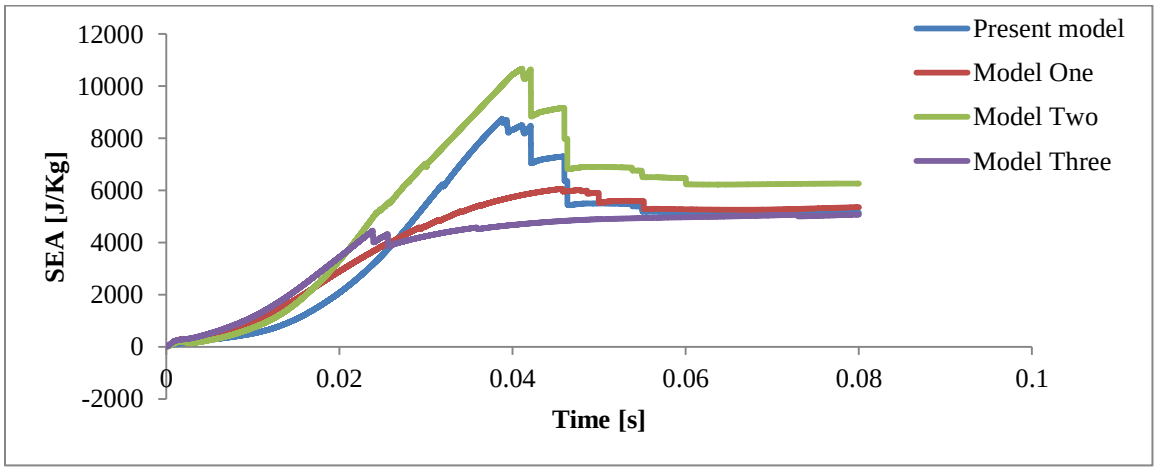

Figure 52 Specific Energy Absorption of Carbon/Epoxy beams

4.3.3 Internal Energy in Beam for Assignment of Material Two (Carbon/PEEK)

The internal energy of each impact beam when the Carbon/Epoxy material assigned is shown in the next graphs.

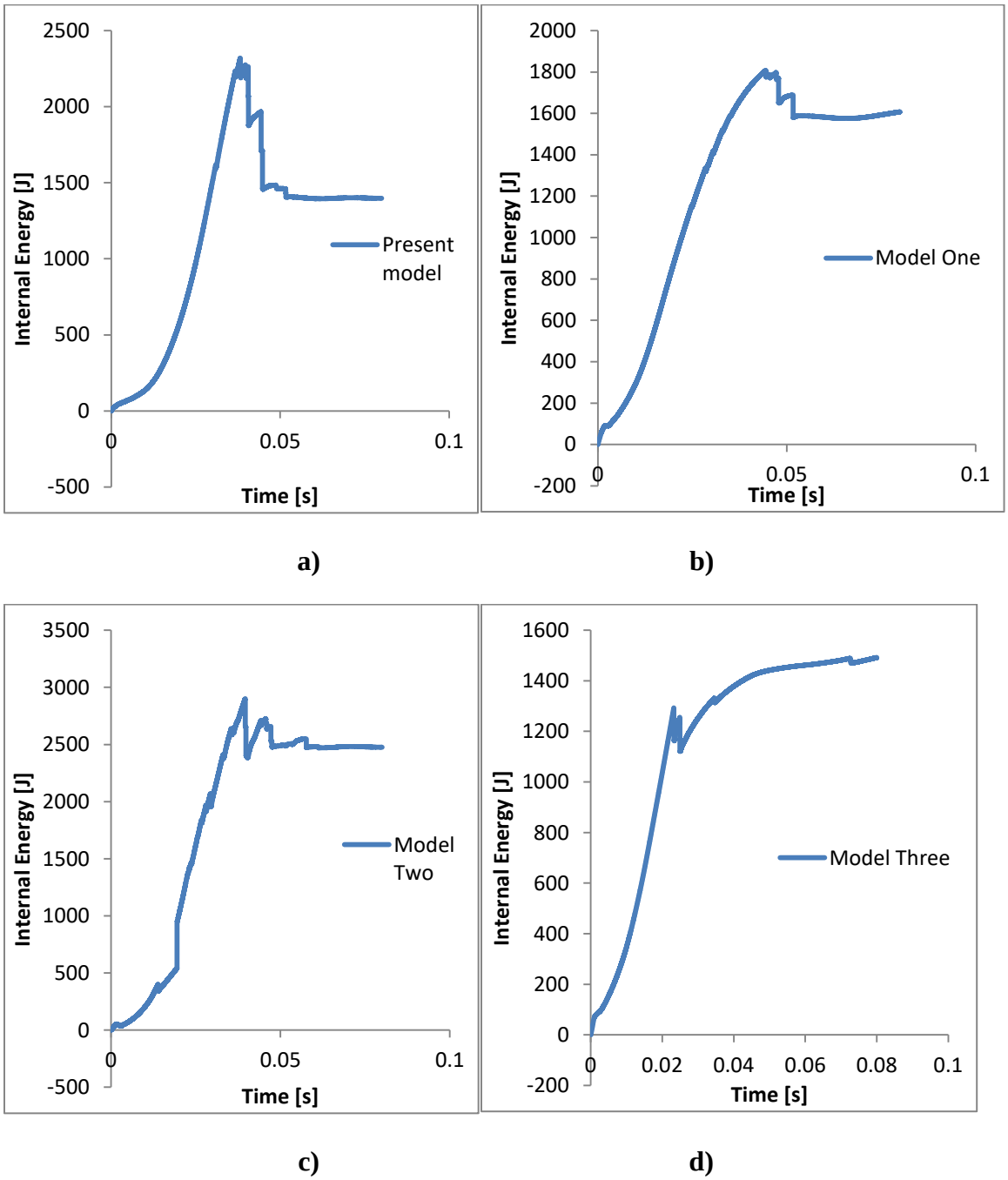

Figure 53 Internal energy in Carbon/PEEK beam **a**) Present Model **b**)Model One **c**) Model Two **d**) Model Three

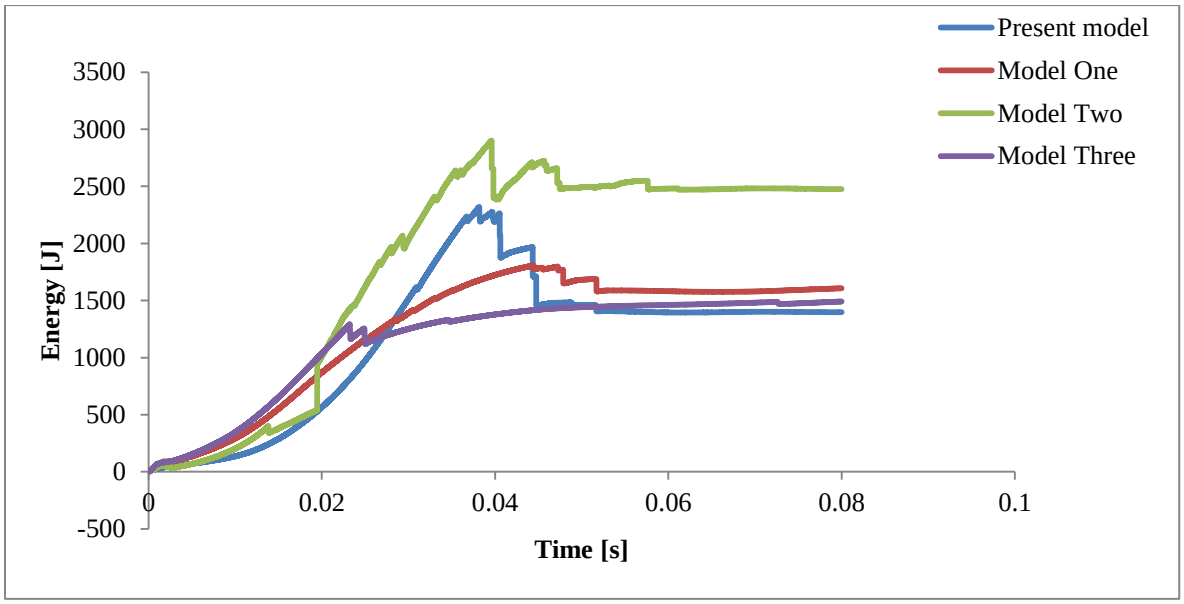

Figure 54 Internal energy absorbed by Carbon/PEEK beams

The maximum energy absorbed by present model, model one, model two and model three were 2320 J, 1807 J, 2901 J and 1492 J, respectively. And also their perspective specific energy absorption, SEA is 10736 J/Kg, 8363 J/Kg, 13425 J/Kg and 6903 J/Kg, respectively.

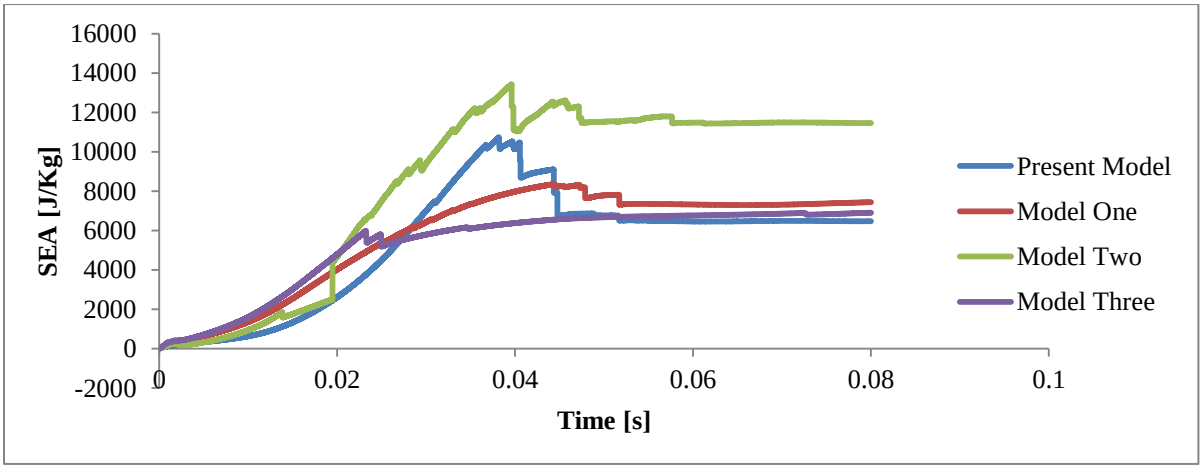

Figure 55 Specific Energy Absorption of Carbon/PEEK beams

As it can be clearly seen from the above graph inserting rib as of model two can increase the maximum specific energy absorption from 10736 to 13425 J/Kg or with 25% improvement. But on the other models (model one and three), less energy is absorbed when comparing with the tube alone beam (present model).

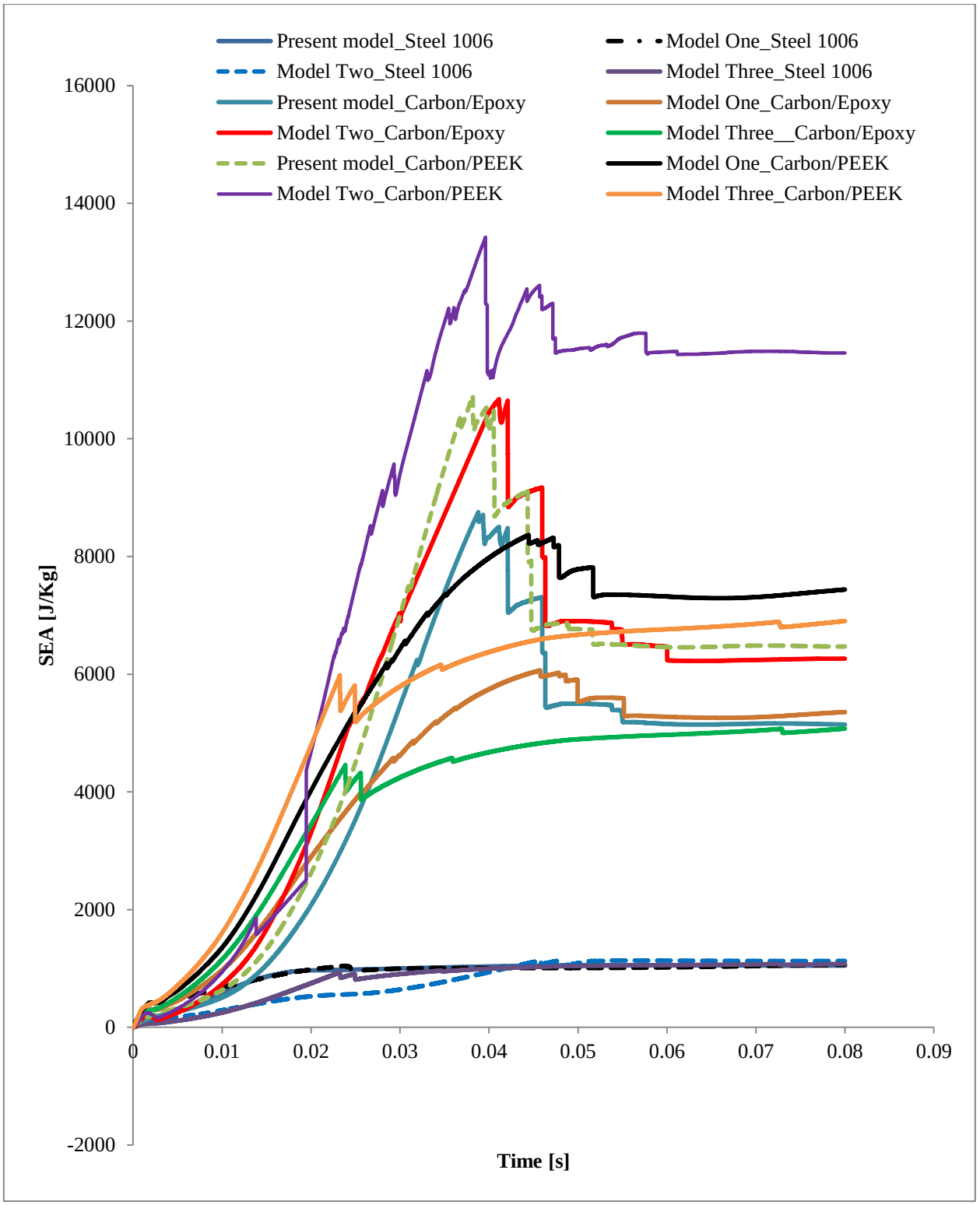

Figure 56 The influence of modification of material and geometry on specific energy absorption

The influence of modification of material on specific energy absorption, SEA is summarized in the next column graph

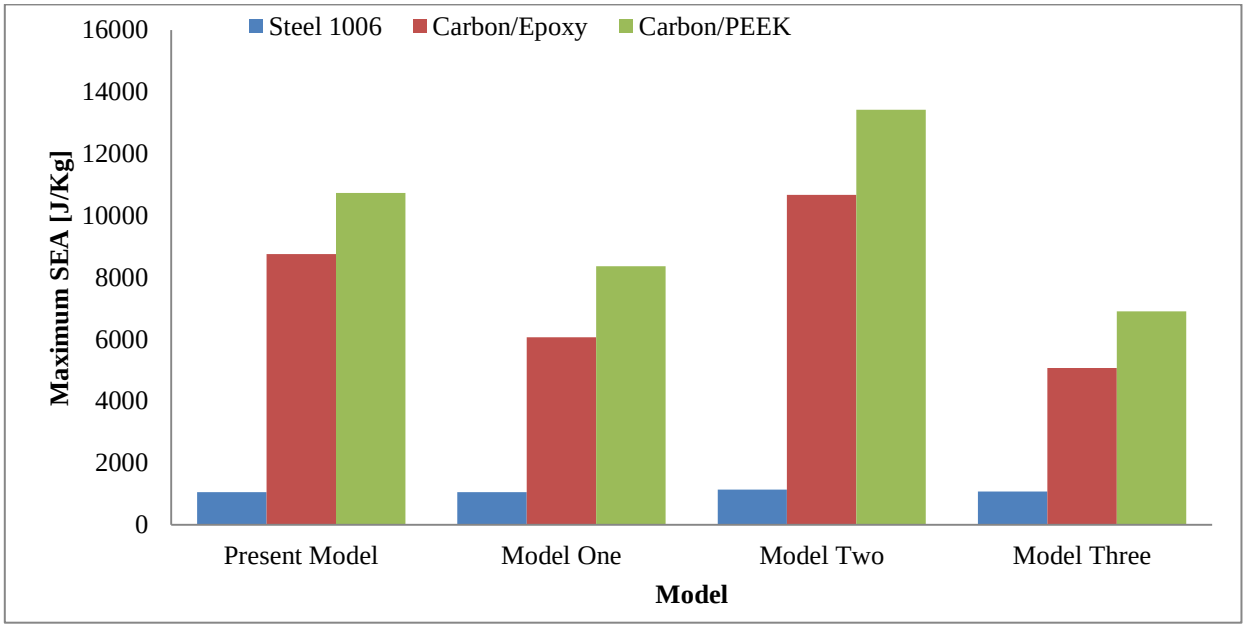

Figure 57 Influence of modification of material on specific energy absorption

The influence of modification of geometry on specific energy absorption, SEA is summarized in the next column graph

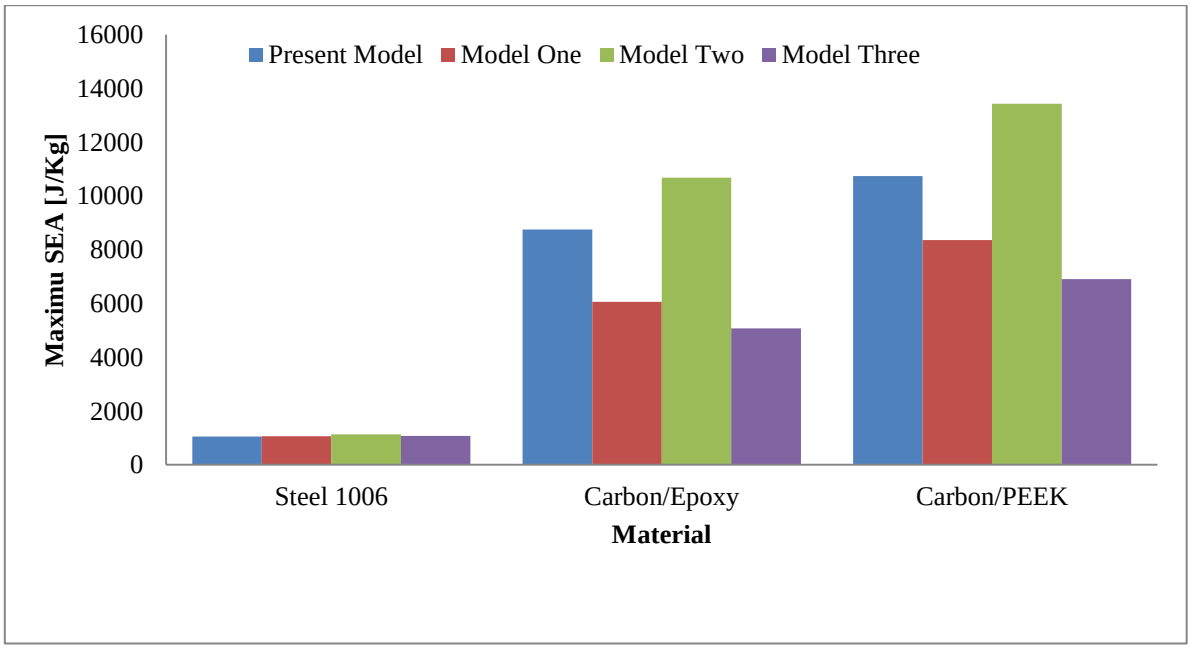

Figure 58 Influence of modification of geometry on specific energy absorption

The influence of modification of material and geometry on specific energy absorption, SEA is summarized in the next column graph. From the previous discussions of SEA, influences of material and geometry modification are compared and discussed. Now the whole resulted SEA on each geometry and their perspective material are summarized as shown in the next column graph.

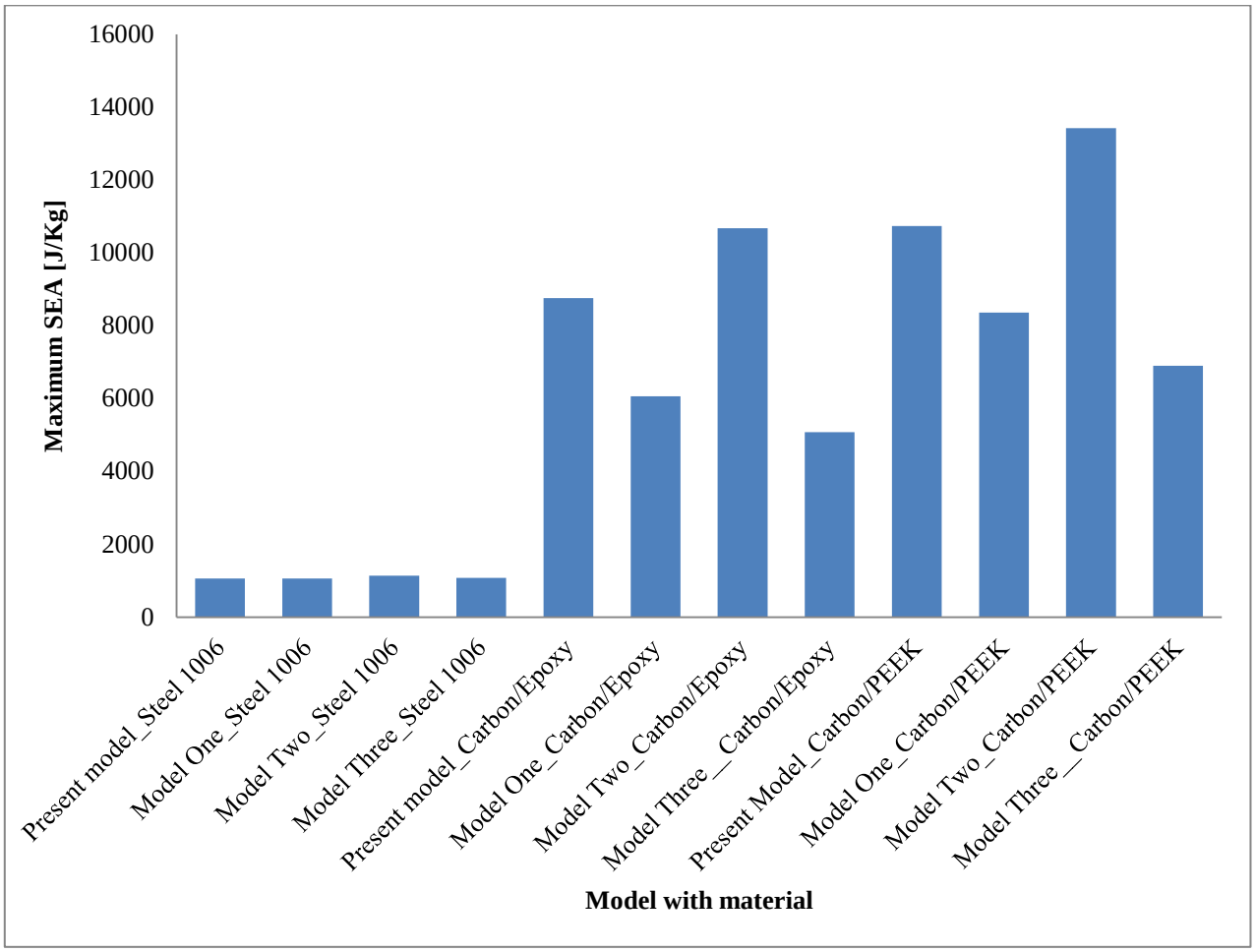

Figure 59 Summary of influence of modifying material and geometry on SEA

Chapter Five

5 Conclusion and Recommendation

5.1 Conclusion

In the design of automobile side-door impact beam, three major factors are usually considered. First, the deflection of beam should be kept below 50 mm for occupant safety. Second, the acceleration of impact beam during collision should not exceed 85 g for avoiding brain skull damage of occupant. Third, the specific energy absorption of side impact beam should be kept high.

From the previous result and discussion the beam with cross-rib arrangement and material implication of Carbon/PEEK could fulfill crashworthiness requirements as compared with other models. So it is selected as a new side door beam.

The improvements of new side door beam design are concluded as follows.

- The peak deflection of beam was decreased by 83 % from 111.6 mm to 18.7 mm due to the geometry and material modification. From the point of side impact beam design requirement, it could be 62 % more safe.
- The acceleration of beam was decreased by 97 % from 765 g to 23 g. From the point of side impact beam design requirement, it could be stable with 72.9 %.
- The specific energy absorption, SEA of beam was increased by 92 % from 1057 J/Kg to 13,425 J/Kg.
- In parallel, the weight of the beam was decreased by 82 % from 1.2026 Kg to 0.2161 Kg due to modification of material.

5.2 Recommendation

The properties of material and geometry have grate role on the deformation, acceleration and specific internal energy of side impact beam. Specially, the properties of composite materials, such as high specific energy absorption, lightweight and high strength are attractive for the construction of lightweight and fuel efficient vehicle structures.

In this study the results of twelve alternative beams were discussed by combining four geometries and three materials and then they were compared and contrasted based on three major factors (deformation, acceleration and SEA). This study shows that side door beam with crossed rib arrangement (⊕-type) and implication of Carbon/PEEK material has better performance than the present beam geometry and present material.

Finally, it recommended that the side impact beam with crossed rib arrangement (⊕-type) and implication of Carbon/PEEK composite material are more suitable for vehicle side impact beam.

5.3 Future Work

Since improvement of crashworthiness factors are depend on material properties and geometries the following research areas are recommended for further study

- Applying Carbon/PEEK material for other components, like impact beam support, trims and consecutive side door components.
- Applying other type of composite material which relatively cheaper than Carbon/PEEK for different ribbed arrangements.
- Varying material and thickness of rib and tube of impact beam.
- Conducting experimental test on the designed beam to check the accuracy of results.
- Doing on other types of rib geometry, orientation and arrangements.
- Re-analyzing the design by considering failure of the bonding between the beam tubes and ribs
- Manufacturing could be expensive for ribbed beams, so other alternatives will figure out.

Reference

[1]. J. Augenstein, injuries in near-side collisions, 1999.

[2]. https://www.daveabels.com/the-dangers-of-side-impact-collisions.html, Abels and Annes P.C. personal Injury lawyers, .

[3]. Ali Ghadianlou, Crashworthiness design of vehicle side door beams under low-speed pole side impact, 2013.

[4]. James Njuguna, The application of energy absorbing structures on side impact protection systems, Journal of computer Application in Technology, Volume 40, 200-208, 2011.

[5]. Clinciu Mihai, Aspects of side impact with vertical cylinder obstacle, 2013.

[6]. Shalabh Yadav, Investigations into Dynamic Response of Automobile components during crash simulation, 2014.

[7]. Panagiotis Bazios, Design and study of door components for a two-seater electric vehicle in side impact conditions, 2015.

[8]. Javier Luzon-Narro, Innovative passive and active countermeasures for near side crash safety, 2010.

[9]. John Townsend, Modular door system for side impact safety of motor vehicles, 2002.

[10]. Sandeep Dalavi, Crashworthiness of car interior door trims in side impact, Journal of Engineering Science, and Innovative Technology, Volume 4, 145-157, 2015.

[11]. Gustavo Zini, Introduction to feasible innovations in side impact safety, eng., 2005.

[12]. Ashwin Sheshadri, Design and analysis of a composite beam for side-impact protection of occupants in a sedan, May 2006.

[13]. Federal Motor Vehicle Safety Standards (FMVSS) No.214 “Side Impact Protection. Apr, 2017.

[14]. IIHS, Crashworthiness Evaluation Side Impact Crash Test Protocol (version III) April 2017.

[15]. George C. Jacob, Energy Absorption in Polymer Composite Materials for Automotive Crashworthiness, 2000.

[16]. Olivier Billot, Pole Impact Test: Study of the Two Current Candidates Interims of Cost and Benefits for France, 2014.

[17]. Abdullatif K. and Dhafer M., Development and Validation of a Us Side Impact Moveable Deformable barrier FE Model, 2010.

[18]. http://www.performancecomposites.com/carbonfibre/mechanicalproperties_2.asp , Mechanical Properties of Carbon Fibre Composite Materials, Fibre / Epoxy resin, January, 14, 2017.

[19]. http://www.lstc.com/products/ls-dyna Livermore Software Technology Corporation, Dec-19-2016.

[20]. http://www.boedeker.com/tecapeek.htm PEEK (PolyEtherEtherKetone) Specifications, Dec-10-2016.

[21]. http://www.matweb.com/search/GetMatlsByTradename.aspx?tn=PEEK, PEEK Technical Data Sheet, January, 16, 2017.

[22]. U.S. Department of Transportation National Highway Traffic Safety Administration FMVSS No. 216. Roof crush resistance.

[23]. Shaik Shaheen , G. Srinivasa Gupta , Design and Stress Analysis of Carbon-Epoxy Composite Rocket Motor Casing, International Journal of Innovative Research in Science, Engineering and Technology, Vol. 4, Issue No:8, August 2015.

APPENDIX A ----------Material Properties/Specification

Table 10 Honey comb material property

Property	**Honeycomb_245psi**	**Honeycomb_45psi**
Density	$8.3x10^{-11}$ t/mm^3	$2.62x10^{-11}$ t/mm^3
Young's Modulus	68950 MPa	68950 MPa
Poisson's Ratio	0.33	0.33
Yield Stress	160 MPa	160 MPa
Elastic Modulus longitudinal	1020 MPa	172 Mpa
Elastic Modulus Transverse	340 MPa	57.2 MPa
Shear Modulus XY	434 MPa	145 MPa
Shear Modulus XZ,YZ	214 MPa	75 MPa

Table 11 Aluminum Face Material Properties

Property	**Aluminum 2024-T3**	**Aluminum 5052-H34**
Density	$2.78x10^{-9}$ t/mm^3	$2.68x10^{-9}$ t/mm^3
Young's Modulus	72400 MPa	70000 MPa
Poisson's Ratio	0.33	0.33
Yield Stress	345 MPa	215 MPa
Plastic Tang. Hardening Modulus	777 MPa	450 MPa
Hardening Parameter	0.5	0.5

Table 12 Carbon/Epoxy 40-60 Properties

Property	**Value**
Density	1580 Kg/m^3
Longitudinal Modulus	142.3 GPa
Transverse Modulus	10.291 GPa
Poisson's Ratio in plane	0.270
Poisson's Ratio intralaminar	0.357
Shear modulus in plane	7.122 GPa
transverse modulus parallel to fiber direction	3.151 GPa
Ply transverse modulus perpendicular to fiber direction	7.124 GPa
Longitudinal tensile strength	1.831 GPa
Longitudinal compressive strength	1.090 GPa
Transverse tensile strength	0.054 GPa
Transverse compression strength	0.220 GPa
Shear strength	0.070 GPa
Longitudinal Coefficient of Thermal Expansion	$-1.913x10^{-7}$ $^oC^{-1}$
Transverse Coefficient of Thermal Expansion	$1.999x10^{-5}$ $^oC^{-1}$

Table 13 Carbon/PEEK 40-60 Properties

Property	Value
Density	1419 Kg/m^3
Longitudinal Modulus	148.101 GPa
Transverse Modulus	12.500 GPa
Poisson's Ratio in plane	0.290
Poisson's Ratio intralaminar	0.4157
Shear modulus in plane	8.142 GPa
transverse modulus parallel to fiber direction	4.051 GPa
Ply transverse modulus perpendicular to fiber direction	8.143 GPa
Longitudinal tensile strength	3.143 GPa
Longitudinal compressive strength	2.004 GPa
Transverse tensile strength	0.114 GPa
Transverse compression strength	0.292 GPa
Shear strength	0.084 GPa
Longitudinal Coefficient of Thermal Expansion	$-2.213x10^{-7}$ $^oC^{-1}$
Transverse Coefficient of Thermal Expansion	$1.899x10^{-5}$ $^oC^{-1}$

Table 14 Steel 1006 Properties

Property	**Value**
Density	7896 Kg/m^3
Yield Strength	350 MPa
Hardening Constant	275 MPa
Haredining Exponent	0.36
Strain rate constant	0.022
Melting Temprature	1538 ^0C
Shear Modulus	81.8 GPa
Specific Heat	452 J/Kg

Table 15 Basic Properties of Fibers and matrix

	Yong's Modulus [GPa]	Tensile Strength [MPa]	Poisson's ratio	Density [Kg/m^3]	Thermal Conductivity coefficient [W/K-m]	Thermal Expansion Coefficient [$1/^0C$]
Carbon IM10	310	6964	0.270	1790	6.140	$-0.7x10^{-6}$
Epoxy 8552	3.45	90	0.350	1300	0.181	$64.3x10^{-6}$
PEEK-Teca	18	184	0.421	1450	0.230	$82.13x10^{-6}$

APPENDIX B ----------Properties of Composite

The property of composite can be estimated numerically by combining the fiber (f) and matrix (m) properties. V is volume fraction, [23].

1. Lamina Density,

$$\rho_c = \rho_f V_f + \rho_m V_m$$

2. Longitudinal Young's Modulus,

$$E_1 = E_f V_f + E_m V_m$$

3. Transverse Young's Modulus

$$\frac{1}{E_2} = \frac{V_m}{E_m} + \frac{V_f}{E_f}$$

4. In-Plane Poisson's Ratio,

$$\upsilon_{12} = \upsilon_f V_f + \upsilon_m V_m$$

5. In-Plane Shear Modulus

$$G_{12} = G_m \left[\frac{(1+V_f) + (1-V_f)\,{G_m}/{G_f}}{(1-V_f) + (1+V_f)\,{G_m}/{G_f}} \right]$$

6. Intralaminar Shear Modulus

$$G_{23} = G_m \left[\frac{V_f + \eta_4(1-V_f)}{\eta_4(1-V_f) + V_f({G_m}/{G_f})} \right]$$

Where $\eta_4 = \dfrac{3-4V_m+{G_m}/{G_f}}{4(1-V_m)}$

7. Longitudinal Coefficient of Thermal Expansion

$$\alpha_1 = \frac{\alpha_f E_f V_f + \alpha_m E_m V_m}{E_1}$$

8. Transverse Coefficient of Thermal Expansion

$$\alpha_2 = \alpha_f \sqrt{V_f} + (1-\sqrt{V_f})(1+V_f V_m \frac{E_f}{E_1})\alpha_m$$

9. Longitudinal Coefficient of Moisture Expansion,

$$\beta_1 = \beta_m (1 - V_f)\frac{E_m}{E_1}$$

10. Transverse Coefficient of Moisture Expansion

$$\beta_2 = \beta_m (1 - V_f)\left[1 + \frac{\sqrt{V_f}(1-\sqrt{V_f})E_m}{\sqrt{V_f}E_2 + (1-\sqrt{V_f})E_m}\right]$$

APPENDIX C ----------Meshed Model

Table 16 Meshed model and statistics for the parts of model

Part Name	Meshed Model	**Number of Element**	**Number of Node**
MDB	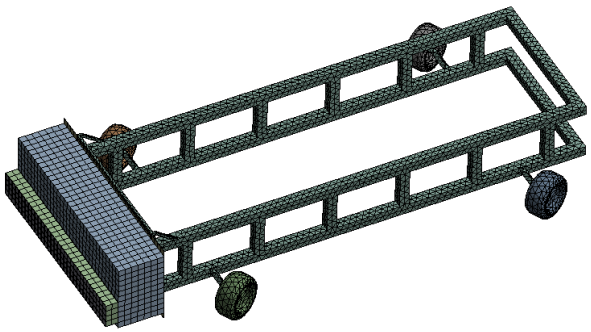	39,537	16,801
Present Model		11,318	19,723
Model One	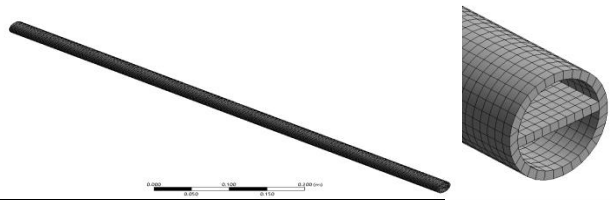	14,856	28,396
Model Two		17,292	30,006
Model Three	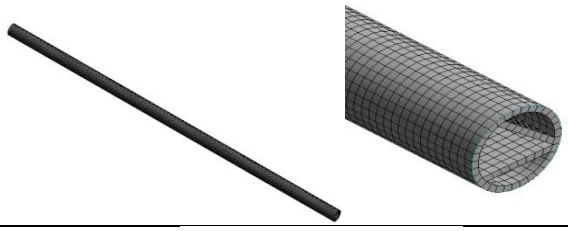	16,686	32,092
Beam Support	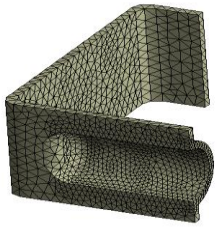	12,080	3,380

APPENDIX D----------Equivalent (Von-Mises) Stress

.

Equivalent Stress in the Assignment of Present Material (Steel 1006)

The equivalent stress of each impact beam when the Steel 1006 material assigned is shown in the next figures.

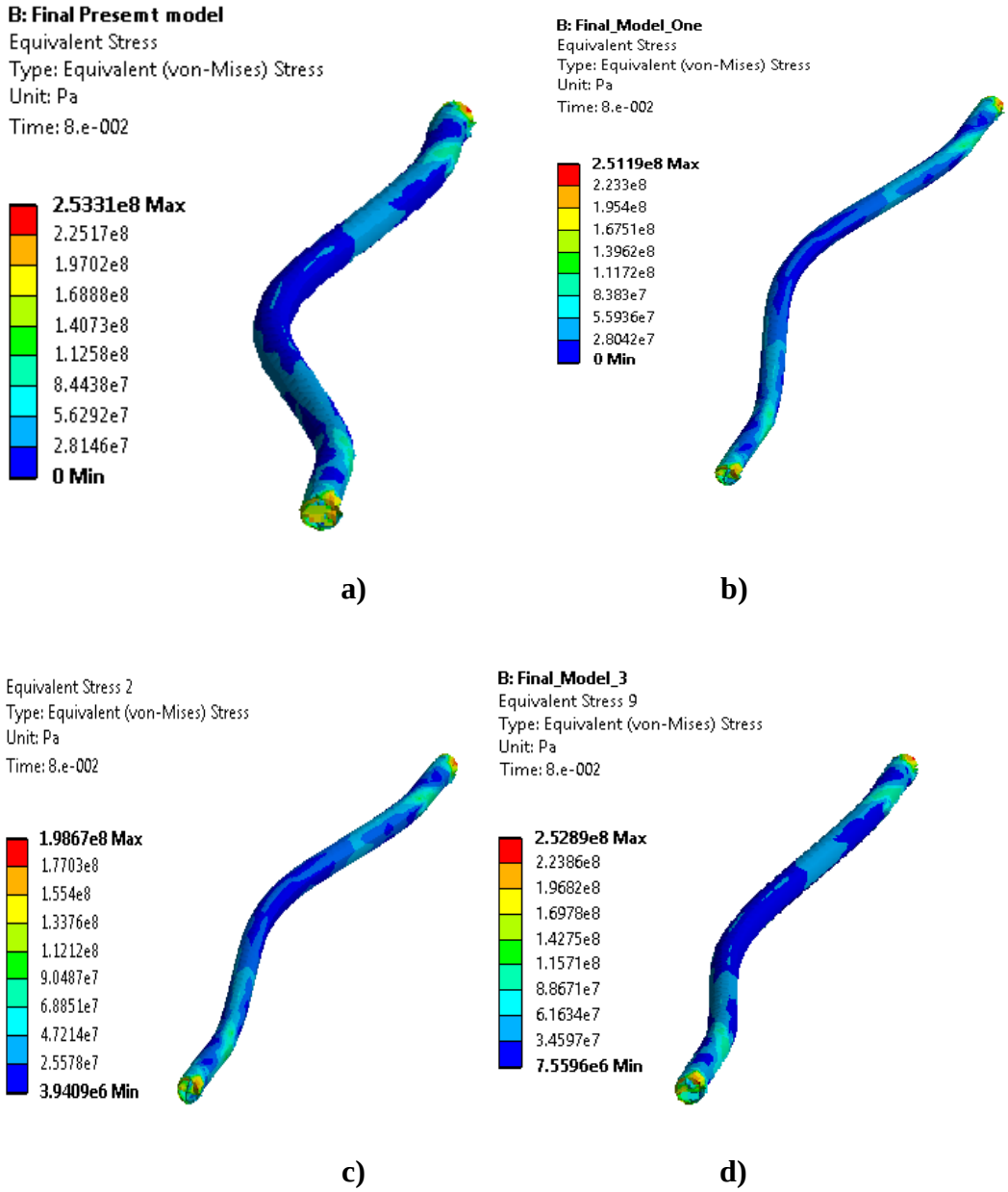

Figure 60 Equivalent Stress in Steel 1006 beam a) Present Model b) Model One c) Model Two d) Model Three

Equivalent Stress in the Assignment of Material One (Carbon/Epoxy)

The equivalent stress of each impact beam when the Carbon/Epoxy composite material assigned is shown in the next figures.

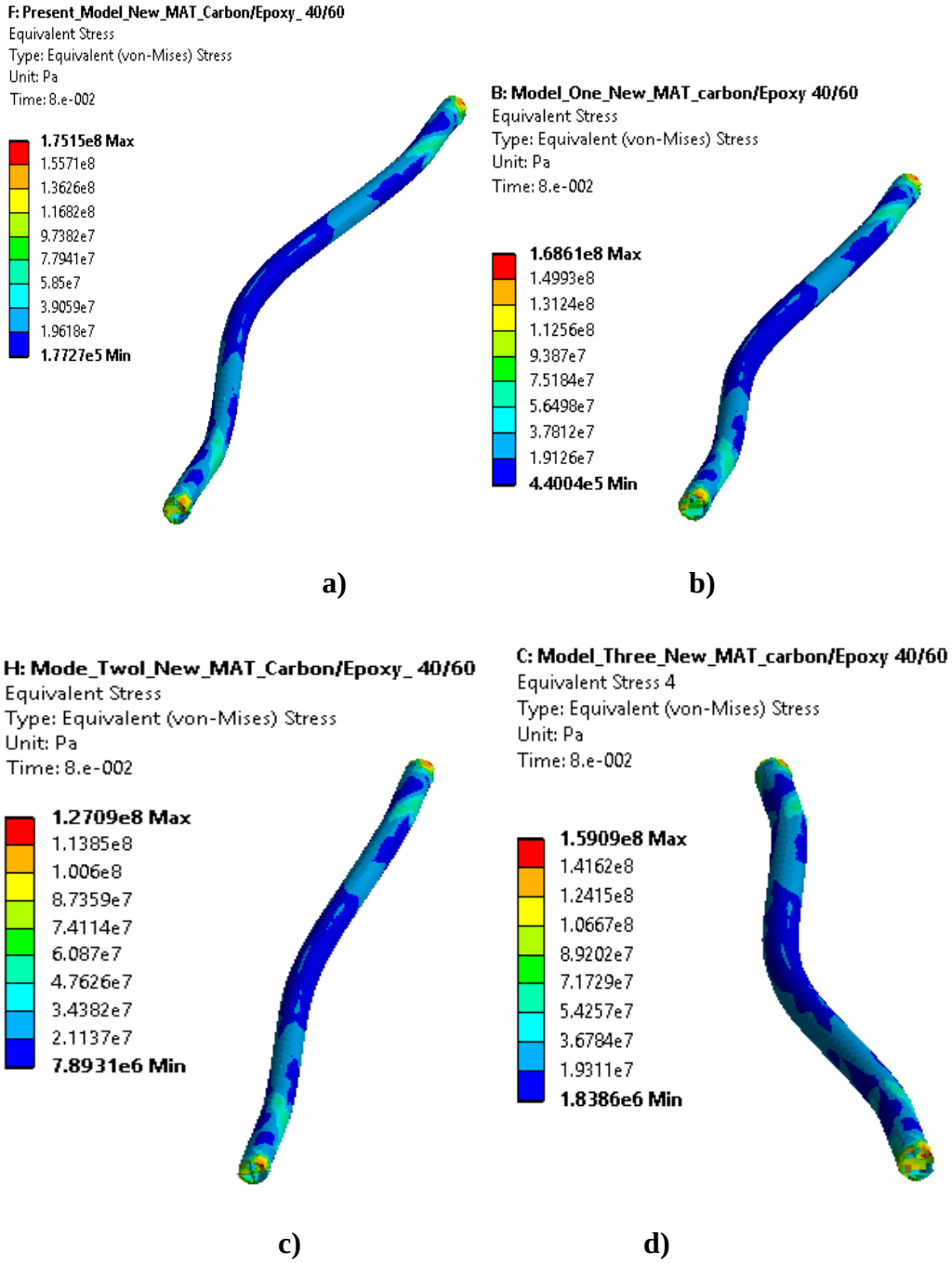

Figure 61 Equivalent Stress in Carbon/Epoxy beam a) Present Model b) Model One c) Model Two d) Model Three

Equivalent Stress in the Assignment of Material Two (Carbon/PEEK)

The equivalent stress of each impact beam when the Carbon/PEEK composite material assigned is shown in the next figures.

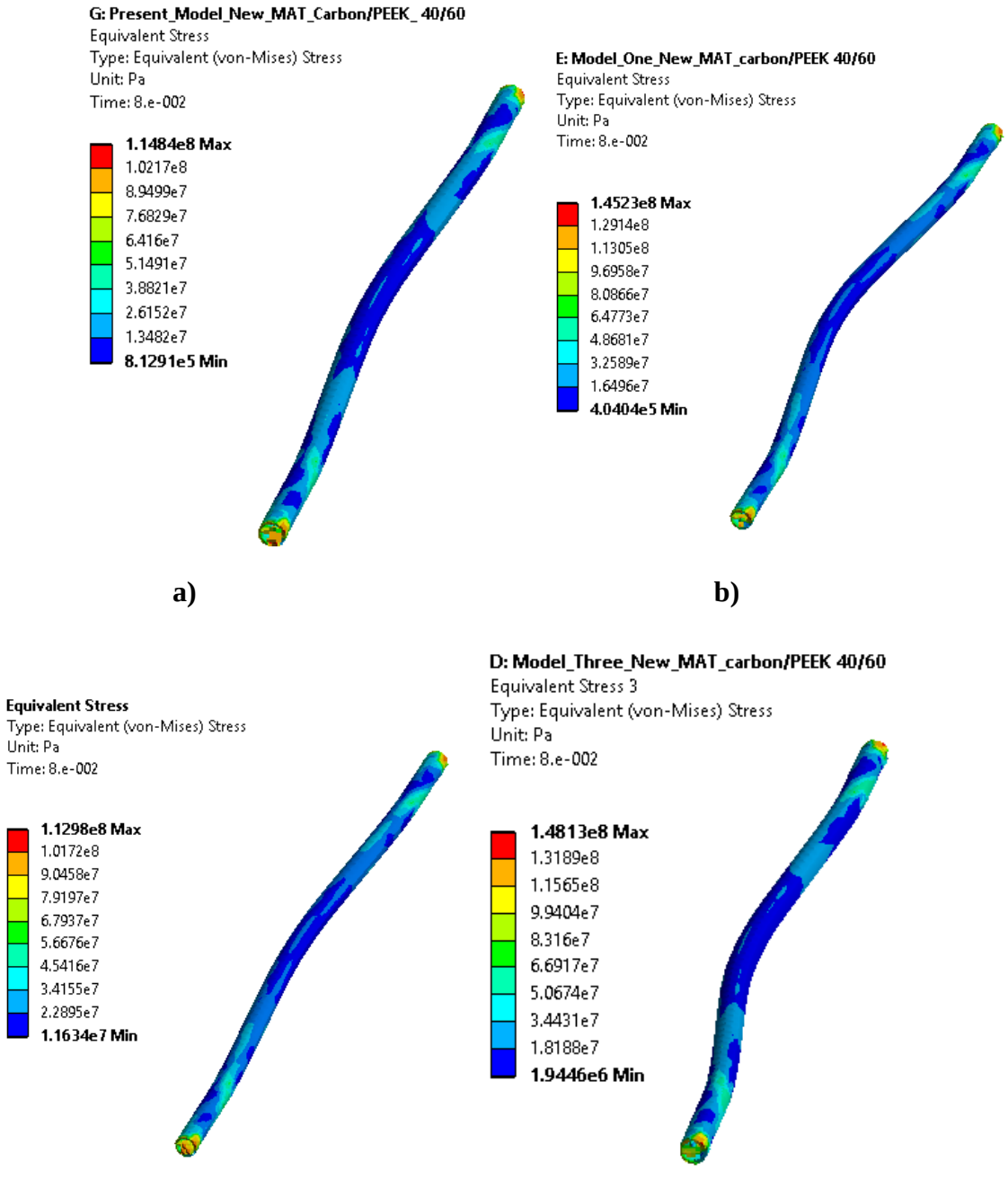

Figure 62 Equivalent Stress in Carbon/PEEK beam a) Present Model b) Model One c) Model Two d) Model Three